Vienna Doctoral Programme on
Water Resource Systems
www.waterresources.at

Doctoral Thesis

From the detection to the attribution of flood changes in Europe

submitted in satisfaction of the requirements for the degree of
Doctor of Science in Civil Engineering
of the TU Wien, Faculty of Civil Engineering

as part of the
Vienna Doctoral Programme on Water Resource Systems

by

Dott.Mag. Ing. **Miriam Bertola**
Matr.Nr.: 1652633

Examiner:	Assoc.Prof. Dr. **Alberto Viglione** Department of Environment, Land and Infrastructure Engineering (DIATI) Polytechnic University of Turin Corso Duca degli Abruzzi 24, 10129 Turin, Italy
Examiner:	Univ.Prof. Dipl.-Ing. Dr.techn. **Günter Blöschl** Institut für Wasserbau und Ingenieurhydrologie, Technische Universität Wien Karlsplatz 13/222, 1040 Wien, Österreich
Examiner:	Univ.Prof. PhD **Koen Blanckaert** Institut für Wasserbau und Ingenieurhydrologie, Technische Universität Wien Karlsplatz 13/222, 1040 Wien, Österreich
Examiner:	Prof. Dr. **Attilio Castellarin** Dipartimento di Ingegneria Civile, Chimica, Ambientale e dei Materiali Università di Bologna Viale del Risorgimento 2, 40136 Bologna, Italy

Vienna, October 2020

Vienna Doctoral Programme on
Water Resource Systems
www.waterresources.at

Dissertation

Von der Detektion zur Attribution von Hochwasserveränderungen in Europa

ausgeführt zum Zwecke der Erlangung des akademischen Grades eines
Doktors der technischen Wissenschaften
eingereicht an der Technischen Universität Wien, Fakultät für Bauingenieurwesen

als Teil des
Doktoratskolleg für Water Resource Systems

von

Dott. Mag. Ing. **Miriam Bertola**
Matr.Nr.: 1652633

Gutachter: Univ.Prof. Ing. **Alberto Viglione**
Department of Environment, Land and Infrastructure Engineering (DIATI)
Polytechnic University of Turin
Corso Duca degli Abruzzi 24, 10129 Turin, Italy

Gutachter: Univ.Prof. Dipl.-Ing. Dr.techn. **Günter Blöschl**
Institut für Wasserbau und Ingenieurhydrologie,
Technische Universität Wien
Karlsplatz 13/222, 1040 Wien, Österreich

Gutachter: Univ.Prof. PhD **Koen Blanckaert**
Institut für Wasserbau und Ingenieurhydrologie,
Technische Universität Wien
Karlsplatz 13/222, 1040 Wien, Österreich

Gutachter: Univ.Prof. Ing. **Attilio Castellarin**
Dipartimento di Ingegneria Civile, Chimica, Ambientale e dei Materiali
Università di Bologna
Viale del Risorgimento 2, 40136 Bologna, Italy

Vienna, im Oktober 2020

Abstract

Floods are the most frequent natural disasters in Europe, causing significant socioeconomic losses. There is a general concern that climate and environmental change may affect the magnitude and frequency of floods. As a consequence, hydraulic structures and flood defences, whose design did not account for those changes, may become inadequate to provide the required protection level over time. Several local and regional trend detection studies have provided evidence of past flood regime changes in Europe. These studies have typically analysed changes in the mean annual flood discharge, while trends in floods associated with large return periods, such as the 100-year flood, have not been studied. Also, their underlying causes have not been explained yet in a quantitative and formally consistent way. The aim of this thesis is to understand whether trends in flood discharges also occurred for larger return periods and to attribute them to their drivers. For this purpose, this thesis proposes new data-based attribution approaches.

In Chapter 2, regional trends in flood quantiles, in particular the median and the 100-year flood, are assessed across Europe with a non-stationary regional flood frequency approach. The flood data analysed in this research consist of a unique pan-European database of annual maximum discharges from 2370 hydrometric stations, covering five decades (i.e. 1960-2010). Results show that in northwestern Europe the trends in flood magnitude are generally positive. In small catchments, the 100-year flood increases more than the median flood, while the opposite is observed in medium and large catchments. In southern Europe flood trends are generally negative. The 100-year flood decreases less than the median flood and, in the small catchments, the median flood decreases less compared to the large catchments. In eastern Europe the regional trends are negative and do not depend on the return period, but catchment area plays a substantial role: the larger the catchment, the more negative the trend.

A data-based attribution approach is proposed in Chapter 3 for selecting which driver best explains variations in time of the flood frequency curve. This approach considers three groups of potential drivers (i.e. atmospheric, catchment and rivers system drivers) and consists of comparing and selecting alternative driver-informed models at the catchment scale, based on an information criterion. This approach is applied to a case study, consisting of 96 gauges in Upper Austria, where flooding has become more intense during the last 50 years. This allowed us to identify changes in extreme daily precipitation as the most probable cause of flood change, as well as to exclude the influence of human intervention on landscape or rivers.

In Chapter 4 we extend the approach of Chapter 3 to estimating the relative contributions of potential drivers to the flood changes across Europe (those detected in Chapter 2) as a function of return period, through a regional non-stationary flood frequency analysis. Extreme precipitation, antecedent soil moisture and snowmelt are the potential drivers considered in this chapter. Results show that, in northwestern Europe, extreme precipitation mainly contributes to changes in both the median and 100-year flood, while the contributions of antecedent soil moisture are of secondary importance. In southern Europe, both antecedent soil moisture and extreme precipitation contribute to flood changes, and their relative importance depends on the return period. Antecedent soil moisture is the main contributor to changes in the median flood, while the contribution of the two drivers to changes in larger floods are comparable. In eastern Europe, snowmelt drives changes in both the median and the 100-year flood.

This thesis contributes to flood change research in two ways: methodologically and factually. It proposes new approaches for the formal attribution of flood changes, which may be relevant in other regions, and it provides continental-scale detection and attribution results for flood changes that improve our understanding of observed flood regime changes across Europe. The understanding of past flood changes is important for better informed flood management strategies.

Kurzfassung

Hochwässer sind die häufigste Naturkatastrophe in Europa und verursachen erhebliche sozioökonomische Schäden. Veränderungen des Klimas und der Umwelt beeinflussen die Größe und die Häufigkeit von Hochwässern. Infolgedessen kann die Bemessung von Wasserbauten und Maßnahmen für den Hochwasserschutz nicht mehr ausreichen, um das erforderliche Schutzniveau aufrecht zu erhalten. Wissenschaftliche Arbeiten zu lokalen und regionalen statistischen Trends haben Hinweise auf Änderungen des Hochwasserregimes in Europa geliefert. In diesen Studien wurden in der Regel Änderungen des mittleren jährlichen Hochwasserabflusses analysiert, während Trends von Hochwassern mit großer Wiederkehrperiode/Jährlichkeit, wie z. B. einem 100-jährigen Hochwasser, nicht untersucht wurden. Ferner wurden die zugrunde liegenden Ursachen für die beobachteten statistischen Trends nicht quantitativ und formal konsistent ausgearbeitet. Ziel dieser Arbeit ist es zu verstehen, ob Trends in Hochwasserdurchflüssen auch bei größeren Wiederkehrperioden aufgetreten sind, und diesen ihre Treibern zuzuordnen. Zu diesem Zweck werden in dieser Arbeit neue datenbasierte Attributionsansätze entwickelt.

In Kapitel 2 werden regionale Trends in Hochwasserquantilen, insbesondere dem Median und dem 100-jährigen Hochwasser, europaweit mit einem instationären, regionalen Hochwasserhäufigkeitsansatz geschätzt. Die in dieser Studie analysierten Hochwasserdaten bestehen aus einer einzigartigen europaweiten Datenbank. Es handelt sich um Beobachtungen von jährlichen Maximaldurchflüssen von 2370 hydrometrischen Stationen, die fünf Jahrzehnte abdecken (d. h. 1960-2010). Die Ergebnisse zeigen, dass in Nordwesteuropa Trends in Hochwasserdurchflüssen im Allgemeinen positiv sind. In kleinen Einzugsgebieten nimmt das 100-jährige Hochwasser stärker zu als das mittlere Hochwasser, während in mittleren und großen Einzugsgebieten das Gegenteil beobachtet wird. In Südeuropa sind die Trends in Hochwasserdurchflüssen im Allgemeinen negativ. Das 100-jährige Hochwasser nimmt weniger ab als das mittlere Hochwasser, und in den kleinen Einzugsgebieten nimmt das mittlere Hochwasser im Vergleich zu großen Einzugsgebieten weniger ab. In Osteuropa sind regionale Trends in Hochwasserquantilen negativ und hängen nicht von der Wiederkehrperiode ab, aber die Einzugsgebietsgröße spielt eine wesentliche Rolle: Je größer das Einzugsgebiet, desto negativer ist der beobachtete Trend.

In Kapitel 3 wird ein datenbasierter Attributionsansatz vorgestellt, um zu quantifizieren welche Treiber die zeitlichen Schwankungen der Hochwasserhäufigkeitskurve am besten erklären. Der Ansatz verwendet drei Gruppen potenzieller Treiber (d. h. atmosphärische, einzugsgebietsbezogene und flusssystembezogene Treiber). Alternative, durch Treiber informierte, Modelle werdenauf der Einzugsgebietsskala anhand eines Informationskriteriums verglichen. Dieser Ansatz wird in einer Fallstudie angewendet, die aus 96 Hochwasserzeitreihen in Oberösterreich besteht, wo Hochwasserdurchflüsse in den letzten 50 Jahren zugenommen haben. Dies erlaubt uns Änderungen des extremen täglichen Niederschlags als wahrscheinlichste Ursache für beobachtete Hochwasserveränderungen zu identifizieren und den Einfluss menschlicher Eingriffe auf Landschaft und Flüsse als dominante Treiber auszuschließen.

In Kapitel 4 erweitern wir den Ansatz aus Kapitel 3 auf die Schätzung der relativen Beiträge potenzieller Treiber zu Hochwasseränderungen in ganz Europa (welche in Kapitel 2 detektiert wurden) als Funktion der Wiederkehrperiode im Kontext einer regionalen instationären Hochwasserhäufigkeitsanalyse. Extreme Niederschläge, Bodenfeuchtigkeit und Schneeschmelze sind die potenziellen Treiber, die in diesem Kapitel berücksichtigt werden. Die Ergebnisse zeigen, dass

in Nordwesteuropa hauptsächlich extreme Niederschläge zu Veränderungen sowohl des mittleren als auch des 100-jährigen Hochwassers beitragen, während Beiträge der Bodenfeuchtigkeit von geringerer Bedeutung sind. In Südeuropa tragen sowohl Bodenfeuchtigkeit als auch extreme Niederschläge zu Hochwasseränderungen bei, und ihre relative Bedeutung hängt von der Wiederkehrperiode ab. Bodenfeuchtigkeit trägt hauptsächlich zu Änderungen der mittleren Hochwasser bei, während der Beitrag der beiden Treiber zu Änderungen größerer Hochwasser vergleichbar ist. In Osteuropa führt Schneeschmelze zu Veränderungen sowohl im Median als auch im 100-jährigen Hochwasser.

Diese Arbeit trägt auf zwei Weisen zur Erforschung der Veränderungen von Hochwassern bei: methodisch und sachlich. Es werden neue Ansätze für die quantitative Attribution von Hochwasseränderungen vorgestellt, die in anderen Regionen relevant sein können. Und es werden Ergebnisse zu Detektion und Attribution von Hochwasseränderungen auf kontinentaler Ebene erarbeitet, die unser Verständnis von beobachteten Änderungen des Hochwasserregimes in Europa verbessern. Damit können Maßnahmen des Hochwassermanagement noch sicherer und effizienter gestaltet werden.

I am very grateful to my supervisors, Prof. Alberto Viglione and Prof. Günter Blöschl for giving me this opportunity and for always providing great guidance. I would like to thank the reviewers of my thesis, Prof. Koen Blanckaert and Prof. Attilio Castellarin, for taking the time to read it.

I wish to thank my fellow students and friends from the Vienna Doctoral Program on Water Resource Systems for sharing all the happy and challenging moments of this journey during these last three years and a half.

Last but not least, I would like to thank my family for always supporting me, despite the distance, and Alberto Trentino for being there, day by day.

Contents

Chapter 1

Introduction

Increasing flood hazard in Europe has become a major concern as a consequence of severe flood events experienced in the last decades, as, for instance, the extreme floods occurred in central Europe in 2002 (Ulbrich et al., 2003) and 2013 (Blöschl et al., 2013a), and the winter floods in northwest England in 2009 (Miller et al., 2013) and 2015-16 (Barker et al., 2016). As a result, past flood regime changes in Europe have been investigated by several local and regional trend detection studies. These studies typically analysed catchments individually and investigated whether spatial clusters or coherent regional patterns of flood trends could be observed (e.g. Petrow and Merz, 2009; Prosdocimi et al., 2014; Mangini et al., 2018). The main limitation of most at-site studies is the limited flood data locally available, which results in high uncertainties in the detected trends. In order to overcome the limitation of at-site studies, regional non-stationary flood frequency methods were proposed (e.g., Renard et al., 2006b; Leclerc and Ouarda, 2007), where flood data are pooled across multiple sites within homogeneous regions (Dalrymple, 1960; Hosking and Wallis, 1997) and the regional estimate depend on time (e.g. Cunderlik and Burn, 2003; Renard et al., 2006a; Leclerc and Ouarda, 2007; Hanel et al., 2009) or on time-varying climatic or anthropogenic covariates (e.g. Lima and Lall, 2010; Renard and Lall, 2014; Prosdocimi et al., 2015). Other approaches analysed coherent regional change by testing for the presence of trends in regional variables, such as the number of annual floods in the region (e.g. Hannaford et al., 2013), or with regional tests (e.g. Douglas et al., 2000; Renard et al., 2008).

The above studies are heterogeneous with respect to flood data types, period of records, detection approaches and spatial coverage (Hall et al., 2014). In recent years, thanks to the release of pan-European and global flood databases (Hall et al., 2015; GRDC, 2016), European-wide trend detection studies have been published (Blöschl et al., 2017; Blöschl et al., 2019; Mangini et al., 2018). They revealed evidence of positive trends in the magnitude of the mean annual flood in north-western Europe and negative trends in southern and eastern Europe. However, few examples exist where observed trends in different flood quantiles (e.g. the 100-year flood) are analysed, as changes in the mean annual (or median) flood are typically investigated.

While a wide body of literature on the detection of flood changes is available, proper methods for the identification of their underlying causes (i.e. flood change attribution) have not been proposed yet. According to Pinter et al. (2006), Merz et al. (2012) and Hall et al. (2014), potential drivers of change in flood regimes can be clustered into three groups: atmospheric, catchment and river system drivers. Atmospheric drivers are changes in climate variables, such as total precipitation, precipitation intensity/duration, temperature, and radiation. These changes typically occur consistently over large regions, resulting in gradual changes in time in the mean or variance of peak discharges. Catchment drivers are changes in runoff generation and concentration processes (e.g. changed infiltration and storage characteristics) caused, for instance, by land-use changes. These processes, such as urbanization or deforestation, are more likely to occur gradually in time and at small scales, with decreasing effects on floods with catchment size. River system drivers are changes in processes affecting flood wave propagation, such as river training, the construction of hydraulic structures, modification of river morphology, roughness or

storage. They typically produce step changes in flood peak discharges with increasing effects with catchment size.

The way attribution is approached in flood trend studies is mainly through qualitative reasoning, attempting to explain the change in flood regime with some climate variables (e.g. precipitation and circulation patterns) or with anthropogenic effects (e.g. river training, dam construction or land use change), and citing literature as support for the hypothesised attribution statements (Merz et al., 2012). In other cases, the detected flood changes are quantitatively related to potential drivers and two different approaches have been used in literature: data-based and simulation-based approaches. The data-based approach, usually, tries to statistically correlate the mean or extreme characteristics of the flood time series to climate drivers. Climate indices or other atmospheric variables (usually precipitation) are used as covariates of the flood frequency distribution parameters, in order to allow a better fit to the data (e.g., Šraj et al., 2016; Silva et al., 2017; Steirou et al., 2019). On the other hand, simulation-based methods, try to reproduce the observed flood changes by introducing, in a hydrological model, changes in a potential driver and by observing their effects on the simulated hydrograph characteristics (e.g., Renard et al., 2008; Vorogushyn and Merz, 2013; Skublics et al., 2016). Rarely more than one driver is taken into consideration and catchments are often analysed individually. One exception is Viglione et al. (2016), who proposed a framework for the estimation of the regional relative contribution to flood trends of each of the three drivers, exploiting the scaling with catchment area.

The aim of this thesis is to contribute to recent research on flood regime changes in Europe through the assessment of trends in flood quantiles (e.g. the median and the 100-year flood) across Europe and their attribution to potential drivers. In particular, this thesis addresses the following research questions:

1. Are changes in small and big floods different?
2. Is it possible to identify the main driver of flood change using a data-based attribution approach?
3. Do small and large floods have the same drivers of change?

Each chapter of this thesis corresponds to a scientific paper (published or in preparation). Chapter 2 investigates and compares trends in small versus big flood events (i.e. the median and the 100-year flood) in the period 1960-2010 across Europe, through a regional non-stationary flood frequency approach. Chapter 3 proposes a local data-based attribution approach, which is applied investigate whether atmospheric, catchment and river drivers determined the river flood changes in Upper Austria. Chapter 4 analyses the relative contribution of three climatic drivers (i.e. extreme precipitation, antecedent soil moisture and snow melt) across Europe on flood changes as a function of the return period. Finally, Chapter 5 presents an overview of the results and the overall conclusion of the thesis.

Chapter 2

Flood trends in Europe: are changes in small and big floods different?

The present chapter corresponds to the following scientific publication in its original form:

Bertola M., Viglione A., Lun D., Hall J. and Blöschl G. (2020). "Flood trends in Europe: are changes in small and big floods different?". Hydrology and Earth System Sciences, 24(4), pp. 1805–1822. doi: 10.5194/hess-24-1805-2020.

Abstract

Recent studies have revealed evidence of trends in the median or mean flood discharge in Europe over the last five decades, with clear and coherent regional patterns. The aim of this study is to assess whether trends in flood discharges also occurred for larger return periods, accounting for the effect of catchment scale. We analyze 2370 flood discharge records, selected from a newly-available pan-European flood database, with record length of at least 40 years over the period 1960-2010 and with contributing catchment area ranging from 5 to 100 000 km^2. To estimate regional flood trends, we use a non-stationary regional flood frequency approach consisting of a regional Gumbel distribution, whose median and growth factor can vary in time with different strengths for different catchment sizes. A Bayesian Markov chain Monte Carlo (MCMC) approach is used for parameter estimation. We quantify regional trends (and the related sample uncertainties), for floods of selected return periods and for selected catchment areas, across Europe and for three regions where coherent flood trends have been identified in previous studies. Results show that in northwestern Europe the trends in flood magnitude are generally positive. In small catchments (up to 100 km^2), the 100-year flood increases more than the median flood, while the opposite is observed in medium and large catchments, where even some negative trends appear, especially in northwestern France. In southern Europe flood trends are generally negative. The 100-year flood decreases less than the median flood and, in the small catchments, the median flood decreases less compared to the large catchments. In eastern Europe the regional trends are negative and do not depend on the return period, but catchment area plays a substantial role: the larger the catchment, the more negative the trend.

2.1 Introduction

Increasing flood hazard in Europe has become a major concern as a consequence of severe flood events experienced in the last decades, as, for instance, the extreme floods occurred in central Europe in 2002 (e.g. Ulbrich et al., 2003) and 2013 (e.g. Blöschl et al., 2013a), and the winter floods in northwest England in 2009 (e.g. Miller et al., 2013) and 2015-16 (e.g. Barker et al., 2016). Hence a growing number of flood trend detection studies has been published in recent years. These studies typically analyse a large set of time series of flood peaks in a region and test them

for the presence of significant gradual or abrupt changes in flood magnitude or frequency. For example, Petrow and Merz (2009) analysed eight flood indicators, from 145 gauges in Germany over the period 1951-2002, and detected mainly positive trends in the magnitude and frequency of floods. Villarini et al. (2011) tested flood time series of 55 stations in central Europe, with at least 75 years of data, for abrupt or gradual changes and found mostly abrupt changes associated with anthropogenic intervention (such as the construction of dams and reservoirs and river training). Mediero et al. (2014) detected a general decreasing trend in the magnitude and frequency of floods in Spain, with the exception of the north-west. Prosdocimi et al. (2014) investigated the presence of trends in annual and seasonal maxima of peak flows in the UK and found clusters of increasing trends for winter peaks in northern England and Scotland, and decreasing trends for summer peaks in southern England. These studies are highly heterogeneous in terms of flood data types, period of records and detection approaches and it is therefore not trivial to deduce regional patterns of flood regime change at the larger continental scale. Despite this fragmentation, Hall et al. (2014) summarized the findings of previous studies in a map of increasing, decreasing and not detectable flood changes for Europe, and showed the existence of consistent regional patterns. In particular, in central and western Europe flood magnitude appeared to increase with time, while it seemed to decrease in the Mediterranean catchments and in eastern Europe.

More recently, thanks to the availability of European and global high spatial resolution databases, large-scale investigation studies across Europe have been published. Mangini et al. (2018) extracted 629 flood records from the Global Runoff Data Center database (GRDC, 2016) and compared the detected trends in magnitude and frequency of floods from different approaches (annual maximum flood and peak over threshold) for the period 1965–2005. Blöschl et al. (2019) analysed 2370 flood records from a newly available pan-European flood database consisting of more than 7000 observational hydrometric stations and covering the last five decades (Hall et al., 2015) and revealed consistent spatial patterns of trends in the magnitude of the annual maximum flood, with clear positive trends in northwestern Europe and decreasing trends in southern and eastern Europe.

Existing studies typically analyse catchments individually and investigate whether spatial clusters or coherent regional patterns of flood trends can be observed (e.g. Petrow and Merz, 2009; Prosdocimi et al., 2014; Mangini et al., 2018). Based on predefined regions or obtained change patterns, some studies aggregate flood records and local test results in order to assess their field significance (e.g. Douglas et al., 2000; Mediero et al., 2014; Renard et al., 2008). The main limitation of most at-site studies is the short length of the flood peak records locally available for the detection of trends, resulting in low signal-to-noise ratio and hence high uncertainties in the detected trend. Increasing the signal-to-noise ratio can be achieved by pooling flood data from multiple sites within homogeneous regions, as in regional frequency analyses (Dalrymple, 1960; Hosking and Wallis, 1997). Several studies propose non-stationary regional frequency analyses for changes in precipitation extremes and flood trends, that consider the dependency of regional estimates on time (e.g. Cunderlik and Burn, 2003; Renard et al., 2006a; Leclerc and Ouarda, 2007; Hanel et al., 2009; Roth et al., 2012) or on climatic and anthropogenic covariates (e.g. Lima and Lall, 2010; Tramblay et al., 2013; Renard and Lall, 2014; Sun et al., 2014; Prosdocimi et al., 2015; Viglione et al., 2016). Other approaches analyse coherent regional change by testing for the presence of trends in regional variables, as the number of annual floods in the region (e.g. Hannaford et al., 2013), or with regional tests (e.g. Douglas et al., 2000; Renard et al., 2008).

However, most of the cited studies investigate changes in the mean annual (or median) flood only, and few examples exist where observed trends in different flood quantiles are analysed. Typically, flood quantiles obtained with stationary and non-stationary flood frequency approaches are compared (see e.g. Machado et al., 2015; Šraj et al., 2016; Silva et al., 2017). The detection of changes in the magnitude of flood quantiles is much more common for precipitation (e.g. Hanel

et al., 2009) or in flood projection studies (e.g. Prudhomme et al., 2003; Leander et al., 2008; Rojas et al., 2012; Alfieri et al., 2015).

To address this research gap, the aim of this study is to assess the changes in small vs. big flood events (corresponding to selected flood quantiles) across Europe over five decades (i.e. 1960-2010), and to determine whether these changes have been subject to different degrees of modification in time. Moreover, given that the impacts of different drivers of change on floods are expected to be strongly dependent on spatial scales (Blöschl et al., 2007; Hall et al., 2014), it is also of interest to assess the effect of catchment area, by comparing changes of flood quantiles for catchments of different sizes. Since the length of at-site flood records is often not sufficient to enable the reliable estimation of flood quantiles associated with high return periods (i.e. low probability of exceedance, e.g. the 100-year flood), in this study we adopt a (non-stationary) regional flood frequency approach, which pools flood data of multiple sites in order to increase the robustness of the estimated regional flood frequency curve and its changes over time. The methods and the flood database are described in detail in Sect. 2.2. The results are presented in Sect. 2.3, where we show the estimation of the flood quantiles and their trends in one example region (Sect. 2.3.1), the patterns of flood regime changes emerging from a spatial moving window analysis across Europe (Sect. 2.3.2) and the flood regime changes in three relevant macro-regions (Sect. 2.3.3).

2.2 Methods

2.2.1 Regional flood change model

In order to quantify the changes in time in flood quantiles corresponding to different return periods for catchments of different size, we propose a regional flood change model that is more robust than local (at-site) trend analysis, in particular regarding trends associated to large quantiles of the flood frequency curve. We assume annual maximum flood peak discharges to follow the Gumbel distribution (i.e. Extreme Value distribution type I), whose cumulative distribution is defined as:

$$F_X(x) = p = \exp\left(-\exp\left(-\frac{x-\xi}{\sigma}\right)\right) = \exp\left(-\exp\left(-y\right)\right),$$

where ξ and σ are the location and scale parameter and

$$y = \frac{x-\xi}{\sigma} = -\ln(-\ln p),$$

is the Gumbel reduced variate. The corresponding quantile function, i.e., the inverse of the cumulative distribution function, is:

$$q(p) = \xi - \sigma \ln\left(-\ln p\right) = \xi + \sigma y,$$

In this chapter we consider two alternative parameters which better relate to the literature on regional frequency analysis, especially to the Index-Flood method of Dalrymple (1960) and Hosking and Wallis (1997). The alternative parameters are: (1) the 2-year quantile or median q_2 (which corresponds to the index-flood), and (2) the 100-year growth factor x'_{100}, which gives the 100-year quantile as $q_{100} = q_2(1 + x'_{100})$ in a similar fashion to the modified quantiles in

Coles and Tawn (1996) and Renard et al. (2006b). The relationships linking these alternative parameters to the Gumbel location and scale parameters are:

$$q_2 = \xi + \sigma y_2$$
$$x'_{100} = \sigma(y_{100} - y_2)/(\xi + \sigma y_2)$$

where $y_2 = -\ln(-\ln(0.5))$ and $(y_{100} - y_2) = -\ln(-\ln(0.99)) + \ln(-\ln(0.5))$. The quantile function, with the alternative parametrisation, is here expressed as a function of the return period $T = 1/(1-p)$ as:

$$q_T = q_2 \left(1 + a_T x'_{100}\right), \tag{2.1}$$

where $a_T = (y_T - y_2)/(y_{100} - y_2)$ and $y_T = -\ln(-\ln(1 - 1/T))$. In particular, a_T=0 for T=2 and a_T=1 for T=100.

In the following we estimate the parameters of the Gumbel distribution both locally and regionally. For the local case, we allow the parameters to change with time according to the following log-linear relationships:

$$\begin{aligned} \ln q_2 &= \ln \alpha_{2_0} + \alpha_{2_1} \cdot t \\ \ln x'_{100} &= \ln \alpha_{g_0} + \alpha_{g_1} \cdot t \end{aligned} \tag{2.2}$$

For the regional case we introduce the scaling of q_2 and x'_{100} with catchment area S, according to the following relationships:

$$\begin{aligned} \ln q_2 &= \ln \alpha_{2_0} + \gamma_{2_0} \ln S + (\alpha_{2_1} + \gamma_{2_1} \ln S) \cdot t + \varepsilon \\ \ln x'_{100} &= \ln \alpha_{g_0} + \gamma_{g_0} \ln S + (\alpha_{g_1} + \gamma_{g_1} \ln S) \cdot t \\ \varepsilon &\sim \mathcal{N}(0, \sigma) \end{aligned} \tag{2.3}$$

where the α and γ terms are parameters to be estimated (the γ terms control the scaling with area) and the ε term accounts for the fact that additional local variability, on top of the one explained by time and catchment area, is affecting the index flood but not the growth curve. In our model, a homogeneous region is thus formed by sites whose growth curve depends on catchment area and time only, and whose index flood also depends on other factors which determine an additional noise (here assumed normal).

We investigate changes in flood quantiles associated with fixed annual exceedance probability $1-p$, or, equivalently, with fixed return period $T = 1/(1-p)$. The relative change in time of the generic flood quantile q_T is thus derived, for the local case, from Eq. 2.1 and Eq. 2.2:

$$\frac{1}{q_T}\frac{dq_T}{dt} = \alpha_{2_1} + \alpha_{g_1} - \frac{\alpha_{g_1}}{1 + a_T x'_{100}}, \tag{2.4}$$

and, for the regional case, from Eq. 2.1 and Eq. 2.3 :

$$\frac{1}{q_T}\frac{dq_T}{dt} = \alpha_{2_1} + \alpha_{g_1} + (\gamma_{2_1} + \gamma_{g_1}) \ln S - \frac{\alpha_{g_1} + \gamma_{g_1} \ln S}{1 + a_T x'_{100}}. \tag{2.5}$$

The model parameters, the quantiles and their local and regional relative trends are estimated by fitting the local and regional models to flood data with Bayesian inference through a Markov chain Monte Carlo (MCMC) approach. One of the advantages of the Bayesian MCMC approach is that the credible bounds of the distribution parameters (and other estimated quantities) can be directly obtained from their posterior distribution, without any additional assumption. The MCMC inference is performed using the R package *rStan* (Carpenter et al., 2017). It generates

samples with a Hamiltonian Monte Carlo algorithm, that uses the derivatives of the density function being sampled to generate efficient transitions spanning the posterior (Stan Development Team, 2018). For each inference, 4 chains, with 100 000 simulations each, are generated with different initial values of the parameters and checked for their convergence. An improper uniform prior distribution over the entire real line is set for the parameters, with the exception of α_{2_0} and α_{g_0} for which we use an improper uniform prior distribution over the entire positive real line. When fitting the regional model we make the assumption of regional homogeneity with regards to the distribution of flood peaks, allowing local variability of the median value and its changes in time.

Spatial cross-correlation between flood time series at different sites is not accounted for in this model (i.e. it assumes independence of flood time series in space), however, it is possible to quantify its effects in first approximation in a Bayesian framework through an approach based on a magnitude adjustment to the likelihood (Ribatet et al., 2012). This approach consists in scaling the likelihood with a proper constant exponent to be estimated between 0 and 1, that results in inflating the posterior variance of the parameters and consequent increase of the width of parameter uncertainty intervals, reflecting the overall effect of spatial dependence in the data (see Appendix B). In the case of spatial independence the magnitude adjustment factor is 1, whereas values of the magnitude adjustment factor close to 0 indicate strong inter-site correlation of floods and substantially larger sample uncertainties resulting from the adjusted model compared to the model where spatial cross-correlation is not accounted for. For further details about the method and its application to hydrological data, see Smith (1990), Ribatet et al. (2012) and Sharkey and Winter (2019). We apply this method to an example region in central Europe, in order to quantify the magnitude of the uncertainty underestimation associated with the model assumption of spatial independence in flood data.

2.2.2 European flood database

In this study, we analyse annual maximum discharge series from a newly available pan-European flood database, consisting of more than 7000 observational hydrometric stations and covering five decades (Hall et al., 2015). Their contributing catchment areas range from 5 to 100 000 km^2 and several nested catchments are included in the database.

For comparability with Blöschl et al. (2019), only the stations satisfying the following selection criteria, based on record length and even spatial distribution, are considered for the estimation of the regional trends. We select stations with at least 40 years of data in the period 1960-2010, with record starting in 1968 or earlier, and ending in 2002 or later. Additionally, in order to ensure a more even spatial distribution across Europe, in Austria, Germany and Switzerland (countries with highest density of stations in the database) the minimum record length accepted is 49 years; in Cyprus, Italy and Turkey 30 years are accepted, and in Spain 40 years without restrictions to the start and end of the record. Figure 2.1 shows the locations of the 2370 station satisfying the above selection criteria. The flood discharge data are accessible at `https://github.com/tuwhydro/europe_floods`.

2.2.3 Experimental design for the regional analyses

In this study, the regional flood change model of Sect. 2.2.1 is initially fitted to flood data of multiple sites that are pooled within spatial windows of size 600x600 km, with an overlapping length of 200 km in both directions. The size and overlapping length of the windows are chosen, after several preliminary tests, in order to ensure a sufficient number of gauges within each window and an appropriate spatial resolution at which to present the regional trends at the

continental scale. Significant differences in spatial change pattern are not observed when changing the window size (not shown). The rationale behind the homogeneity assumption is that the spatial windows, given their size, are characterized by comparatively homogeneous climatic conditions (and hence flood generation processes) and processes driving flood changes. Figure 2.1 shows the resulting 200x200 km grid cells. Each of the 600x600 km windows considered in this analysis is composed of 9 neighbouring cells as represented, for example, by the black rectangular region, whose regional trend estimates are shown in detail in Sect. 2.3.1. The example region is selected in central Europe because of the number of available gauges with different ranges of contributing catchment areas. In each window we estimate the regional relative trend in time of q_2 and q_{100}, as defined in Eq. 2.5, for small and big catchment sizes (i.e. assuming S=100 and 10 000 km^2 in the model). Note that this analysis intends to show the estimated flood trends in hypothetical catchments with a specific size, which may not be represented in the database or may not exist everywhere across Europe, based on fitting the model to existing catchments. The idea is here to compare between trends in small vs large catchments, therefore the trends are shown also for regions where they represent an extrapolation for the hypothetical catchment areas. We plot the resulting trends on a map by assigning their values to the respective central 200x200 km cell (e.g. the light red area in Fig. 2.1). The number of stations within each of the considered 600x600 km windows is shown in Fig. A.1 for several ranges of catchment size.

Figure 2.1 shows three macro-regions (numbers 1-3) located in northwestern Europe, southern Europe and eastern Europe, respectively. These regions were identified in Blöschl et al. (2019) by visual inspection of the flood trend and flood seasonality patterns and represent large homogeneous regions in terms of changes in the mean annual flood discharges. According to Köppen-Geiger climate classification (Köppen, 1884), northwestern Europe (region 1) corresponds approximately to the temperate oceanic climate zone, in southern Europe (regions 2) the hot and warm summer Mediterranean climate zones prevail, and eastern Europe (region3) is dominated by warm summer humid continental climate. Table 2.1 shows some related regional summary statistics. In this study, the same regions are analysed in terms of changes in flood quantiles, to allow a more detailed assessment of existing research and to allow for ready comparability of the results. The regional change model is consequently fitted to the pooled flood data of the sites within each of the three regions and trends in small and big floods for small to large catchments are analysed (Sect. 2.3.3).

In summary, the following regional analyses are carried out:

- In Sect. 2.3.1 regional flood regime changes in central Europe are investigated. As an example, the regional model is fitted to the black rectangular region of Fig. 2.1, which contains 601 hydrometric stations. For this example region, the regional model flood quantiles and their trends in time are shown as a function of catchment area and of return period (as defined in Eq. 2.1 and Eq. 2.5, respectively). The regional trends in q_2 and q_{100} are compared for five hypothetical catchment sizes (S=10, 100, 1000, 10 000 and 100 000 km^2) and local trend estimates (as in Eq. 2.4) are shown together with the regional trends. In this example region we also investigate the overall effect of spatial dependence in flood data on the width of the estimated credible bounds, with the approach based on the magnitude adjustment to the likelihood.

- In Sect. 2.3.2 regional flood regime changes across Europe are investigated. The regional model is fitted to overlapping windows across Europe, of size 600x600 km, and the regional trends in q_2 and q_{100} are estimated for small and big hypothetical catchments (S=100 and 10 000 km^2, respectively). Maps of the estimated trends are shown, where the trend values are plotted in the respective central 200x200 km cell of each region. Differences among the estimated trends across Europe are calculated for further comparison.

- In Sect. 2.3.3 regional flood regime changes are investigated in three macro-regions, i.e. (1) northwestern Europe, (2) southern Europe and (3) eastern Europe. The regional model is fitted to these regions and the regional trends in q_2 and q_{100} are estimated and compared for five hypothetical catchment sizes (S=10, 100, 1000, 10 000 and 100 000 km^2).

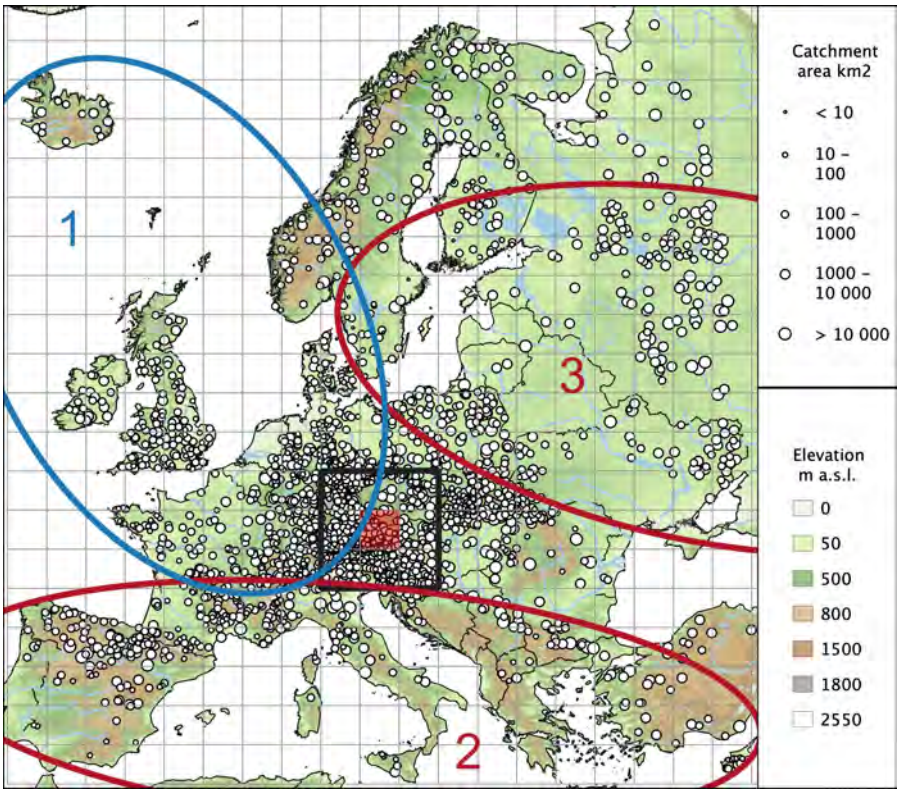

Fig. 2.1: Location of the selected 2370 hydrometric stations in Europe and regions considered in this study. The size of the circles is representative for the contributing catchment area. The size of the grid cells is 200x200 km. The black rectangle shows the size of the spatial moving windows analysed in Sect. 2.3.2. It consists of 9 cells, corresponding to 600x600 km. The three ellipses (numbers 1-3) mark homogeneous macro-regions, analysed in Sect. 2.3.3, and consist of (1) northwestern Europe, (2) southern Europe and (3) eastern Europe, respectively.

Region	No. of stations	Mean catchment area (km^2)	Mean outlet elevation (m a.s.l.)	Mean record length (years)
1. North-western Europe	895	1300.0	274.4	49.6
2. Southern Europe	458	2900.2	327.9	45.7
3. Eastern Europe	282	4959.4	101.5	49.7
Europe	2370	2472.3	286.0	48.8

Tab. 2.1: Regional summary statistics (number of stations, mean catchment area, mean outlet elevation, mean record length) of the flood database for the considered macro-regions (1-3 in Fig. 2.1) and for Europe.

2.3 Results

2.3.1 Regional flood regime changes in central Europe

In this section, we show a detailed example of the (local and) regional model estimates for the black rectangular 600x600 km window of Fig. 2.1, located in central Europe and containing 601 hydrometric stations. The annual maximum discharge series of these stations are shown in Fig. 2.2 (with thin lines and box-plots in panels a and b, respectively). In the same figure, the regional flood quantiles q_2 (panels a and b) and q_{100} (panel b), estimated with Eq. 2.1, are shown (thick lines and shaded areas) as a function of time for five selected catchment areas (S=10, 100, 1000, 10 000 and 100 000 km^2, indicated by different colours), in panel a, and as a function of catchment area for 1985 (i.e. the median year of the analyses period), in panel b. In both panels, the 90% credible bounds (shaded areas) are shown together with the median (thick lines) of the posterior distribution of the regional flood quantiles. In general, both q_2 and q_{100} (not shown) increase with time and their trend is larger for smaller catchment areas. The uncertainties in the quantile estimates also vary with catchment area: for very small (e.g. 10 km^2) and very large (e.g. 100 000 km^2) catchments the credible bounds get larger, reflecting the scarcity of samples with these (extremely small and extremely large) sizes in the considered region (see Fig. 2.2b).

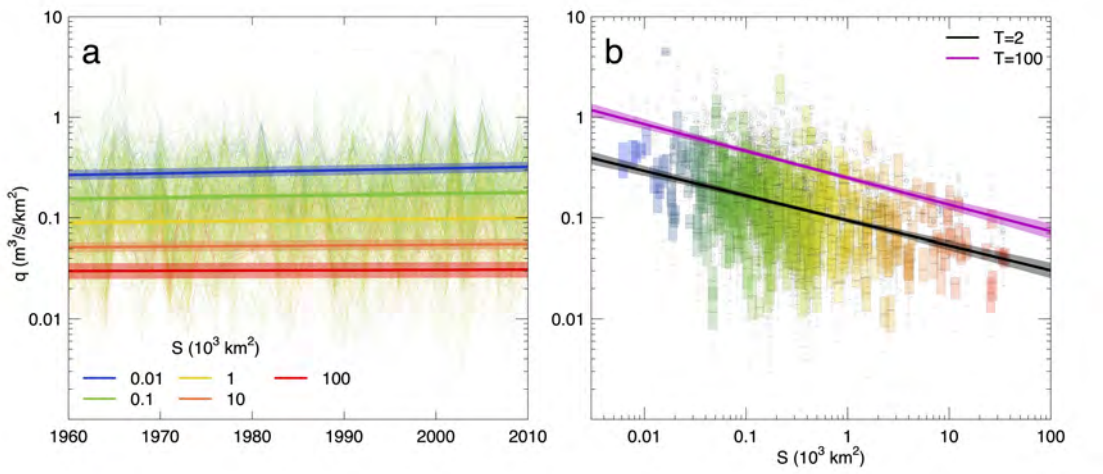

Fig. 2.2: Fitting the regional model to flood data of 601 hydrometric stations in central Europe. In panel a, annual maximum discharge series are shown with thin lines, with colours referring to catchment area. The thick lines and the shaded areas represent respectively the median and the 90% credible intervals of the posterior distribution of the 2-year flood, for five hypothetical catchment areas (S=10, 100, 1000, 10 000 and 100 000 km^2, indicated by different colours). In panel b, the box-plots represent flood data as a function of catchment area. The thick lines and the shaded areas represent respectively the median and the 90% credible intervals of the posterior distribution of flood quantiles, corresponding to return periods of 2 and 100 years. The curves are shown for 1985, i.e. the median year of the period analysed.

The two panels of Fig. 2.3 show the relative change in time, in % per decade, of the regional flood quantile estimates q_T (as defined in Eq. 2.5) as a function of catchment area and of the return period, respectively. The curves are shown for 1985, the median year of the analysed period. The trends in q_T are mostly positive and their values tend to decrease with increasing catchment area, approaching zero and moving towards negative values for higher return periods and for very large catchment areas (S=100 000 km^2). For small catchment areas (S<100 km^2) the trend tends to be bigger for floods with large return periods (q_{100}) than for small return periods (q_2). The opposite is observed for larger catchments. As in Fig. 2.2, we observe larger 90% credible bounds of the quantile estimates for very small and very large catchment areas. In this case, the overall effect of spatial cross-correlation between flood time series at different sites is investigated through the magnitude adjustment to the likelihood. The credible bounds for the regional trends obtained with the likelihood adjustment (dashed lines in Fig. 2.3) are 17.6 to 23.8% larger compared to the case where spatial cross-correlation is not accounted for (estimated magnitude adjustment factor 0.669).

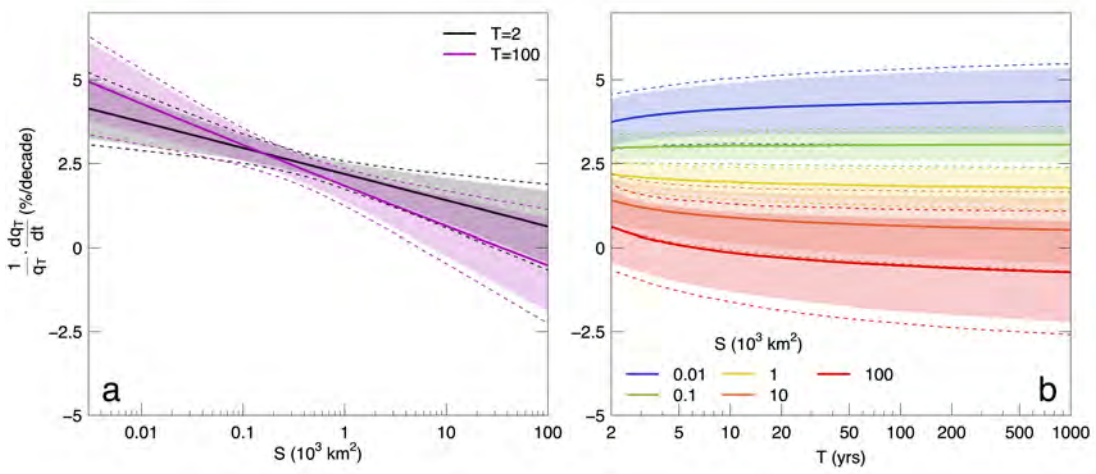

Fig. 2.3: Estimates of the regional relative trend of q_T in %/decade as a function of catchment area and return period in central Europe. The thick solid lines and the shaded areas represent respectively the median and the 90% credible intervals of the posterior distribution of the regional trends. Panel a shows the trend as a function of catchment area for selected values of the return period (T=2 and 100 years). Panel b shows the trend as a function of return period and for five hypothetical catchment areas (S=10, 100, 1000, 10 000 and 100 000 km^2). The curves are shown for the median year of the period analysed (i.e. 1985). The credible bounds obtained with the magnitude adjustment to the likelihood are shown with dashed lines.

Figure 2.4 summarizes the relative flood trends in the considered region for big (q_{100}) vs. small floods (q_2) and for small (10 km^2) to large catchment areas (100 000 km^2). Panel a shows a scatter plot (light transparent dots) of the local relative trends in q_{100} vs. q_2, as defined in Eq. 2.4, with the respective 90% credible intervals (error bars) for 1985. On top of the local trend estimates, the regional relative trends, calculated with Eq. 2.5, are plotted (dark solid dots). Again colours refer to catchment area for both the local and regional estimates. Regional flood trends are generally positive in the considered region (Fig. 2.4b), with the exception of big floods (T=100) in the hypothesized very large catchments (S=100 000 km^2). For both big and small events, the trend is generally larger in smaller catchments and it diminishes with increasing catchment area, approaching zero, for small floods (q_2), and moving towards negative values for big floods (q_{100}, according to the credible intervals, we cannot determine if its trend for big catchments is different from zero). The credible bounds obtained with the likelihood adjustment (dashed lines in Fig. 2.4b) result slightly wider (about 20%) compared to the case where spatial cross-correlation is not accounted for.

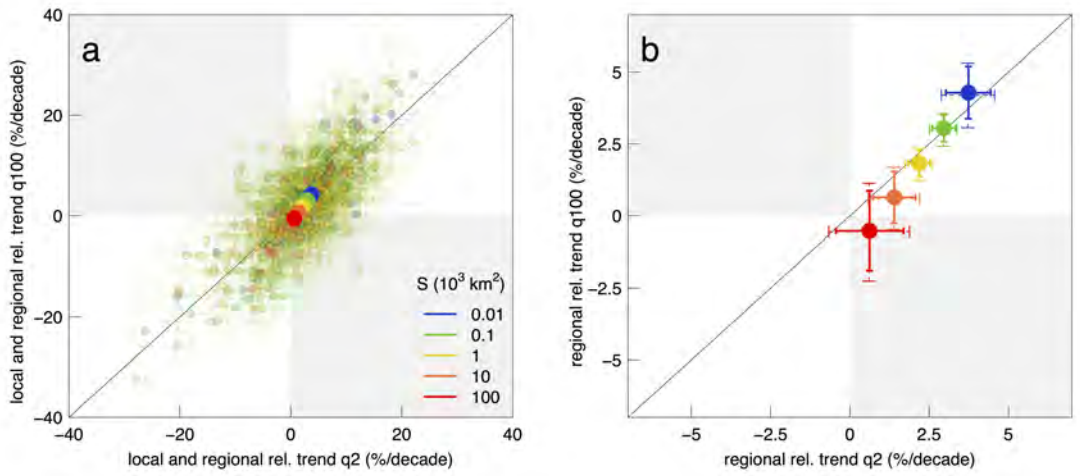

Fig. 2.4: Local and regional relative trend in %/decade in large (q_{100}) vs. small floods (q_2) in central Europe. Panel a shows the median of the posterior distribution of the local trends in q_{100} vs. q_2 (light transparent dots in the background), with the respective 90% credible intervals (error bars). On top of them, the estimated regional trends (dark solid dots) are shown. Panel b shows the median of the posterior distribution of the regional trends in q_{100} vs. q_2 (dark solid dots), with the respective 90% credible intervals (error bars with solid lines). Colours refer to catchment area in both panels and for both the local and regional estimates. The figure is obtained for 1985, i.e. the median year of the analyses period. The credible bounds obtained with the magnitude adjustment to the likelihood are shown with dashed lines.

2.3.2 Regional flood regime changes across Europe

Figure 2.5 shows the results of the regional trend analysis with moving windows across Europe. It is obtained by fitting the regional model to overlapping 600x600 km windows and by plotting the estimated trend values in the respective central 200x200 km cell. Panels a and b show the percentage change of the median flood (i.e. T=2 years) and panels c and d of the 100-year flood. Panels a and c refer to small (i.e. 100 km^2) catchment area and panels b and d to big catchment area (i.e. 10 000 km^2). The white circles represent a measure of the uncertainty in the estimation of the regional relative trend, with their dimension being proportional to the width of the respective 90% credible intervals. The larger the circle, the larger the uncertainty associated with the value of flood trend provided in the map.

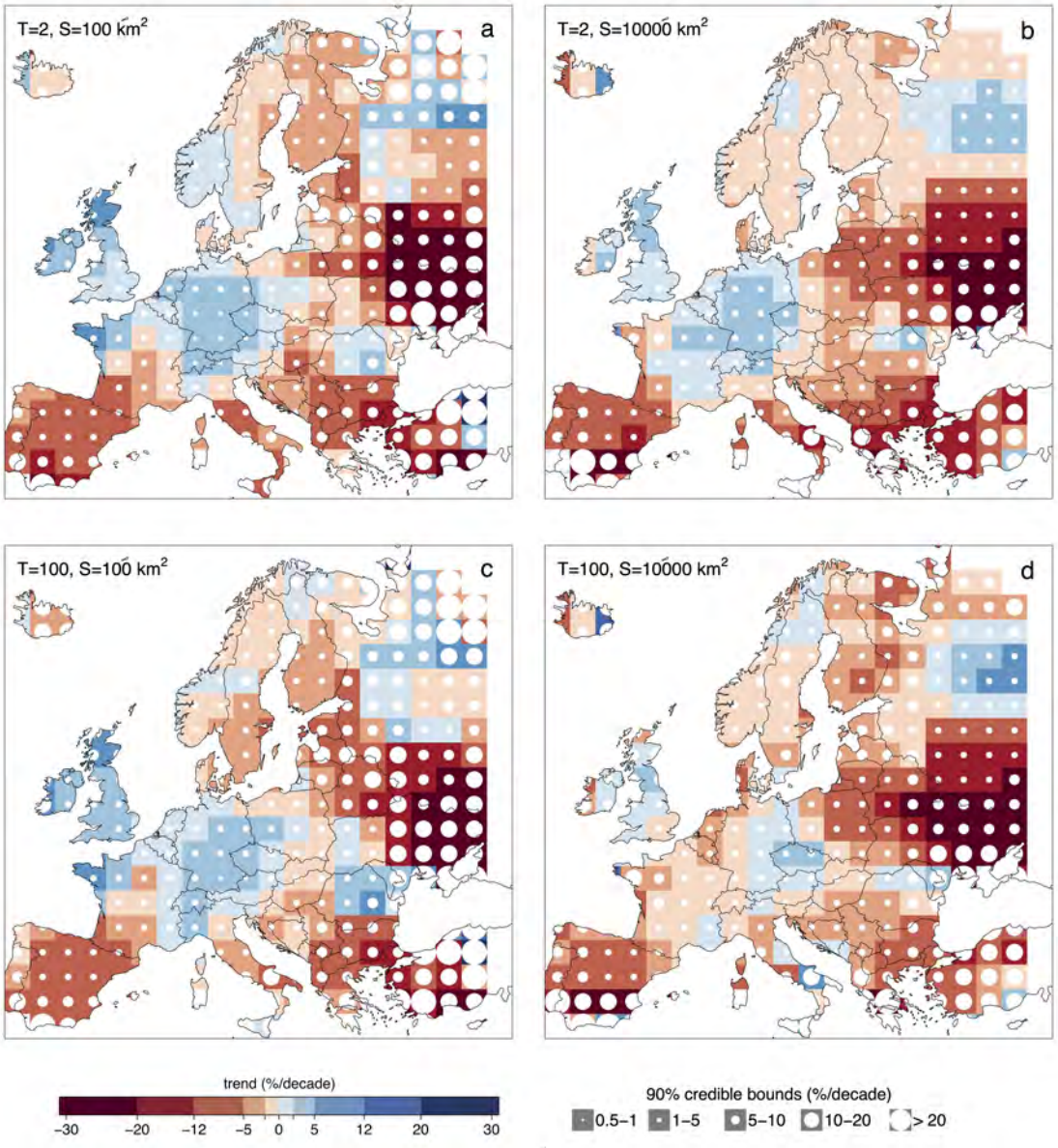

Fig. 2.5: Flood trends in Europe: small vs big floods. The panels show the median of the posterior distribution of the regional relative trends of flood quantiles in time (i.e. the percentage change in %/decade). Positive trends in the magnitude of flood quantiles are shown in blue and negative trends in red. Circle size is proportional to the width of the 90% credible intervals. Results are shown for the median flood (i.e. T=2 years), in panel a and b, and for the 100-year flood, in panel c and d. Flood trends refer to small (i.e. 100 km^2) in panel a and c and to large catchment area (i.e. 10 000 km^2) in panels b and d.

When analysing the panels of Fig. 2.5, regional patterns of flood change appear: flood magnitudes increase in general in the British-Irish Isles and in central Europe, whereas they decrease in the Iberian Peninsula, in the Balkans, in eastern Europe and in most of Scandinavian countries. The larger uncertainties associated with the regional trends are evident in eastern Europe, Turkey, Iceland and the countries surrounding the Mediterranean, where the density of the hydrometric stations in the flood database is low. In the British-Irish Isles, the positive

trends in small catchments (up to 10-12% per decade, Fig. 2.5a and c) appear to be larger for bigger return periods (Fig. 2.5c), whereas for larger catchments the trends are smaller in absolute value (up to 5% per decade) and, in some cases, they disappear or even tend to become negative. In central Europe, the magnitude of positive trends (2-5% per decade) tends to decrease for large catchments and large return periods where, in most cases, the regional trends are between 0 and 2% per decade (Fig. 2.5b and d). Positive flood trends are also observed in northern Russia, especially in large catchments (Fig. 2.5b and d). These positive trends are however accompanied by strong uncertainties in the case of small catchments (Fig. 2.5a and c). In the Iberian Peninsula, southwestern France, Italy and in the Balkans, negative trends appear and they are particularly consistent for the median floods (i.e. return period T=2 years), where the regional flood trends are mostly between -5 and -12% per decade (Fig. 2.5a and b). Trends in the magnitude of the big flood events (T=100 years) are less negative and some isolated positive trends do appear. The lower number of large catchments in this areas is generally reflected in larger uncertainties (Fig. 2.5b and d). In eastern Europe strong negative trends in flood peak magnitude are detected for small and big floods and small and large catchments. In eastern Europe, contrary to the Mediterranean countries, the dataset contains mostly big catchments, hence the uncertainties are larger for small catchments (Fig. 2.5a and c). In Scandinavia the regional trends are, in general, neither clearly positive nor negative, with spatial patterns changing with return period and catchment area. However, in Finland negative trends are prevalent (mostly between -5 and -12% per decade) and they become less negative (0-5% per decade) for big catchments and small return periods (Fig. 2.5b). Overall, in more than half of the cases the 90% credible bounds do not include 0 (i.e. 68.9%, 59.2%, 58.5% and 50.2% respectively in panel a, b, c and d). Positive (negative) trends occur in 26.3 to 34.95% (65 to 76%) of the cases and their credible bounds do not include zero in 4.9 to 20.8% (39.5 to 48.1%) of the total cells. These percentages depend on the assumptions made, such as regional homogeneity and no spatial cross-correlation, and may, therefore, be overestimated.

For further comparison, we estimate the differences between the regional relative trends in the panels of Fig. 2.5. In particular, Fig. 2.6a and 2.6b show the difference between the trend in q_{100} and the trend in q_2, for a hypothetically big (i.e. 10 000 km^2) and small catchment areas (i.e. 100 km^2) respectively. Figure 2.6c and 2.6d show the difference between the trend in large and the trend in small catchments, for small (T=2 years) and big (T=100 years) return periods respectively. Positive differences are shown in blue and negative ones in red. The circle size is proportional to the width of their 90% credible intervals.

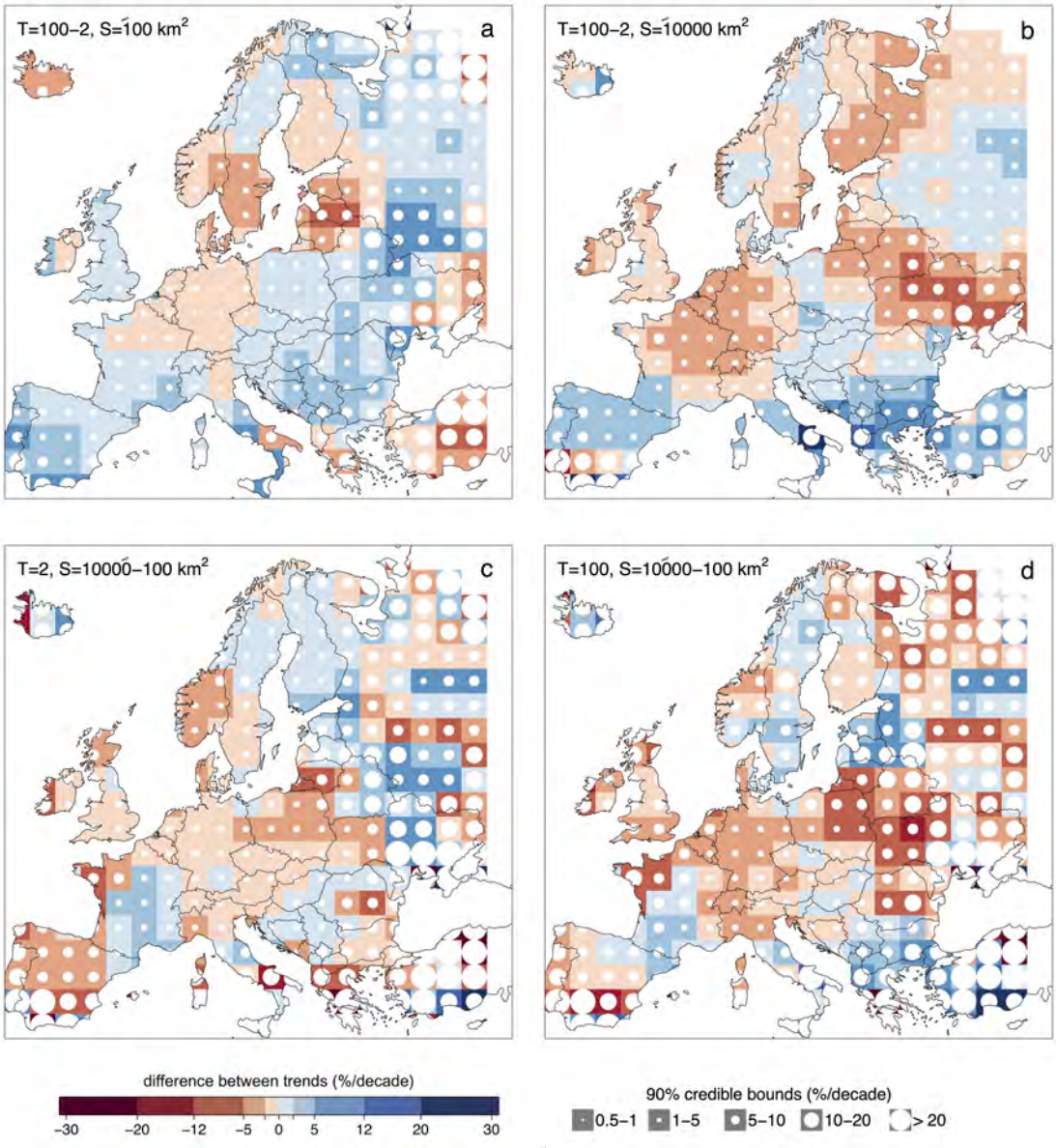

Fig. 2.6: Differences between flood trends of big vs small floods (i.e. T=100 and 2 years, respectively) and in large vs small catchments (i.e. S=10 000 and 100 km^2, respectively). The panels show the differences (in % per decade) between the trends of Fig. 2.5. Positive differences are shown in blue and negative in red. Circle size is proportional to the width of the 90% credible intervals. The panels in the first row show the difference between the trend in q_{100} and the trend in q_2 for small (a) and big catchment area (b). The panels in the second row show the difference between the trend in large and the trend in small catchments for small (c) and big (d) return periods.

In small catchments (Fig. 2.6a) positive differences between the trend in q_{100} and in q_2 prevail in the British-Irish Isles, the Iberian Peninsula and southern France, the Balkans, eastern Europe and northern Russia. This indicates that, in the small catchments of these regions, the trend of the extreme flooding events is more positive (or less negative) than the median flood. Negative differences appear in central Europe, Baltic countries, southern Scandinavia and Turkey. The magnitude of this difference varies in a narrow range (-2 to +2% per decade) in most parts of

Europe and it gets larger (up to -12 to +12% per decade) in several regions in southern and eastern Europe.

In the case of big catchments (Fig. 2.6b), negative differences between the trend in q_{100} and in q_2 are more widespread across Europe, compared to those in smaller catchments. In the British-Irish Isles, southern France, northwestern Italy, eastern Europe and northern Russia the difference becomes in fact negative. This suggests that, in the big catchments of these regions, the trend of the extreme flooding events is less positive (or more negative) than the median flood. Positive values of this difference appear mostly in southern Europe and Russia. The magnitude of these differences, in the case of big catchments, varies in a wider range (generally from -5 to +5% per decade) with larger differences in few regions in southern and eastern Europe.

The patterns appear more fragmented when analysing the differences between trends in catchments with big and small catchment areas (Fig. 2.6c and d) and their magnitude is generally larger (mostly from -12 to +12 % per decade). Negative differences between trends in large and trends in small catchments prevail in western and central Europe (with the exception of France), for both the median and the 100-year flood, and they extend towards eastern countries, in the case of the 100-year flood (Fig. 2.6d). This indicates that trends in large catchments are more negative (or less positive) than those in small catchments. Positive differences appear in central and southern France, in the Balkans, Baltic countries and northern Russia, for both T=2 and 100 years (Fig. 2.6c and d), and in Finland and eastern Europe, for T=100 years (Fig. 2.6d).

2.3.3 Regional flood regime changes in northwestern, southern and and eastern Europe

The regional trends shown in Sect. 2.3.2 highlight the presence of predominantly positive trends in northwestern Europe and negative trends in southern and eastern Europe. In this section we fit the regional model of Sect. 2.2.1 by pooling flood data over each of these three regions and we estimate the regional relative trends for five hypothetical catchment areas (S=10, 100, 1000, 10 000 and 100 000 km^2) and for two selected values of return period (T=2 and 100 years). The resulting trends are shown together with their 90% credible intervals in Fig. 2.7.

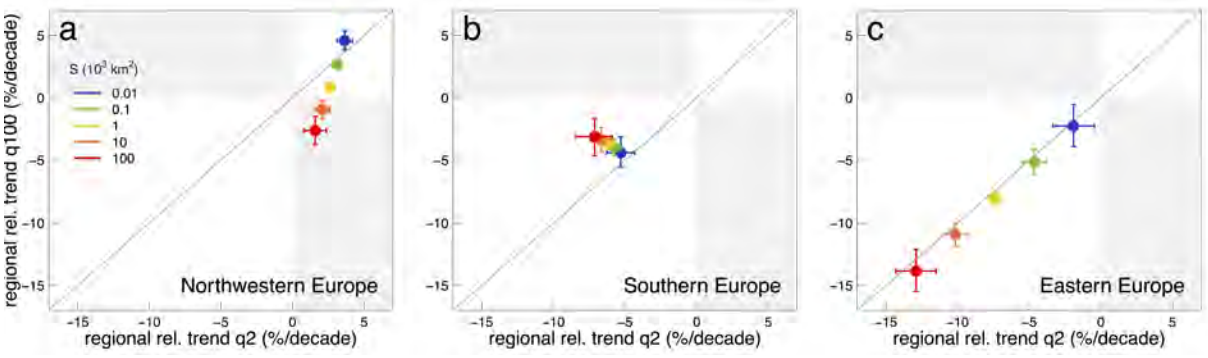

Fig. 2.7: Regional relative trend in large (q_{100}) vs. small floods (q_2) in (a) northwestern Europe, (b) southern Europe and (c) eastern Europe for five hypothetical catchment areas (S). The figure shows the median (solid dots) and the 90% credible intervals (error bars) of the posterior distribution of the regional trends. Catchment area is shown with different colours. The figure is obtained for 1985, i.e. the median year of the period analysed.

In northwestern Europe (Fig. 2.7a) the trends in flood magnitudes are predominantly positive, with the exception of very large catchments for the 100-year flood. The magnitude of the

positive trend tends to decrease with increasing catchment area for the 2-year flood, whereas for the 100-year flood the positive trend decreases, it goes to zero for catchment sizes of about 10 000 km^2, and then becomes negative and increases in absolute value for increasing catchment area. Generally, trends are bigger for the 2-year flood compared to the 100-year flood, with the exception of very small catchments (S=10 km^2). Overall there is large variability of the trend in q_{100}, which ranges from about -2.5 to 5% per decade with catchment area, while the trend in q_2 is around 2-3% per decade for all areas considered.

In southern Europe the trends are negative in all the considered cases and larger in absolute value for the 2-year flood. This means that the more frequent flood events tend to decrease more than the rare, more extreme events. However, there is small variability of the trends (especially in q_{100}) with catchment size. In the smaller catchments the regional relative trends in q_2 and q_{100} are both about -5% per decade. As catchment area increases, the trend in q_2 decreases from -5.2 to -7.1% per decade, while the trend in q_{100} increases from -4.4 to -3.1% per decade.

In eastern Europe the regional relative trends are all negative. The estimates lay close to the 1:1 line, which means that the trends are similar for big and small events and that there is little variability with the return period. Catchment area seems to play a more important role in determining flood trends, as the magnitude of the negative trend appears to be very sensitive to the catchment size and ranges from about -13.8% per decade for the big catchments, to -1.9% per decade for smaller ones.

In all regions analysed, it is also evident that the uncertainties in the trend estimates vary with catchment area: the credible bounds are narrower for mid-sized catchments that are represented by more hydrometric stations in the database.

2.4 Discussion and conclusions

In this study we assess and compare the changes that have occurred over five decades (i.e. 1960-2010) in small vs. big flood events, for catchments of different hypothetical sizes across Europe. We propose a regional flood change model that is more robust than local (at-site) trend analysis, in particular regarding trends associated with large quantiles of the flood frequency curve (e.g. the 100-year flood). Flood peaks are assumed to follow a regional Gumbel distribution, accounting for time dependency of two parameters alternative to the location and scale parameters: the 2-year flood q_2 and the 100-year flood growth factor x'_{100}. The two parameters are modelled as varying in time according to log-linear relationships. Other relationships with time could be investigated as well as the use of physical covariates potentially driving flood trends, which will be analysed and discussed in Chapter 3 and Chapter 4. In flood frequency analysis, the Generalized Extreme Value distribution (GEV) is commonly used to estimate flood quantiles. The suitability of the GEV distribution in the European context is discussed in detail in Salinas et al. (2014b) and Salinas et al. (2014a). The estimate of the shape parameter of the GEV distribution is extremely sensitive to record length (Papalexiou and Koutsoyiannis, 2013), with strong bias and uncertainty for short records (Martins and Stedinger, 2000) and, when corrected for the effect of record length, it varies in a narrow range (Papalexiou and Koutsoyiannis, 2013). For these reasons, in regional frequency analyses the GEV shape parameter is commonly assumed to be identical for all sites within a region (see e.g. Renard et al., 2006a; Lima et al., 2016). Here, we fix the shape parameter equal to 0 (i.e. we assume a Gumbel distribution) which leads to more robust relationships, without compromising the general validity of the study (i.e. the analysis can be repeated with a more complex GEV distribution if longer flood records are available). A Bayesian Markov chain Monte Carlo (MCMC) approach is used for parameter estimation, allowing to directly obtain information about their associated uncertainties.

Spatial cross-correlation between flood time series at different sites is not accounted for in this model and may affect the estimation of sampling uncertainty (see e.g. Stedinger, 1983; Castellarin et al., 2008; Sun et al., 2014). Because of this, the sampling uncertainties estimated in this chapter should be considered as a lower boundary. We expect that the effect of spatial correlation on the identified spatial patterns is negligible, since the cross-correlation length is about 50 km (calculated from flood time series and distances between catchment outlets, using a nonlinear regression model proposed by Tasker and Stedinger (1989)), which is much shorter than the size of the spatial patterns. A possible way of taking into account spatial cross-correlation between sites is a magnitude adjustment to the likelihood, that reflects the overall effect of spatial dependence and results in increased width of uncertainty intervals of the estimated quantiles (see Ribatet et al., 2012). The application of this approach to the specific example region in central Europe shows that the 90% credible bounds of the regional trends in q_2 and q_{100} result, on average, 20% wider compared to the case where the likelihood is not adjusted. However, further research is needed to properly characterize the effect of spatial dependence between flood peaks in regional trend analyses.

We analyse 2370 flood records, selected from a newly-available pan-European flood database (Hall et al., 2015). We estimate regional trends (and the related uncertainties) in the magnitude of floods of selected return periods (T=2 and 100 years) and for selected catchment areas (S=10 to 100 000 km^2), by fitting the proposed regional flood change model to flood data pooled within defined regions. The trend patterns are investigated at the continental scale, by fitting the model to 600x600 km^2 overlapping windows, with a spatial moving window approach. Flood trends are then analysed in three macro-regions (i.e. northwestern, southern and eastern Europe), based on previously published change patterns of the mean annual flood magnitude and seasonality. When fitting the model to these regions, we allow for local spatial variations in the median, but assume homogeneity with regards to the growth curves of flood peaks to changes in time and the dependency of the trends on catchment area and on the return period. The assumption is that these regions are characterized by comparatively homogeneous climatic conditions (and hence flood generation processes) and processes driving flood changes. We have not assessed the statistical homogeneity of the regions in terms of the flood change model used here. One reason is that formal procedures to assess the regional homogeneity, such as for example those used in regional flood frequency analysis (e.g. Hosking and Wallis, 1993; Viglione et al., 2007), are not available at the moment. Also, while deviation from regional homogeneity would probably invalidate estimates of local flood change statistics from the regional information (e.g., as in the prediction in ungauged basins, see Blöschl et al., 2013b), we expect its effect on the average regional behavior to be less relevant. This is because we have not observed significant differences in the spatial change pattern when changing the size of the moving windows (not shown here). As a limiting case, the results obtained using the three macro-regions (Sect. 2.3.3) are consistent with those obtained by the moving window analysis across Europe (Sect. 2.3.2).

The results of this study show that the trends in flood magnitude are generally positive in northwestern Europe, where floods occur predominantly in winter (Mediero et al., 2015; Blöschl et al., 2017; Hall and Blöschl, 2018). The increasing winter runoff in UK is typically explained in the literature by increasing winter precipitation and soil moisture (Wilby et al., 2008). Recent studies show that extreme winter precipitation and flooding events in northwestern Europe are positively correlated with the North Atlantic Oscillation (NAO) and the East Atlantic (EA) pattern (Hannaford and Marsh, 2008; Steirou et al., 2019; Zanardo et al., 2019; Brady et al., 2019). Furthermore the largest winter floods in Britain occur simultaneously with Atmospheric Rivers (AR) (Lavers et al., 2011), which are expected to become more frequent in a warmer climate (Lavers and Villarini, 2013). When comparing trends in flood events associated with different return periods, we observe two opposite behaviours depending on catchment area. In

small catchments (up to 100 km^2) the 100-year flood increases more than the median flood, while the opposite is observed in medium and large catchments, where even some negative trends appear, especially in northwestern France. Furthermore, in medium and large catchments the magnitude of the trends is in general smaller compared to the small catchments. This could be explained by different types of weather events and their changes affecting the flood trends in catchments of different sizes in different ways, for example, long-duration synoptic weather events are probably more influential in producing floods in medium and large catchments, in contrast to small catchments in western Europe where the largest peaks are often caused by summer convective events with high local intensities (Wilby et al., 2008), which are expected to increase in a warmer climate (IPCC, 2013).

In southern Europe flood trends are negative, possibly due to decreasing precipitation and soil moisture, caused by increasing evapotranspiration and temperature (Mediero et al., 2014; Blöschl et al., 2019). The big flood events (i.e. T=100 years) decrease less in time compared to more frequent events (i.e. T=2 years), leading to higher flood variability and steeper flood frequency curves. The reason for this may be (decreasing) soil moisture driving flood changes in southern Europe, causing direr catchments and consequent negative trends in flood magnitudes, that are particularly strong for small floods (q_2), where the influence of soil moisture is stronger (as shown for e.g. by Grillakis et al., 2016). The magnitude of big flood events is also decreasing (probably, as an effect of decreasing precipitation) but in this case soil moisture is less influential, resulting in less strong negative trends compared to q_2. The flood trends do not vary significantly with catchment area. In smaller catchments we observe similar negative trends in q_2 and q_{100} (about 5%/decade). With increasing catchment area the trends in q_2 become more negative, while the opposite is observed for q_{100}. Notice, however, that the small catchments analysed in southern Europe have sizes of the order of 10 km^2 and are, therefore, larger than catchments where flash floods are the dominant flood type and infiltration excess runoff is the main generation mechanism (Amponsah et al., 2018). For these very small catchments ($<$ 10 km^2), floods may become larger due to more frequent thunderstorms (Ban et al., 2015) and land management changes, e.g. deforestation and urbanisation (Rogger et al., 2017).

In eastern Europe trends in flood peak magnitude are strongly negative for both small and big floods, and small to large catchments. These negative flood trends have been linked in past studies with increasing spring air temperature, earlier snow-melt and reduced spring snow-cover extents (Estilow et al., 2015), producing increased infiltration and consequent earlier and decreasing spring floods (Madsen et al., 2014; Blöschl et al., 2017; Blöschl et al., 2019). The resulting trends in eastern Europe do not seem to depend on the return period (i.e. for a given catchment area, the trend in q_2 and the trend in q_{100} are almost identical), whereas catchment area plays a substantial role: the larger the catchment area, the more negative the trend. These results suggest that, in these region, snow-melt affects flood events of different magnitude in the same way and it represents a relevant processes for flood (trend) generation especially in large catchments. The explanation for the importance of these processes in large catchments could be found in the characteristics of snow-melt flooding, which originates from large-scale gradual processes, i.e. snowfall and temperature changes, that may be more influential for large scale events, compared to smaller-scale catchments, where other local conditions may prevail.

The uncertainty associated with the regional trend estimates is here assessed through their 90 % credible bounds. The results show that the uncertainties in the trend estimates varies with catchment area: the credible bounds are generally narrower for mid-sized catchments, that are represented by more samples in the database, and the bounds become wider for very small and very large values of catchment area, where less samples are available. Spatial patterns in trend uncertainties are also observed. As expected, the uncertainty is lower in the regions where the density of stations is very high (i.e. central Europe and UK), while the estimated trend

is very uncertain in the data-scarce regions (i.e. southern and eastern Europe). Overall the obtained uncertainties associated with the trends in q_{100} do not seem to increase much compared to q_2, while a relevant increase would be reasonably expected. These results are valid under the assumption of the adopted model (i.e. Gumbel distribution and homogeneous regions) which may be too stringent. The model assumptions could be relaxed (e.g. adopting a Generalized Extreme Value distribution) in order to allow for larger model flexibility.

This study provides a continental-scale analysis of the changes in flood quantiles that have occurred across Europe over five decades, however further research is needed to formally attribute the resulting regional change patterns to potential driving processes. According to flood hazard projections, the past flood regime changes found in this study, are likely to further occur in the next decades, led by increasing precipitation over northwestern Europe, decreasing precipitation over southern Europe and increasing temperature in eastern Europe (see e.g. Alfieri et al., 2015; Kundzewicz et al., 2017; Thober et al., 2018). This has relevant implications since flood risk management has to adapt to these new realities.

Chapter 3

Informed attribution of flood changes to decadal variation of atmospheric, catchment and river drivers in Upper Austria

The present chapter corresponds to the following scientific publication in its original form:

Bertola M., Viglione A., and Blöschl G. (2019). "Informed attribution of flood changes to decadal variation of atmospheric, catchment and river drivers in Upper Austria". Journal of Hydrology, 577(November 2018), p. 123919. doi: 10.1016/j.jhydrol.2019.123919.

Abstract

Flood changes may be attributed to drivers of change that belong to three main classes: atmospheric, catchment and river system drivers. In this work, we propose a data-based attribution approach for selecting which driver best relates to variations in time of the flood frequency curve. The flood peaks are assumed to follow a Gumbel distribution, whose location parameter changes in time as a function of the decadal variations of one of the following alternative covariates: annual and extreme precipitation for different durations, an agricultural land-use intensification index, and reservoir construction in the catchment, quantified by an index. The parameters of this attribution model are estimated by Bayesian inference. Prior information on one of these parameters, the elasticity of flood peaks to the respective driver, is taken from the existing literature to increase the robustness of the method to spurious correlations between flood and covariate time series. Therefore, the attribution model is informed in two ways: by the use of covariates, representing the drivers of change, and by the priors, representing the hydrological understanding of how these covariates influence floods. The Watanabe-Akaike information criterion is used to compare models involving alternative covariates. We apply the approach to 96 catchments in Upper Austria, where positive flood peak trends have been observed in the past 50 years. Results show that, in Upper Austria, one or seven day extreme precipitation is usually a better covariate for variations of the flood frequency curve than precipitation at longer time scales. Agricultural land-use intensification rarely is the best covariate, and the reservoir index never is, suggesting that catchment and river drivers are less important than atmospheric ones. Not all the positive flood trends correspond to a significant correlation between floods and the covariates, suggesting that other drivers or other flood-driver relations should be considered to attribute flood trends in Upper Austria.

3.1 Introduction

In recent years, a large number of major floods occurred, triggering many studies to focus on flood trend detection at local and regional scale (see e.g. Mudelsee et al., 2003; Petrow and Merz,

2009; Blöschl et al., 2017; Mangini et al., 2018, for an European overview). Despite trends in flood regime are detected in numerous studies, the identification of their driving processes and causal mechanisms is still far from being properly addressed (Merz et al., 2012). Understanding the reasons why the detected flood changes occurred (i.e. flood change attribution) is a complex task, since different processes, influencing flood magnitude, frequency and timing, can act in parallel and interact in different ways across spatial and temporal scales (Blöschl et al., 2007). According to Pinter et al. (2006), Merz et al. (2012) and Hall et al. (2014), potential drivers of flood regime change belong to three groups: atmospheric, catchment and river system drivers.

The Atmospheric driver includes the meteorological forcing of the system (e.g. total precipitation, precipitation intensity/duration, temperature, snow cover/melt and radiation) whose changes can be related to both natural climate variability and anthropogenic climate change. They usually occur at large spatial scales, affecting flood regime consistently within a region, with gradual changes in time of the mean or the variance of peak discharges (Mudelsee et al., 2003; Blöschl et al., 2007; Petrow and Merz, 2009; Renard and Lall, 2014).

The Catchment driver includes runoff generation and concentration processes, which are quantified, for instance, by the infiltration capacity or the runoff coefficient. They are susceptible to land-cover and land-use changes (e.g. urbanization, deforestation, change in agricultural practices) and are likely to occur gradually in time, usually with diminishing effects with increasing catchment area (Blöschl et al., 2007; O'Connell et al., 2007; Rogger et al., 2017; Alaoui et al., 2018).

The River System driver includes flood wave propagation processes into the river network. River training and hydraulic structures produce modifications of river morphology, roughness, water levels, discharge and inundated area, resulting typically in step changes in the time series of flood discharge peaks. Usually, these changes occur in proximity (e.g. flood flow acceleration and channel incision) or downstream (e.g. loss of floodplain storage) of the river modification, e.g. downstream of reservoirs or downstream urban areas, where structural flood protection measures are developed (Graf, 2006; Pinter et al., 2006; Volpi et al., 2018).

In the past, as pointed out by Merz et al. (2012), the attribution of flood changes has been mainly done through qualitative reasoning, suggesting relationships with changes in climate variables (e.g. precipitation or circulation patterns) or anthropogenic impacts (e.g. river training, dam construction or land-use change), and citing literature to support these hypotheses. Recently, however, in several studies the detected flood changes are quantitatively related to one or, more rarely, to more than one of the potential drivers. This has been done essentially in two different ways: the data-based and the simulation-based approach.

The data-based approach consists in identifying the relationship between drivers and floods from data only, in a statistical way. For example, studies exist that analyze the correlation and geographic cohesion between flood characteristics and large-scale climate indices (Archfield et al., 2016) or the long-range dependencies of precipitation and discharge (Szolgayova et al., 2014) and their spatial and temporal co-evolution (Perdigão and Blöschl, 2014). Many studies use the so called "non-stationary flood frequency analysis" to improve the reliability of flood quantile estimation by relating the parameters of flood frequency distributions to covariates, such as large-scale climate indices or large-scale atmospheric or oceanic fields (i.e. climate-informed frequency analysis, see e.g. Renard and Lall, 2014; Steirou et al., 2019), extreme precipitation (Villarini et al., 2009; Prosdocimi et al., 2014), annual precipitation (Šraj et al., 2016), reservoir indices (López and Francés, 2013; Silva et al., 2017), population measures (Villarini et al., 2009), etc. The advantage of the data-based approach, when compared to other methods, is that, due to its relative simplicity, it is easily applicable to many sites, at the regional or even continental scale. Its drawback is that it identifies correlations between covariates and flood dynamics,

usually without investigating whether the magnitude of these correlations are consistent with what process understanding would suggest.

Cause-effect mechanisms are instead included in the simulation-based approach, which consists in reproducing the observed flood changes by introducing, in hydrological models, changes in the potential driver(s) and observing the effects on the simulated hydrograph characteristics (Merz et al., 2012). Several simulation-based studies analyze the effects of extensive river training on flood regime (Lammersen et al., 2002; Vorogushyn and Merz, 2013; Skublics et al., 2016, see e.g.). The effect of land-use changes (e.g. forestry management, agricultural practices and urbanization) on discharge is often investigated, in simulation-based studies, for specific catchments and flood events, under different land-management scenarios (see e.g. Niehoff et al., 2002; Bronstert et al., 2007; O'Connell et al., 2007; Salazar et al., 2012). The advantage of the simulation-based approach is that process understanding is explicitly taken into account. However, due to the complexity of the models, simulation-based methods are usually applied to single (or few) catchments at a time.

Clearly, it would be of interest to make use of the advantages of both approaches, when performing attribution studies. Viglione et al. (2016), propose a framework for attribution of flood changes, based on a regional analysis, that make use of process understanding in a data-based analysis. They exploit information, obtained through rainfall-runoff modelling, on how different drivers should affect floods for catchments of different size. The estimation of the relative contribution of the drivers is framed in Bayesian terms and the process-based information is quantified by prior knowledge about the scaling parameters of the regional model.

In this chapter we also make use of knowledge accumulated in previous studies relating floods to dominant drivers, when performing attribution. We use the same study region of Viglione et al. (2016), where positive trends in flood peak series are observed, but differently from them, who focus on attribution at the regional level, we are interested in the attribution at the local (site-specific) scale. We apply the non-stationary flood frequency method, here called "driver-informed" flood frequency method (consistently with Steirou et al., 2019), to 96 sites in Upper Austria, using local (rather than regional) covariates on atmospheric, catchment and river system drivers. Differently from Viglione et al. (2016), we allow the drivers to act in opposite directions when contributing to positive flood peak changes. We use Bayesian inference for parameter estimation, with prior information on the connection between covariates and flood peaks taken from previous studies, both data-based and simulation-based ones. The attribution is performed by comparing alternative models (with alternative covariates) using an information criterion that quantifies how well the flood frequency model fits the flood data (accounting for prior information) and penalize models that are too complex given the information available. The attribution model is therefore informed in two ways: by the use of covariates, representing the drivers of change, and by the priors, representing the hydrological understanding of how these covariates influence floods.

Section 3.2 describes the driver-informed flood frequency model and the way attribution is performed. Section 3.3 describes the data used, including how information from the literature is translated into prior knowledge on the model parameters. Section 3.4 reports the results of the analysis, investigating the sensitivity of the attribution results to different time-scales of the atmospheric driver and the dependency of the driver effects on the catchment area (as hypothesized by Hall et al., 2014; Viglione et al., 2016).

3.2 Methods

3.2.1 Flood Frequency analysis and alternative driver-informed models

For simplicity, we assume the maximum annual peak discharges to follow a two-parameter Gumbel distribution. Visual inspection of the data in Gumbel probability diagrams shows consistency with this assumption for most of the sites (note that the following procedure can be applied using more flexible distributions, i.e. with more parameters, without loss of generality). The Gumbel cumulative distribution function is defined as:

$$G(z) = \exp\left\{ -\exp\left\{ \frac{z-\mu}{\sigma} \right\} \right\} \tag{3.1}$$

where μ and σ are respectively the location and scale parameter of the distribution. These parameters are usually assumed invariant in time.

In recent studies, climate variables have been used as covariates for the extreme value distribution parameters, which are therefore not constant in time. This approach is usually called "non-stationary" even if the resulting distribution can be considered non-stationary only if the covariates exhibit a deterministic change in time (Montanari and Koutsoyiannis, 2014; Serinaldi and Kilsby, 2015).

We use local covariates of the extreme value distribution parameters, representative for the three drivers of flood change (i.e. the atmospheric, catchment and river system processes) in the study region, and, similarly to the climate-informed statistics of Steirou et al. (2019), we refer to this as driver-informed distribution/parameters.

The following models are considered:

$$G_0) \qquad \mu = \mu_0, \qquad \sigma = \sigma_0 \tag{3.2}$$

$$G_1) \qquad \log(\mu) = a + b\log(X), \qquad \sigma = \sigma_0 \tag{3.3}$$

$$G_2) \qquad \log(\mu) = a + bX, \qquad \sigma = \sigma_0 \tag{3.4}$$

where X is a general covariate (e.g. one of the drivers) and a and b are regression parameters to be estimated locally. The location parameter μ only is conditioned on the external covariate, with two different dependence structures in model G_1 and G_2. Practically speaking, they introduce one additional parameter to be estimated, compared to the time-invariant Gumbel distribution G_0. The parameters are estimated by fitting the alternative models to flood data with Bayesian inference through a Markov Chain Monte Carlo approach. The R package *rStan* (Carpenter et al., 2017) is used to perform the MCMC inference. rStan makes use of Hamiltonian Monte Carlo sampling, which speeds up convergence and parameter exploration by using the gradient of the log posterior (Stan Development Team, 2018). For each inference, we generate 4 chains of length $N_{sim} = 10000$, each starting from different parameter values, and check for their convergence.

One advantage of the Bayesian framework is the possibility to take into account additional prior belief (e.g. expert knowledge) or external a priori information about the parameters in their estimation. Herein, we set informative priors on the parameter b, based on the results of published studies (see Section 3.4), in order to limit the possibility for spurious correlations to bias the attribution. In model $G1$ the parameter b is defined as:

$$b = \frac{X}{\mu} \cdot \frac{d\mu}{dX} \tag{3.5}$$

and represents the percentage change of the location parameter of the distribution of annual maxima, following a 1% change in the covariate X. In other words, the parameter b represents

the elasticity of (the location parameter of) flood peaks with respect to the covariate, similarly to the temporal sensitivity coefficient of flood to precipitation defined in Perdigão and Blöschl (2014). In model $G2$ instead, the parameter b is defined as:

$$b = \frac{1}{\mu} \cdot \frac{d\mu}{dX} \tag{3.6}$$

It represents the relative change occurring in the location parameter of the distribution of annual maxima, following a unit change in the covariate.

3.2.2 Model selection and flood change attribution

The Widely Applicable or Watanabe-Akaike Information Criterion (WAIC) is used in this study for model comparison and selection. Its measure represents a trade-off between goodness of fit and model complexity. The WAIC, originally proposed by Watanabe (2010), is one of the Bayesian alternatives of the Akaike Information Criterion (AIC) (Akaike, 1973). It estimates the out-of-sample predictive accuracy ($elppd$) by subtracting, to the computed log pointwise posterior predictive density ($lppd$), a penalty for the complexity of the model expressed in terms of effective number of parameters (p_{WAIC}) (Gelman et al., 2014). We evaluate the WAIC as defined in Gelman et al. (2014) and in Vehtari et al. (2017):

$$WAIC = -2 \cdot \widehat{ellpd}_{WAIC} = -2 \cdot (lppd - p_{WAIC}) \tag{3.7}$$

Where the multiplication factor -2 scales the expression, making it comparable with AIC and other measures of deviance. The R package *loo* is used for the calculations.

3.3 Study area and drivers of flood change

As in Viglione et al. (2016), the study area considered is Upper Austria, where annual maximum daily discharges (AM) for 96 river gauges (catchment areas ranging from 10 to 79500 km^2) are available with record lengths of at least 40 years after 1961. Figure 3.1 shows the extension and the elevation of the considered catchments and Table 3.1 contains percentiles of some catchment attributes.

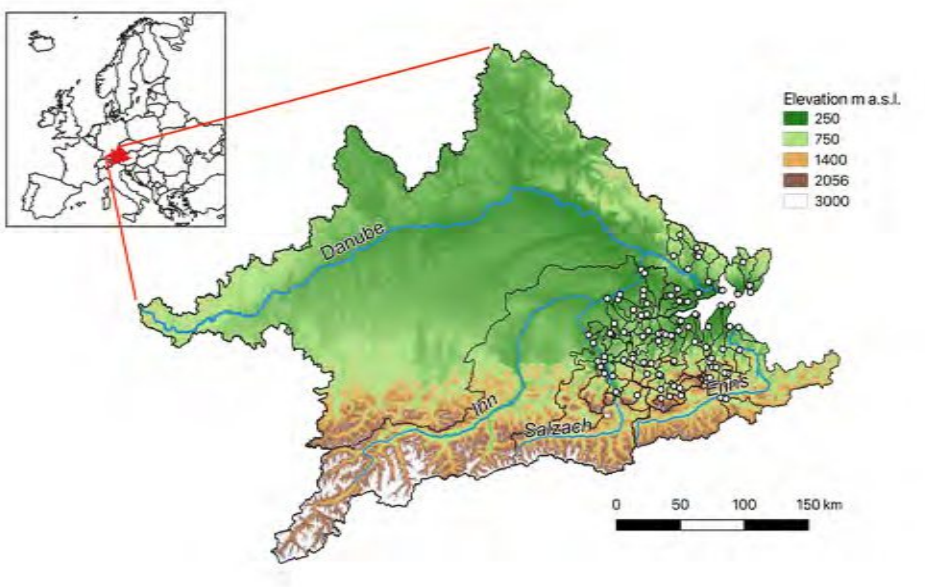

Fig. 3.1: Study region. Location and elevation of the 96 catchments, with outlets in Upper Austria.

Percentile:	0%	25%	50%	75%	100%
Catchment area (km2):	10.5	68.6	159.4	428.2	79490.1
Elevation of the outlet (m a.s.l.):	246.7	357.0	442.1	504.1	763.5
Mean annual flow (m^3/s):	0.2	1.6	3.9	10.9	1583.0
Mean annual flood (m^3/s):	6.2	24.5	46.7	138.1	4415.3
Length of the flood series (years):	40	54	64	96	182

Tab. 3.1: Percentiles of catchment attributes (catchment area, outlet elevation, mean annual flow, mean annual flood and length of records) over the 96 considered catchments

In the considered region, clear evidences of positive trends in flood peaks have been detected in previous studies (Blöschl et al., 2011; Blöschl et al., 2012; Viglione et al., 2016). Figure 3.2 (panel a) shows the trends in the logarithm of the flood peaks (this is equivalent to the percentage change in time), together with their 95% confidence intervals, resulting from a simple least square linear regression, taking 1961 as a common starting year of the AM series. Mostly positive trends are detected, with magnitude between -1 and 3.5 % change per year. A common Mann-Kendall test with 5% significance is performed to identify significant trends (shown in orange in the figure). Panel b shows that more than one third of the catchments in the region has a positive significant trend over time.

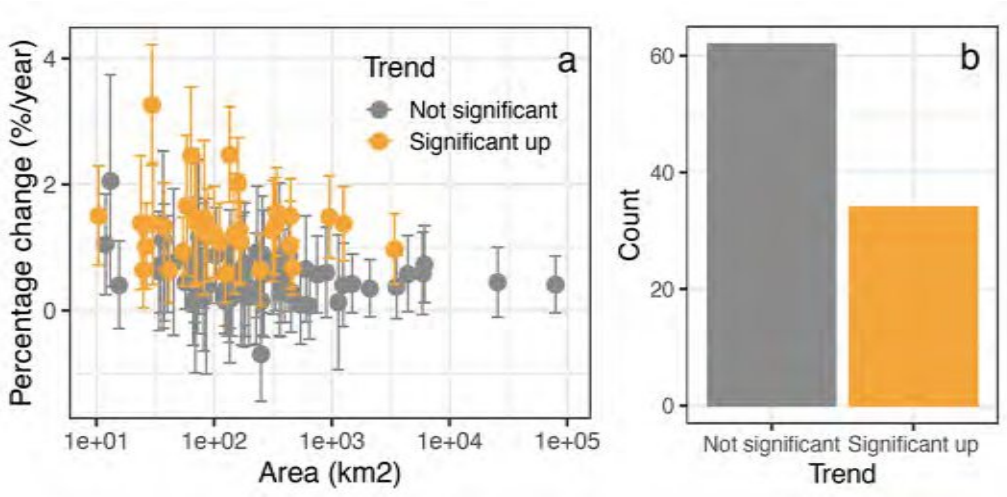

Fig. 3.2: Detected trends (in % $year^{-1}$) in the annual maximum discharge with 95% confidence intervals, as a function of catchment area (as in Viglione et al., 2016) (panel a). Significant upward trends (based on Mann-Kendall test at 5% significance level) are represented in orange. Panel b shows the occurrence of significant upward vs not significant trends in the region.

In this study, instead, we search for relationships between flood temporal variations and the long term evolution of precipitation (atmospheric driver), land-use and agricultural intensification (catchment driver) and the construction of reservoirs (river system driver). Table 3.2 contains some statistics of the covariates (and related quantities) that we use, as possible drivers of flood change, in the driver-informed models G_1 and G_2.

Percentile:	0%	25%	50%	75%	100%
Mean annual precipitation (mm):	762.4	1081.2	1353.5	1641.6	2153.2
30-day annual max. precipitation (mm):	164.7	218.4	257.4	308.5	413.7
7-day annual max. precipitation (mm):	81.6	103.3	126.8	155.5	214.8
1-day annual max. precipitation (mm):	35.0	44.1	51.6	61.9	82.2
Crop area fraction (%):	0.0	1.5	4.7	14.2	91.6
Mean maize yield in year 2000 (t/ha):	0.00	2.10	6.09	9.23	9.68
Mean Land-use intensity Index (-):	0.00	0.01	0.03	0.13	0.83
Reservoir capacity sums (10^6 m^3):	0.0	0.0	0.0	0.0	1376.1
Mean Reservoir Index (-):	0.00	0.00	0.00	0.00	0.05

Tab. 3.2: Percentiles of the covariates and some covariate-related quantities, calculated over the 96 catchments

3.3.1 Long-term evolution of precipitation

Daily precipitation records from 1961, averaged over each catchment, are obtained from the Spartacus gridded dataset of daily precipitation sum (spatial resolution 1x1 km) (Hiebl and Frei, 2018). We extract extreme precipitation series (i.e. 30-day, 7-day and 1-day annual maximum precipitation), commonly used as covariates in the literature (e.g. Prosdocimi et al., 2014; Villarini et al., 2009), and annual total precipitation (see Table 3.2). This latter is the preferred predictor of flood frequency changes in some studies (e.g. Perdigão and Blöschl, 2014; Sivapalan and

Blöschl, 2015; Šraj et al., 2016) and is here considered as a proxy of the antecedent soil moisture condition before a flood event (Mediero et al., 2014) as well as of the event precipitation.

In this study, we consider the decadal variation of the mean annual maximum precipitation for different durations and the annual total precipitation as potential drivers of the decadal variation of the annual flood peak discharges. Therefore, as we are interested in this long term evolution rather than in the year-to-year variability, we smooth the precipitation series with the locally weighted polynomial regression LOESS (Cleveland, 1979) using the R function *loess*. The subset of data over which the local polynomial regression is performed is 10 years (i.e. 10 data-points of the series) and the degree of the local polynomials is set equal to 0. This is equivalent to a constant local fitting and turns LOESS into a weighted 10-years moving average. The weight function used for the local regression is the tri-cubic weight function. The locally weighted polynomial regression is used, rather than a common moving average, in order to preserve the original length of the series. The 10-year moving average filter is typically used when long-term temporal evolution of floods and their drivers (see e.g. Blöschl et al., 2017) Longer time windows could be analysed to investigate the correlation between floods and climatic signals at longer time scales, if longer flood time series were available."

3.3.2 Land-use change and intensification of field crop production

We investigate the impact (at the catchment scale) on floods of modern agricultural management practices and heavy machineries, producing soil compaction and degradation (Van Der Ploeg et al., 1999; Van der Ploeg and Schweigert, 2001; Ploeg et al., 2002; Niehoff et al., 2002; Pinter et al., 2006). With the exception of the mountainous catchments located mainly in the southern part of the region, agricultural areas cover significant portions of the catchments, with 290000 *ha* (i.e. $\sim$ 25% of the region area) of cropland in total over the region (Krumphuber, 2016).

A catchment-related land-use intensity index LI, with a structure similar to the Reservoir Index, proposed by López and Francés (2013), is built here. It is defined as:

$$LI = \sum_{i=1}^{N} \frac{A_{c,i}}{A_T} \cdot \frac{Y_i}{Y_{ref}} \tag{3.8}$$

where N refers to the number of sub-areas (i.e. the grid cells) contained into the catchment boundaries, $A_{c,i}$ is the cropland area, Y_i is the yield in tons/ha, A_T is the total catchment area and Y_{ref} is the Reference yield.

This land-use intensity index takes into account both the intensification of agricultural production (represented by the ratio Y_i/Y_{ref}, similar to the τ-factor in Dietrich et al., 2012, as a proxy agricultural land use-intensity), and the land-use of the catchment (represented by the ratio $A_{c,i}/A_T$) with its potential change in time.

Cropland area $A_{c,i}$ is derived for each catchment from the globally available dataset of cropland and pasture areas for the year 2000, provided by Ramankutty et al. (2008) on a 5 min by 5 min latitude/longitude ($\sim$ 10 km by 10 km) grid. It combines agricultural inventory data with satellite-derived land cover data. We considered the ratio $A_{c,i}/A_T$ constant over time, since there are no substantial evidences of land-use changes over the period of interest in the region. In other words, the changes of LI are, in this case, due to the intensification of the agricultural production only.

For what concerns yield data, we focus on the production of maize, which is the most important crop in Upper Austria (Krumphuber, 2016). Furthermore, Beven et al. (2008) list maize among the cropping systems associated with compaction and soil structural damage, due to the required practices (e.g. they keep bare soil surface) and type of operations, their timing (i.e. late harvested

crops, requiring access to the soil during the wettest soil period, causing compaction, and leaving bare soil exposed to winter storms) and depth of cultivation (Chamen et al., 2003). Maize yield data for the year 2000 (provided by Monfreda et al., 2008) and its linear trend in time (provided by Ray et al., 2012) are globally available, in form of 5 min by 5 min latitude/longitude gridded data-sets. Time series of maize yield for each catchment are derived from spatial aggregation of the gridded information and by extrapolation of the linear trends over the period 1961-2014.

The reference yield Y_{ref}, differently from Dietrich et al. (2012) where it represents the obtainable yield under standard and static agricultural management practices and varies with space, is here assumed to be a single value for the entire region, representative for its average maize production. It is calculated by averaging over time the field crop production data for maze in Upper Austria provided by Statistik Austria (2017) (in tons and hectares) and available for the period 1971-2017. The resulting Y_{ref} is 8.72 ton/ha. See Table 3.2 for statistics about the LI in the region.

3.3.3 Potential impact of reservoirs

Within the 96 considered catchments, 21 reservoirs and the corresponding dams, are identified using the Global Reservoir and Dam GRanD database (Lehner et al., 2011). Dam location, year of construction, capacity and drainage area of the reservoir are extracted from the GRanD database and used in this framework (see Table S1 in the Supplementary material for details). The potential impact of reservoirs on flood regime is here quantified using the Reservoir Index (RI) proposed by López and Francés (2013) and defined as follows:

$$RI = \sum_{i=1}^{N} \frac{A_i}{A_T} \cdot \frac{C_i}{C_T} \tag{3.9}$$

Where N is the number of reservoirs upstream of the gauge station, A_i and C_i are the catchment area and the capacity of each reservoir and A_T and C_T are the catchment area and the mean annual flow volume at the gauge station. The construction of a dam represents a step change in the RI. López and Francés (2013) find 0.25 to be RI threshold value between low and high flow alteration. See Table 3.2 for statistics about the RI in the region.

3.3.4 Driver-informed models and prior knowledge

We use the drivers of change, described in section 3.1, 3.2 and 3.3, as covariates X of the driver-informed models of section 2.2. We adopt the model G_1 when investigating the effects on floods of the long-term evolution of precipitation (i.e. where X is one of the smoothed precipitation series described in section 3.1, here generally indicated as P), otherwise we adopt model G_2, when investigating the effects of the agricultural soil degradation or reservoir (i.e. where X is the LI or RI). The alternative Gumbel distributions, with location parameter conditioned on the covariates are:

$$G_A) \qquad \log(\mu) = a_A + b_A \log(P), \qquad \sigma = \sigma_{0,A} \tag{3.10}$$

$$G_C) \qquad \log(\mu) = a_C + b_C \cdot LI, \qquad \sigma = \sigma_{0,C} \tag{3.11}$$

$$G_R) \qquad \log(\mu) = a_R + b_R \cdot RI, \qquad \sigma = \sigma_{0,R} \tag{3.12}$$

This choice comes from the hypothesis that, when investigating the effects of the agricultural soil degradation or reservoir on floods, the actual magnitude of the covariate and its absolute variation is important, and not the relative change (e.g. an increase of 10% of the cropland area may be not influential for floods if the initial cropland area is very small). This corresponds to the

model structure G_2 and the related regression parameter b as defined in Eq.6. On the contrary, when considering the atmospheric driver, we want the regression parameter b to represent the elasticity of floods to precipitation. This is consistent with the temporal sensitivity coefficient of flood to precipitation of Perdigão and Blöschl (2014) and corresponds to model G_1 and Eq.5. Note that the structure of the driver-informed models and the drivers/covariates considered are both assumptions that may be varied. With the proposed framework, we compare alternative models, that reflect/contain these assumptions for the considered region. Other models can be easily formulated to reflect other hypotheses.

Informative a priori on the parameters b_A, b_C and b_R are retrieved from a selection of published studies, listed in Table 3.3 (as for the model structure and the drivers, they are also part of the assumptions made). They evaluate the effects of the change in one of the drivers on the magnitude of flood peaks (i.e. they provide information on the value of the parameters b, as defined in Eq. 10, 11 and 12). The following paragraphs describe in detail the procedure followed to retrieve an estimate of the mean and the variance of their prior distribution, for each of the three drivers of change.

Atmospheric driver Perdigão and Blöschl (2014) provide, in their Table 2, spatiotemporal sensitivity coefficients α and β of floods to annual precipitation, together with 95% confidence intervals, for Austria and its five hydroclimatic regions, obtained analyzing AM series of 804 catchments. The mean and standard deviation of the prior distribution of the parameter b_A, defined consistently with the sensitivity coefficient β in the time domain, are taken respectively equal to 0.61 (value provided in the study for β) and 0.06 (obtained from its 95% confidence bounds with the assumption of normality). We adopt these values as moments of the prior normal distribution of b_A when the covariate is annual precipitation (as in Perdigão and Blöschl, 2014), but also when the covariate is one of the extreme precipitation series. In these latter cases, in order to reflect the additional uncertainty related to this choice, we arbitrarily increase the standard deviation to three times the one in Perdigão and Blöschl (2014) (i.e. 0.18).

Catchment driver The impact of agricultural soil compaction on flood peaks at the catchment scale is still underdeveloped in the scientific literature (Rogger et al., 2017) and it is not possible to directly retrieve a priori on the regression parameter b_C, as defined in this framework. For this reason, we assume that the available prior information related to land-use change can be transferred and used when analyzing the effect of land-use intensification on floods. Fraser et al. (2013) present an application of metamodeling that upscales physics-based model predictions to make catchment scale predictions of land-management change impacts on peak flows. They consider four land-management scenarios, involving changes of land-use between 3 and 30% of catchment area in one catchment (river Hodder at Footholme in north-west England, 25.3 km^2), whose size and agricultural nature is consistent with most of the catchments in this study. For each scenario they provide, in their Table 4, the minimum, median and maximum reduction of the mean catchment peak flow predicted with two different modelling approaches. The mean of the prior distribution of b_C is obtained dividing the predicted mean catchment peak flow reductions (we consider the values in the column "median") by the imposed fraction of area under land-use change of the corresponding scenario, and finally averaging over the scenarios. The resulting mean of the distribution of b_C is 0.13. The predicted minimum and maximum reductions of the mean peak flow are also divided by the corresponding land-use change and averaged over the scenarios, obtaining a minimum and maximum predicted value for b_C. We treat these latter as 95% confidence bounds of reduction of the mean catchment peak flow, from which the standard deviation is easily calculated (with the assumption of normality and by averaging the left and right distance to the mean). The resulting standard deviation of the distribution of b_C is 0.13.

River system driver Graf (2006) analyzes the downstream hydrologic effects of 36 large dams in American rivers. In his Table 8 he provides regional values of the dam-capacity/yield ratio and of the percentage reduction in maximum annual discharge. Given that it is a large-scale study, we assume that the results are general enough to be reasonably transferred to our study region. We assume that this reduction is registered right downstream of the dam (i.e. the ratio A_i/A_T in Eq.9 is equal to 1), therefore it equals ΔRI (before and after the dam construction). We divide the reduction in maximum annual discharge by the capacity/yield ratio, to obtain regional estimates of the parameter b_R, and we consider the value corresponding to "all regions" (resulting equal to -0.30) as the mean of the prior distribution of b_R. We calculate the standard deviation of the b_R values over the six regions in Graf (2006) in order to obtain the standard deviation of the prior distribution of b_R (resulting equal to 0.18).

The mean and standard deviation of the prior distribution of the parameters b_A, b_C and b_R are summarized in the third column of Table 3.3, with prior distribution assumed to be normal. Additional prior information is included about the shape of the prior distribution, based on the authors' understanding of the way the drivers may affect the magnitude of flood peaks.

Increased (decreased) magnitude of flood peaks may result from an increase (a decrease) in the magnitude of precipitation. This is associated with a positive value of the regression parameter b_A (i.e. the changes in the magnitude of flood peaks and in the covariate occur in the same direction/with the same sign). For this reason the lower tail of the prior normal distribution (contained in the third column of Table 3.3) of the parameter b_A is truncated for negative values, in order to constrain the sign of the parameter. Similarly, we truncate the prior distribution of b_C for negative values since soil degradation processes occurring in the catchment, associated with the intensification of agricultural practices, are expected to produce increased flooding. The construction of reservoirs (reflected in a positive step change in the reservoir index) may instead mitigate flood peaks in the downstream catchment. In this case the value of the parameter is negative and the upper tail of its prior normal distribution is truncated for positive values. The final types (lower- or upper- truncated normal) of the prior distribution of the regression parameters b_A, b_C and b_R are summarized in the fourth column of Table 3.3 and represented in Figure 3.3.

Model and parameter	Study	Normal prior moments	Prior type
G_A, b_A	Perdigão and Blöschl (2014)	N(0.61, 0.06) with annual precipitation. N(0.61, 0.18) otherwise	Truncated normal with lower tail truncated in 0
G_C, b_C	Fraser et al. (2013)	N(0.13, 0.13)	Truncated normal with lower tail truncated in 0
G_R, b_R	Graf (2006)	N(-0.30, 0.18)	Truncated normal with upper tail truncated in 0

Tab. 3.3: Sources, moments and type of the prior distribution of the model parameters b_A, b_C and b_R.

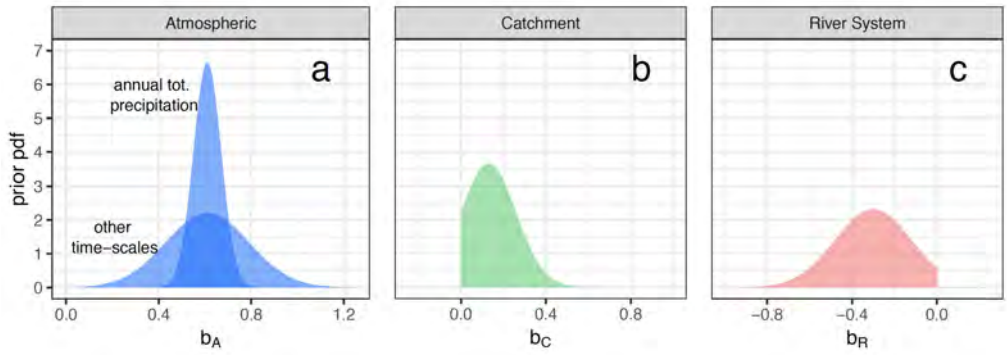

Fig. 3.3: Prior distribution of the model parameters b_A, b_C and b_R, linking the changes of the drivers (i.e. the covariates of the alternative driver-informed models) to the changes of flood peaks. Each panel refers to a different driver (i.e. to a different driver-informed model): atmospheric driver (panel a), catchment driver (panel b) and river system driver (panel c). For the atmospheric driver we adopt different prior distributions for annual and extreme precipitation.

3.4 Results

In order to illustrate the methodology, we apply it first to one site (Section 3.4.1). The results for all other sites in Upper Austria are then presented in Section 3.4.2.

3.4.1 Attribution of flood changes in a single catchment

We analyze the river Traun catchment (gauge station in Wels-Lichtenegg, shown in panel a of Figure 3.4), where the AM series of flood peaks (panel b) presents a significant upward trend ($1.0 \pm 0.6\%$ change per year). We apply the attribution framework in order to try to understand whether the magnitude of flood peaks is related to the temporal evolution of precipitation at the different time-scales (panels c, d, e and f), of the land-use intensity (panel g) or of the reservoir index (panel h) (i.e. if it can be attributed to one of the three drivers of change). In particular, we assume that, the use of a covariate is informative if the WAIC value associated with the driver-informed model is lower than the one associated with the time-invariant model and their absolute difference is larger than a threshold, that we set to 2 using the same interpretation done with the AIC by Burnham and Anderson (2002, pp. 700–71).

	G_0	G_A				G_C	G_R
	Time-invariant	Annual Total P	30-day maximum P	7-day maximum P	1-day maximum P	LI	RI
Non-informative priors	-126.9	-125.0	-125.2	-127.7	-133.4	-133.0	-130.0
Informative priors		-126.6	-127.1	-129.1	-133.7	-127.6	-126.2

Tab. 3.4: Comparison of the alternative time-invariant and driver-informed models for the river Traun catchment, gauge station in Wels-Lichtenegg. The values of the Widely-applicable information criterion, associated with each alternative model, are shown. The first row refers to the use of non-informative priors, while the second one refers to the priors of Table 3.3

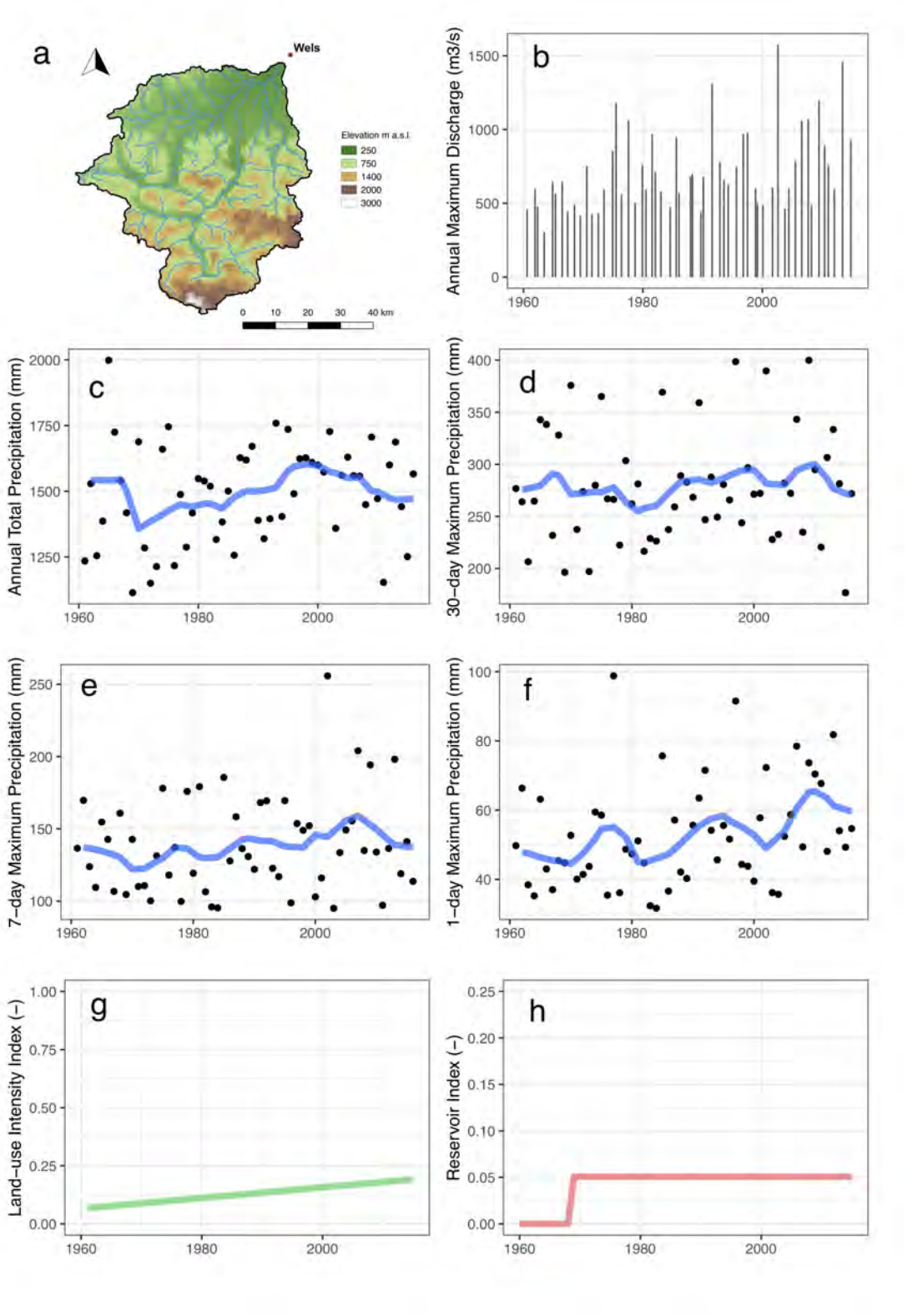

Fig. 3.4: River Traun catchment, gauge station in Wels-Lichtenegg (panel a) and related flood series (panel b) and covariates representative for the three drivers of change: annual total precipitation (c), 30-day (d), 7-day (e) and 1-day maximum precipitation averaged over the catchment (f), land-use intensity index (g) and reservoir index (h).

Table 3.4 shows the values of the WAIC associated with the alternative driver-informed models G_A, G_C, G_R and the time-invariant G_0 in two cases: (i) when no prior information on the parameter b is used (through a non-informative improper uniform distribution with infinite range), and (ii) with the priors of Figure 3.3. In the first case, by comparing the alternative models in terms of differences of WAIC (Table 3.4, first row), it emerges that the 1-day extreme precipitation (model G_A) and land-use intensity (model G_R) are the best covariates and the correspondent models outperform all others, including the time invariant model G_0. This is because, as for the flood peak series, both 1-day extreme precipitation and land-use intensity index have a positive trend over time (panels f and g). Also the model G_R, that uses the reservoir index as covariate, provides a relatively good fit to the data (e.g. better than the time invariant model) since the Gmunden dam was built along the River Traun in 1969 (the location of the dam is shown in panel a of Figure 3.4), which is reflected in a step change in the reservoir index time series in the corresponding year (panel h).

When prior information is used, the WAIC values (Table 3.4, second row) suggest that the model G_A with the 1-day extreme precipitation is still the best one, but the models G_C and G_R, using the land-use intensity and reservoir indexes, do not rank as well as they did before. This is because, in one case, crops cover less than 20% of the total catchment area and, therefore, the land-use intensity varies in a low-value range. Crop areas are, in fact, concentrated in the northern part of the catchment, while the southern and middle part are mountainous areas (panel a of Figure 3.4). In the other case, the reservoir index value after the dam construction ($\sim$0.05) is still significantly lower than the threshold value (0.25) between low and high flow alteration set by López and Francés (2013). This is due to a small dam-capacity/mean-annual-flow-volume ratio. In fact, the reservoir storage capacity (514×10^6 m^3) is significantly smaller than the mean annual flow volume of the catchment (4137×10^6 m^3), as well as the dam drainage area (1395 km^2) compared to the catchment area (3426 km^2). Furthermore both flood peaks and the RI increase in time, suggesting a positive value of the parameter b_R, which is in contrast with its informative prior distribution.

When using prior information on the parameter b (see Figure 3.3), it becomes improbable that small values of the two indexes can produce significant flood changes, even though they vary in time in the same direction as the floods do (as in the case of the land-use intensity). In this case, therefore, we attribute the temporal variability of floods to the long-term variation of the 1-day maximum precipitation.

3.4.2 Attribution of flood changes in Upper Austria

In each of the 96 sites in Upper Austria the model G_A is locally compared to the time-invariant model in terms of WAIC, which represents a trade-off between goodness of fit and model complexity. We alternatively consider different time scales of precipitation as covariate of the driver-informed model. In particular, we are interested in determining the most suitable time-scale for the atmospheric driver to be employed in the attribution study over the entire region, i.e. whether the long-term changes in annual precipitation or in the extreme precipitation drive flood changes in the region.

The results of this analysis are shown in Figure 3.5 where, in each panel, a different time scale of the atmospheric driver is taken as covariate of the model G_A. We mark the catchments in blue if the goodness of fit of the driver-informed model significantly improves with the inclusion of the covariate (accounting for the increased model complexity), with respect to the time-invariant case (i.e. if $WAIC_{G_A}$ is lower than $WAIC_{G_0}$ and their absolute difference is larger than a threshold, arbitrarily set to 2). Otherwise, we mark them in grey (meaning that the time-invariant model is still preferable).

The analysis shows that annual total precipitation as covariate improves the model performance only for a small number of catchments in the region (panel a). On the contrary, extreme precipitation series with short durations (i.e. 7-day and 1-day maximum precipitation) seem to be regionally more suitable covariates for the distribution of AM (panels c and d).

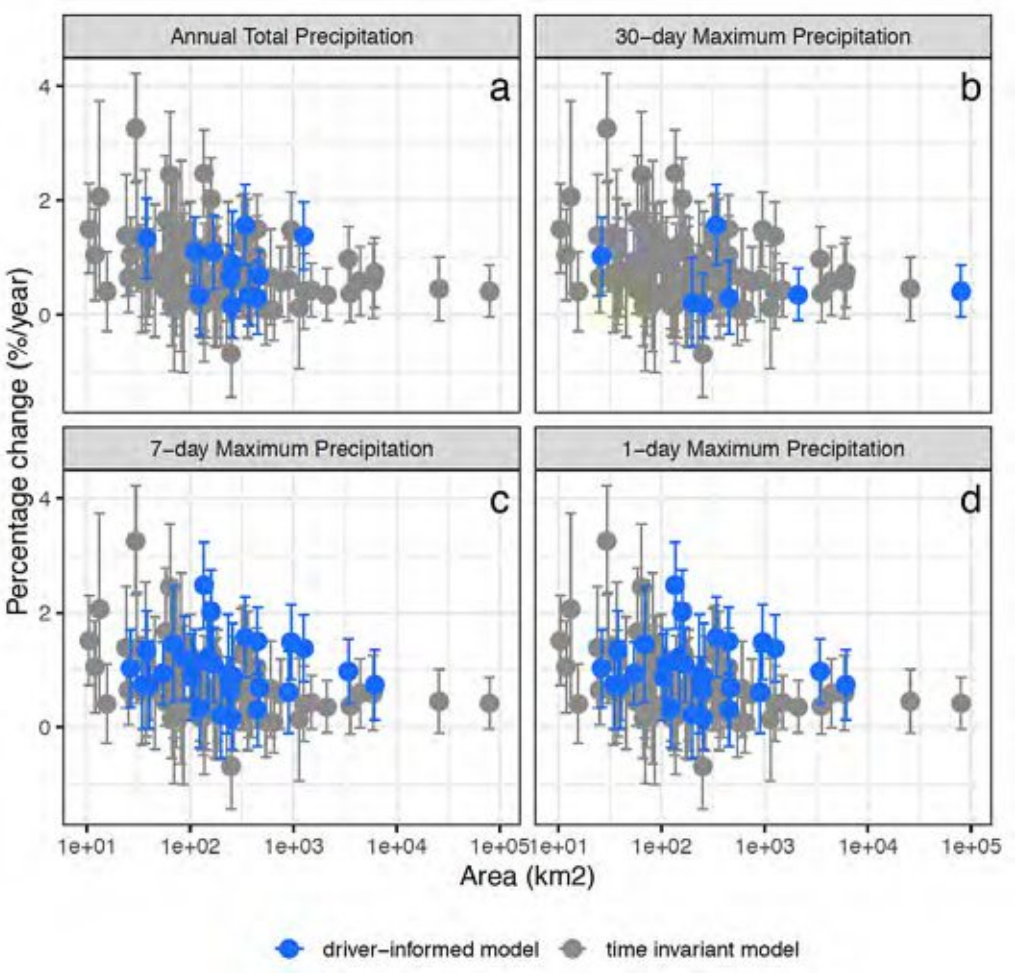

Fig. 3.5: Comparison between the driver-informed model (in blue), with precipitation as covariate, and the time-invariant model (in grey). The panels show the detected trends in flood series as a function of catchment area, with colors referring to the resulting best alternative model (i.e. time-invariant or driver-informed). The selection of the best fitting model is carried out, in each site, through the Widely-Applicable information criterion. Each panel refers to a different time scale of precipitation used as covariate (annual total precipitation in panel a, 30-day maximum precipitation in panel b, 7-day maximum precipitation in panel c and 1-day maximum precipitation in panel d).

Based on this analysis, we select 1-day maximum precipitation as covariate representative for the atmospheric processes driving flood change for the study region. In each catchment we compare the WAIC values associated with four alternative models: G_0 (i.e. the time-invariant model), G_A with 1-day maximum precipitation as covariate, G_C and G_R. Similarly to Figure 3.5, in Figure 3.6 a catchment is marked in grey if the model G_0 is associated with the lowest value of WAIC. Flood changes are instead attributed to one of the drivers (in Figure 3.6 with colors) if the WAIC value of the corresponding driver-informed model is significantly lower than

the one of the model G_0 (we use the same arbitrary threshold of WAIC difference equal to 2) and if it is the lowest among the competing driver-informed models.

In a significant fraction of the catchments, the time-invariant model (in grey) is still the preferred choice while the atmospheric driver (in blue, represented by 1-day max precipitation as covariate) is the main driving process among the alternatives considered. The catchment driver (in green) instead plays a very marginal role, together with the river system driver, which never results as best fitting model. The long-term evolution of floods is attributed to the land-use intensification index only in three catchments with small catchment area (panel a).

Panel b shows the occurrence of the attributed drivers with a distinction between the catchments where the trends in time of flood peaks resulted significant or not significant (see Figure 3.2). The flood series in around half of the sites, where trends in time of the floods are significant, are associated to the long-term evolution of extreme precipitation series. However, the other half of them does not correlate significantly with any of the covariates used here, even though the correlation with time is significant. All of these sites have relatively small catchments and one third of them are in the mountains (Figure 3.7a). Figure 3.7b shows that, in terms of seasonality of floods, the sites with trends but no correlated covariate are not significantly different from the others.

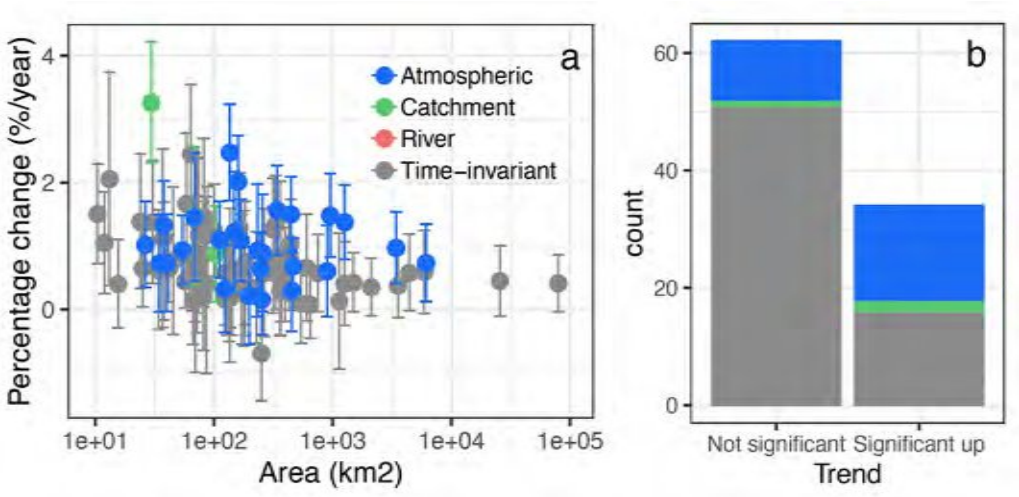

Fig. 3.6: Attribution of flood changes in Upper Austria to the atmospheric (blue), catchment (green) and river system driver (red). Panel a shows the detected trends in flood series as a function of catchment area, with colors referring to the resulting best alternative driver-informed model. Catchments where the time-invariant model is still preferred are shown in grey. Panel b shows the occurrence of the selected alternative (driver-informed and time-invariant) models with a distinction between the catchments where the trends in flood peaks resulted significant (upward) or not significant. The atmospheric driver is here represented by 1-day maximum precipitation.

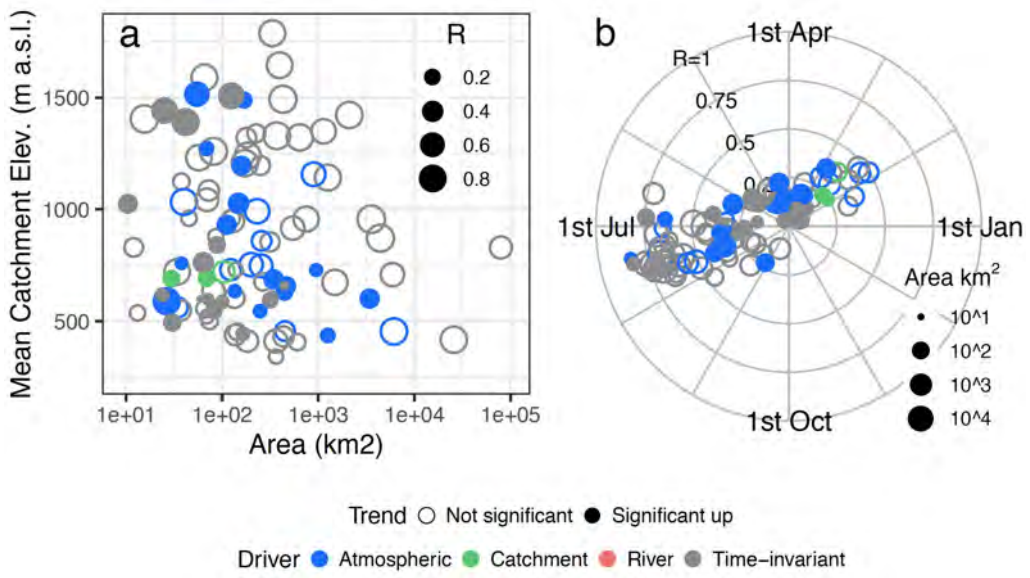

Fig. 3.7: Mean catchment elevation as a function of catchment area (panel a) and seasonality of floods (panel b) in Upper Austria. The results of the attribution analysis (see Figure 3.6) are represented with colors and filled (empty) dots represent catchments with significant (not significant) flood trends. The size of the dots scales with the concentration of the date of occurrence of floods in panel a and with catchment area in panel b. The angular coordinate in panel b represents the average date of occurrence of floods and the distance from the center is the concentration of the date of occurrence R ($R = 0$ when floods are evenly distributed throughout the year and $R = 1$ when all floods occur on the same day). Both are calculated as in Blöschl et al. (2017).

Figure 3.8 compares the posterior distribution of the parameters b_A, b_C and b_R, obtained with the MCMC approach, to their corresponding prior distribution. When the evolution of flood peaks in one catchment is attributed to one driver, the posterior distribution of the corresponding regression parameter is represented in black, otherwise (i.e. if the flood changes are attributed to other drivers or the time-invariant model is preferred) in grey. In the upper panels non-informative priors are used while, in the lower panels, the informative priors, shown in Figure 3.3, are used, consistently with Figure 3.5 and 3.6. This figure shows the influence of the informative priors in the attribution process. By introducing additional external information about how the connection between these covariates and flood peaks should be, we obtain very different posterior estimates of the parameters b and, consequently, of the extreme value distribution parameters and of the attribution results.

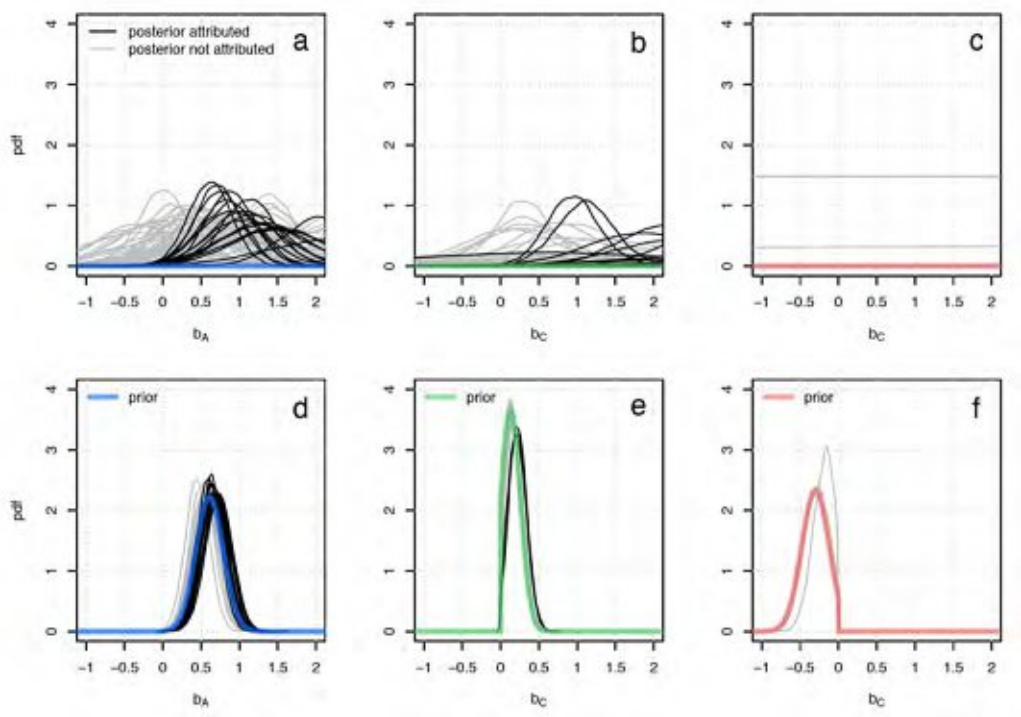

Fig. 3.8: Prior distribution of the regression parameters b_A (Atmospheric driver, panels a and d), b_C (Catchment driver, panel b and e) and b_R (River system driver, panel c and f) with the corresponding posterior distributions for each catchment. Upper panels refer to the use of non-informative priors and lower panels of the informative priors of Figure 3.3. When the evolution of flood peaks in one catchment is attributed to one driver, the posterior distribution of the corresponding parameter is shown in black, otherwise in grey.

Similarly to panel b of Figure 3.6, Figure 3.9 shows the number of occurrence of attributed driver types for the other precipitation time-scales. Different covariates (annual precipitation, 30-day maximum precipitation and 7-day maximum precipitation) for the model G_A are considered in the different panels. The changes in the decadal annual precipitation correspond to only around one fourth of the significant trends in time detected in flood series (even less for the 30-day maximum precipitation). The 7-day maximum precipitation series as covariate show instead a similar results as the 1-day maximum precipitation (see figure 3.6, panel b).

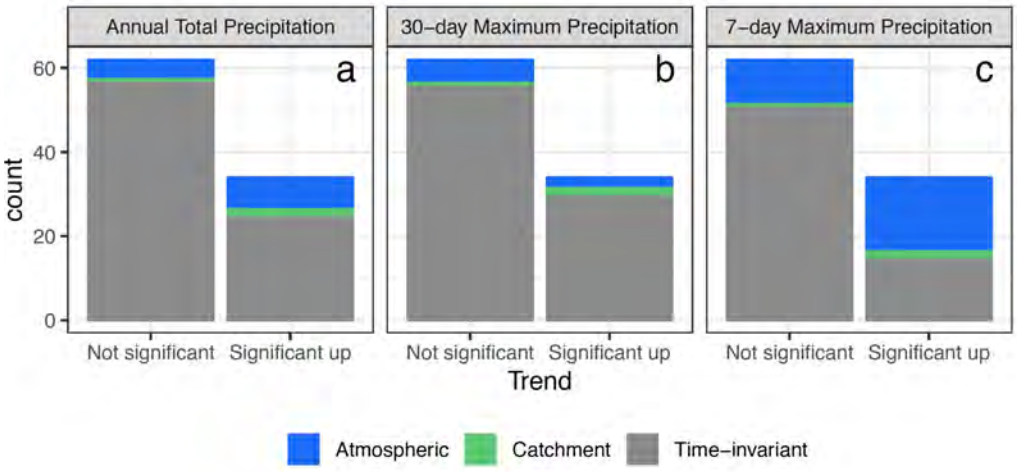

Fig. 3.9: Same as panel b of Figure 3.6 but for different time scales of precipitation. Occurrence of the selected alternative (driver-informed and time-invariant) models is shown, with a distinction between the catchments where the trends in flood peaks resulted significant (upward) or not significant. The considered precipitation time-scales for the atmospheric driver are: annual precipitation (panel a), 30-day maximum precipitation (panel b) and 7-day maximum precipitation (panel c).

3.5 Discussion and conclusions

In this study we apply a simple data-based approach for the attribution of flood changes to potential drivers: atmospheric, catchment and river system drivers. The method is applied to a large number of catchments in a study region, Upper Austria, where significant positive trends are detected in maximum annual peak discharge series. We assume the maximum annual peak discharges to follow a two-parameter Gumbel distribution. We include information on the three drivers through covariates (smoothed/decadal annual precipitation, smoothed/decadal 30-day, 7-day, 1-day maximum annual precipitation, land-use index and reservoir index) that control the location parameter of the Gumbel distribution through simple log-linear and log-log models. The attribution is performed by comparing the different models, using different covariates, fitted using Bayesian inference. The comparison is based on the trade-off between goodness of fit and model complexity, using the Watanabe-Akaike information criterion (WAIC). Prior information on the slope parameters of these models (i.e. on the elasticity of the covariates to floods), based on results of published studies, is also provided in order to limit the possibility for spurious correlations to bias the attribution. Without using information on the expected elasticity, the attribution procedure is ill posed in that it would prefer the covariate better correlated to the flood temporal fluctuations, no matter if the correlation is physically plausible.

Our results suggest that precipitation change is the main driver of flood change in the study region (no matter which time-scale is used for precipitation), which is consistent with the results in Viglione et al. (2016). Differently from what suggested in Sivapalan and Blöschl (2015) and Šraj et al. (2016), annual precipitation is not as good as extreme precipitation in explaining the long-term evolution of floods in this context. This is due to the fact that, while Šraj et al. (2016) are interested in how floods correlate to precipitation at the annual scale, here we are looking at long-term (decadal) variation of precipitation. The smoothing of the annual precipitation time series results in averaging wet years and dry years, thus destroying the correlation to floods. On the contrary, the extreme precipitation series, even after the smoothing, do not contain the

influence of droughts and are therefore more correlated to long-term fluctuations of the flood statistics. In Upper Austria, because of the relatively small size of the catchments, the 7-day and the 1-day maximum annual precipitation decadal fluctuations correlate best with the fluctuations of the flood statistics.

Land-use intensity changes are significant in very few small catchments, which are mostly covered by agricultural land. Differently from what has been assumed in Viglione et al. (2016), these are not the smallest catchments, which are located in the mountains where there is almost no agriculture and there has not been a significant deforestation nor afforestation in the last 50 years. For most of the catchments, land-use intensity changes (note that we investigated the changes related to late-harvested crops, see Section 3.2) do not correlate meaningfully with flood changes (we get a good correlation only if we use non-informative priors for the elasticity parameter, resulting in not credible posterior distributions). This is consistent with the fact that, in Upper Austria, big floods occur generally in summer, in correspondence of precipitation events with high magnitude, and smaller floods are in spring or winter. Few floods occur in autumn, when we would expect a greater soil susceptibility to erosion and compaction (potentially leading to increased flooding) as a consequence of the agricultural practices for late-harvested crops (Chamen et al., 2003; Beven et al., 2008).

Reservoirs do not produce relevant effects on floods neither, because the capacity/yield ratio is generally small. Most of the dams are built for hydroelectricity purposes, but even for those built for flood control we do not detect significant flood attenuation at the gauging stations because these effects are mainly local (Ayalew et al., 2017; Volpi et al., 2018). This result is not surprising given that we expect reservoirs to attenuate flood peaks and that we observe mostly upward trends in flood peak magnitude in the region.

In half of the catchments where we detect significant trends in flood peaks, the driver-informed model, with extreme precipitation as covariate, outperforms the time-invariant model. In the other cases we observe significant trends but not a significant correlation to the covariates, suggesting that the long-term temporal evolution of the selected drivers is overall not sufficient to explain the observed trends in the peak discharge series and that other covariates should be considered or covariates informative on other drivers of flood change. For example, we did not consider changes in snow related processes here (e.g. by taking air temperature as covariate), which may be important for mountainous catchments (see e.g. Blöschl et al., 2017), and changes in precipitation of shorter durations (e.g. hourly precipitation), which may be more appropriate covariate for the smaller catchments. Indeed, all of the sites where we do detect a trend in flood peaks but no correlation with the covariates are small (and some mountainous) catchments. The fact that in these catchments we have not identified a suitable driver may also suggest that other flood-driver relations should be explored in future analyses, representing for example the combined effect of multiple drivers on flood change.

In some of the catchments where we do not detect significant trends in flood peaks, the driver-informed model, with extreme precipitation as covariate, outperforms the time-invariant model. Through the driver informed models used here, long term flood fluctuations are related to the covariates, even in cases where no monotonic trend in time is detected. This is in line with our objective to research the relationships between flood temporal variations and the long-term evolution of the drivers.

This study considers many sites in one region, but the analysis is essentially local, i.e. every site is analysed independently using locally defined covariates. There is potential for extending the method to something in line with Viglione et al. (2016), in which a regional model is fitted to all the sites jointly explicitly using covariates for the drivers.

The framework used here is easily generalizable and applicable in other contexts (i.e. by changing the covariates or the model structure). Different drivers could be considered, that may

have positive or negative effects on floods. The key issue, as shown in this chapter, is to gather prior information on how sensitive are floods to changes in the drivers, which could be achieved through derived-distribution (see e.g. Eagleson, 1972; Sivapalan et al., 2005; Volpi et al., 2018) and comparative process studies (see e.g. Falkenmark and Chapman, 1989; Viglione et al., 2013a; Blöschl et al., 2013b). This is in line with the concept of Flood Frequency Hydrology (Merz and Blöschl, 2008a; Merz and Blöschl, 2008b; Viglione et al., 2013b), which highlights the importance of combining flood data with additional types of information, including causal mechanisms, to improve flood frequency estimation and, as in this case, to support change analyses.

Chapter 4

Do small and large floods have the same drivers of change? A regional attribution analysis in Europe

The present chapter corresponds to the following scientific publication in its original form:

Bertola M., Viglione A., Vorogushyn S., Lun D., Merz B. and Blöschl G. (2020). "Do small and large floods have the same drivers of change? A regional attribution analysis in Europe". To be submitted to Hydrology and Earth System Sciences

Abstract

Recent studies have shown evidence of increasing and decreasing trends in mean annual floods and flood quantiles across Europe. Studies attributing observed changes in flood peaks to their drivers have mostly focused on mean annual floods. This chapter proposes a new framework for attributing flood changes to potential drivers, as a function of return period, in a regional context. We assume flood peaks to follow a non-stationary regional Gumbel distribution, where the median flood and the 100-year growth factor are used as parameters. They are allowed to vary in time and between catchments as a function of the drivers quantified by covariates. The elasticities and contributions of the drivers to flood changes are estimated by Bayesian inference. The prior distributions of the elasticities of flood quantiles to the drivers are estimated by hydrological reasoning and from the literature. The attribution model is applied to European flood and covariate data and aims at attributing the observed flood trend patterns to specific drivers for different return periods. We analyse flood discharge records from 2370 hydrometric station in Europe over the period 1960-2010. Extreme precipitation, antecedent soil moisture and snowmelt are the potential drivers of flood change considered in this study. Results show that, in northwestern Europe, extreme precipitation mainly contributes to changes in both the median (q_2) and 100-year flood (q_{100}), while the contributions of antecedent soil moisture are of secondary importance. In southern Europe, both antecedent soil moisture and extreme precipitation contribute to flood changes, and their relative importance depends on the return period. Antecedent soil moisture is the main contributor to changes in q_2, while the contribution of the two drivers to changes in larger floods (T>10 years) are comparable. In eastern Europe, snowmelt drives changes in both q_2 and q_{100}.

4.1 Introduction

There is widespread concern that river flooding has become more frequent and severe during the last decades, and that human-induced climate change and other drivers will further increase flood discharge and damage in many parts of the world (IPCC, 2012; Hirabayashi et al., 2013) This

concern has given rise to a large number of studies investigating past changes in flood hazard, i.e. changes related to flood discharge, and flood risk, i.e. related to damage. The global pattern of increasing flood damage has been mainly attributed to increasing population, economic activities and assets in flood-prone areas (Bouwer, 2011; IPCC, 2012; Visser et al., 2014). In terms of changes in flood discharge, a variety of changes has been found (for shift in timing and trends in the magnitude of European floods, see Blöschl et al. (2017) and Blöschl et al. (2019)), and attempts to attribute detected changes have not resulted in a clear picture about the contribution of the underlying drivers (for a review on detecting and attributing flood hazard changes in Europe see Hall et al. (2014)).

The large majority of studies on past changes in flood hazard analysed the mean flood behaviour, using, for instance, the Mann-Kendall test to detect gradual changes or the Pettitt test for step changes of the mean or median annual flood (e.g. Petrow and Merz, 2009; Villarini et al., 2011; Mediero et al., 2014; Mangini et al., 2018). This focus may be misleading, since changes in large floods may differ from those in the average behaviour. An illustrative example is the Mekong River, where studies found negative trends in the mean flood discharge, whereas the public perception suggested that the frequency of damaging floods had increased in the past decades. Delgado et al. (2009) resolved this mismatch by analysing the temporal change in flood discharge variability. They found an upward trend in interannual variability which outweighed the decreasing mean behaviour leading to contrasting trends in the mean flood and rare floods. This change in flood variability could be attributed to changes in the Western Pacific monsoon (Delgado et al., 2012). Another recent example is the large-scale study of Bertola et al. (2020) which compared trends of small with those of large floods (i.e. the 2-year and the 100-year flood) across Europe. They found distinctive patterns of flood change which depend on the return period and catchment scale.

It has been widely acknowledged that drivers can differently affect small and large floods (e.g. Hall et al., 2014) and yet the focus has been mainly on changes in the mean flood behaviour. One reason for this may be the ability of quantifying changes in the mean more robustly than those of larger floods. However, both from theoretical and practical perspectives, detection and attribution of flood changes as a function of the return period are of considerable interest for understanding how the non-linearity in the hydrological system plays out and for providing guidance for flood risk management. The shape of the flood frequency curve and its changes in time are a reflection of the interplay between atmospheric processes and catchment state (soil moisture and snow), with different characteristics depending on the region, climate and runoff generation processes (Blöschl et al., 2013b).

Rainfall itself may increase at different rates for small and extreme events in a changing climate. These changes may strongly differ depending on the region and season. In addition, changes in rainfall may be translated in a non-linear way into changes of various flood magnitudes due to the non-linearity of the catchment response. For example, Rogger et al. (2012) detected a change in the slope of the flood frequency curve and linked it to the interplay of catchment saturation and rainfall. Several studies indicated changes in precipitation amounts/intensities for different rainfall quantiles that might translate into different changes of small and large floods. For Germany, Murawski et al. (2016) found an increasing variability of precipitation along with increasing mean in seasons other than summer, which leads to a disproportional increase of heavy precipitation. Besselaar et al. (2013) detected a decrease of the return period of extreme precipitation (5, 10 and 20 years) over Europe in the past 60 years between 2 and 58%. Berg et al. (2013) found a disproportional increase of high-intensity, convective precipitation with increasing temperature that goes beyond the Clasius-Clapeyron rate (7% per degree of temperature increase) compared to low-intensity, stratiform precipitation. The review of a number of regional studies on past precipitation trends in Europe by Madsen et al. (2014) suggested a tendency for increasing

extreme rainfalls. This trend seemed not to translate directly into positive trends in observed streamflow over large scales in Europe (Madsen et al., 2014). Similarly, Hodgkins et al. (2017) suggested that occurrence of floods with return periods of 25 to 100 years is dominated by multi-decadal climate variability rather than by long-term trends based on the analysis of more than 1200 gauges in Europe and North America. The study suggested that occurrence rate of larger floods (50 and 100 years) increased slightly stronger compared to smaller floods (25 years) in Europe over the past about 50 years.

It has been observed that increases in precipitation extremes often do not translate in increasing floods (Madsen et al., 2014; Sharma et al., 2018). This is attributable to other factors which modulates flood response, such as initial soil moisture. For example, Tramblay et al. (2019) found that, despite the increase in extreme precipitation, the fewer detected annual occurrences of extreme floods in 171 Mediterranean basins were likely caused by decreasing soil moisture. The relationship between the flow rate and the initial saturation state of the soil is often non-linear and the effect of antecedent soil moisture strongly depends on soil type and geology. The sensitivity of floods to initial soil moisture depends on flood magnitude, and runoff generation is more influential for smaller events. Vieux et al. (2009) analysed several watersheds in the Korean peninsula with a distributed hydrologic model and found that the sensitivity of the watershed response to the initial degree of saturation is dependent on event magnitude. Zhu et al. (2018) simulated peak discharges for return periods of 2 to 500 years for several sub-watersheds in Turkey River in the Midwestern United States and found that antecedent soil moisture modulates the role of rainfall structure in simulated flood response, particularly for smaller events. Grillakis et al. (2016) analysed flash flood events in two Greek and one Austrian catchments, and found higher sensitivity of the smallest flood events to initial soil moisture, compared to larger events. These results are consistent throughout the different regions and climates, confirming that the effects of initial soil moisture on flood response depend on flood magnitude.

Snow storage and melt are other important factors that modulate flood response in temperate and cold regions. Snowmelt represents the dominant flood generating process in northeastern Europe and rain-on-snow is relevant for regions in central and northwestern Europe (Berghuijs et al., 2019; Kemter et al., 2020). It was observed that in catchments where snowmelt and rain-on-snow are the dominant flood generating processes, the shape of the flood frequency curve is likely to flatten out at large return periods due to the upper limit of energy available for melt (Merz and Blöschl, 2003; Merz and Blöschl, 2008a). Reduction in spring and summer snow cover extents have been detected as a result of increasing spring temperature in the Northern Hemisphere (Estilow et al., 2015). Several studies from regions dominated by snowmelt-induced peak flows reported decrease in extreme streamflow and earlier spring snowmelt peak flows, likely caused by increasing temperature (Madsen et al., 2014). The effects of changing snow storage and melt on the flood frequency curves likely depend on flood regimes and mixing of different flood generating processes in the catchments. For example, in Carinthia, in the very south of Austria, the major floods tend to occur in autumn, and spring snowmelt floods represent a smaller fraction of events with small magnitude (Merz and Blöschl, 2003). Hence, changes in snow cover and melt are expected to mainly affect the smaller floods in these climates. In contrast, in northeastern Europe where snowmelt is the dominant flood generating process of both small and large floods, the effects of decreasing snowmelt are likely important for the entire flood frequency curve.

Overall, the contributions of different drivers to flood changes as a function of return period are currently not well understood. This is partly due to detection and attribution studies focusing generally on the mean annual flood. Several studies applied non-stationary frequency analysis to attribute past flood changes to potential drivers. These studies typically allowed the parameters of the probability distribution of floods to vary in time, using time-varying climatic covariates

(e.g. Prosdocimi et al., 2014; Šraj et al., 2016; Steirou et al., 2019) and, more rarely, catchment and river covariates (e.g. López and Francés, 2013; Silva et al., 2017; Bertola et al., 2019). They attempted to identify and select covariates in the non-stationary model that provide a better fit than the alternative stationary model to the flood data. However, these studies still aimed at attributing changes in the mean annual flood and did not separate the effects of drivers on floods associated with different return periods.

The aim of this chapter is to address two science questions: (a) Is it possible to identify the relative contributions of different drivers to observed flood changes across Europe as a function of the return period, and if so, (b) what is the magnitude and sign of these contributions across Europe? Regarding the first question, one possible outcome is for the data to provide evidence that the relative contributions differ, or alternatively, the data may contain insufficient information to separate the effects by return period. Regarding the second question, the interest resides in understanding the relative importance of potential drivers as a function of return period (and catchment scale), provided such information can be inferred from the data. In this study, we adopt a non-stationary flood frequency approach to attribute observed flood changes to potential drivers, used as covariates of the parameters of the regional probability distribution of floods. Extreme precipitation, antecedent soil moisture and snowmelt are the potential drivers considered. The relative contribution of the different drivers to flood changes is quantified through the elasticity of flood quantiles with respect to each driver.

4.2 Methods

4.2.1 Regional driver-informed model

In this study, we use non-stationary flood frequency analysis to attribute observed flood changes across Europe (see e.g., Blöschl et al., 2019; Bertola et al., 2020) to potential drivers, used as time-varying covariates. In the spirit of Bertola et al. (2020), we formulate the flood model as a regional Gumbel model. The Gumbel distribution has two parameters (i.e. the location μ and scale σ parameters) and its cumulative distribution function is:

$$F_X(x) = p = e^{-e^{-\frac{x-\xi}{\sigma}}} \tag{4.1}$$

The two Gumbel parameters can be inferred from knowledge of two flood quantiles, e.g., the 2-year and the 100-year flood. We adopt here the same alternative parameters as in Bertola et al. (2020), i.e. the 2-year flood q_2 and the 100-year growth factor x'_{100}. The T-year flood can be obtained with the following relationship:

$$q_T = q_2 \left(1 + a_T x'_{100}\right) \tag{4.2}$$

where $a_T = (y_T - y_2)/(y_{100} - y_2)$, with y being the Gumbel reduced variate, which is related to the return period by:

$$y_T = -\ln\left(-\ln\left(1 - \frac{1}{T}\right)\right) = -\ln\left(-\ln p\right) \tag{4.3}$$

We adopt the following change model accounting for catchment area:

$$\ln q_2 = \ln \alpha_{2_0} + \gamma_{2_0} \ln S + \alpha_{2_1} \ln X_1 + \alpha_{2_2} \ln X_2 + \alpha_{2_3} \ln X_3 + \varepsilon \tag{4.4a}$$

$$\ln x'_{100} = \ln \alpha_{g_0} + \gamma_{g_0} \ln S + \alpha_{g_1} \ln X_1 + \alpha_{g_2} \ln X_2 + \alpha_{g_3} \ln X_3 \tag{4.4b}$$

$$\varepsilon \sim \mathcal{N}(0, \sigma)$$

Where X_1, X_2 and X_3 are three covariates (i.e. time series of the potential drivers of flood change), S is catchment area and the Greek symbols represent the parameters of the model to be estimated. The ε term, here assumed normally distributed, accounts for additional local variability (i.e. not explained by catchment area and the covariates) of q_2.

The elasticity of the generic flood quantile q_T with respect to the covariate X_i is defined as:

$$S_{T,X_i} = \frac{X_i}{q_T}\frac{\partial q_T}{\partial X_i} = \alpha_{2_i} + \alpha_{g_i}\left(1 - \frac{1}{1 + a_T x'_{100}}\right) \tag{4.5}$$

It represents the percentage change in q_T, due to a 1% change in X_i, i.e., how sensitive flood peaks are to changes of the drivers. However, the elasticity alone does not tell how much the flood quantiles have actually changed (in time) due to observed changes of the drivers. Hence, we define the contribution of X_i to the changes in q_T as:

$$C_{T,X_i} = \frac{X_i}{q_T}\frac{\partial q_T}{\partial X_i} \cdot \frac{1}{X_i}\frac{dX_i}{dt} \tag{4.6}$$

It represents the percentage change in q_T, due the actual change in X_i. The total change in q_T due to the changes in the drivers, assuming that the contributions are additive, is:

$$\frac{1}{q_T}\frac{dq_T}{dt} = \sum_i C_{T,X_i} = \sum_i \frac{X_i}{q_T}\frac{\partial q_T}{\partial X_i} \cdot \frac{1}{X_i}\frac{dX_i}{dt} \tag{4.7}$$

A measure of relative contribution of X_i to the change in q_T is expressed here by:

$$R_{T,X_i} = \frac{abs(C_{T,X_i})}{\sum_i abs(C_{T,X_i})} \tag{4.8}$$

where $\sum_i R_{T,X_i} = 1$

In the change model, the flood and covariates data are pooled and used simultaneously to attribute any observed changes in floods to their drivers. This pooling increases the robustness of the estimates (see e.g., Viglione et al., 2016) but requires an assumption of homogeneity. Specifically, we assume here that for a given return period and catchment scale, the elasticities of the flood discharges to their drivers are uniform within the region. We do allow the drivers to vary between catchments.

We frame the estimation problem in Bayesian terms through a Markov chain Monte Carlo (MCMC) approach, using the R package rStan (Carpenter et al., 2017) which makes use of a Hamiltonian Monte Carlo algorithm to sample the posterior distribution (Stan Development Team, 2018). For each inference, we generate four chains of 10 000 simulations each with different initial values and we check for their convergence. We use prior information on the model parameters to constrain their estimation to hydrologically plausible values (see Sect. 4.2.5).

4.2.2 Spatial correlation of floods

Spatial correlation of floods is not directly accounted for in the proposed regional change model of Sect. 4.2.1 and it may result in underestimated sample uncertainties (see e.g., Stedinger, 1983; Castellarin et al., 2008; Sun et al., 2014). Here, we adopt an approach proposed by Ribatet et al. (2012) and based on the work of Smith (1990), consisting in a magnitude adjustment to the likelihood function in a Bayesian framework, which accounts for the overall dependence in space and allows to obtain reliable credible intervals. The adjusted likelihood is defined as:

$$L^*(\theta, \mathbf{y}) = L(\theta, \mathbf{y})^k \tag{4.9}$$

where L is the likelihood under the assumption of spatial independence, θ is the vector of unknown parameters and k is the magnitude adjustment factor to be estimated, such as $0 < k \leq 1$ (see Appendix B). The magnitude adjustment factor k represents the overall reduction of hydrological information in the data caused by the presence of spatial correlation and results in an inflated posterior variance of the parameters. If floods at different sites are spatially independent, k is 1; on the contrary, if floods are strongly cross-correlated, k assumes values close to 0. In this latter case, the sample uncertainty resulting from the adjusted likelihood will be larger, compared to the model where spatial cross-correlation is not accounted for. For further details on the adjustment to the likelihood and its application to hydrological data see Smith (1990), Ribatet et al. (2012) and Sharkey and Winter (2019).

4.2.3 Data

Consistently with Blöschl et al. (2019) and Bertola et al. (2020), we analyse long series of annual maximum discharges between 1960 and 2010, from 2370 hydrometric stations in 33 European countries (`https://github.com/tuwhydro/europe_floods`). Stations affected by strong artificial alterations (such as large reservoirs in the proximity of the gauges) are not included in this database (Blöschl et al., 2019). The location of the stations is shown in Fig. 4.1. Their contributing catchment areas range from 5 to 100 000 km^2 and the median record length is 51 years. The catchment boundaries relative to each hydrometric station are derived from the CCM River and Catchment Database (Vogt et al., 2007). Daily gridded precipitation and mean surface temperature is obtained from the E-OBS dataset (version 18.0e, resolution 0.1 deg; Cornes et al. (2018)). It covers the area 25N-71.5N x 25W-45E for the period 1950-2018.

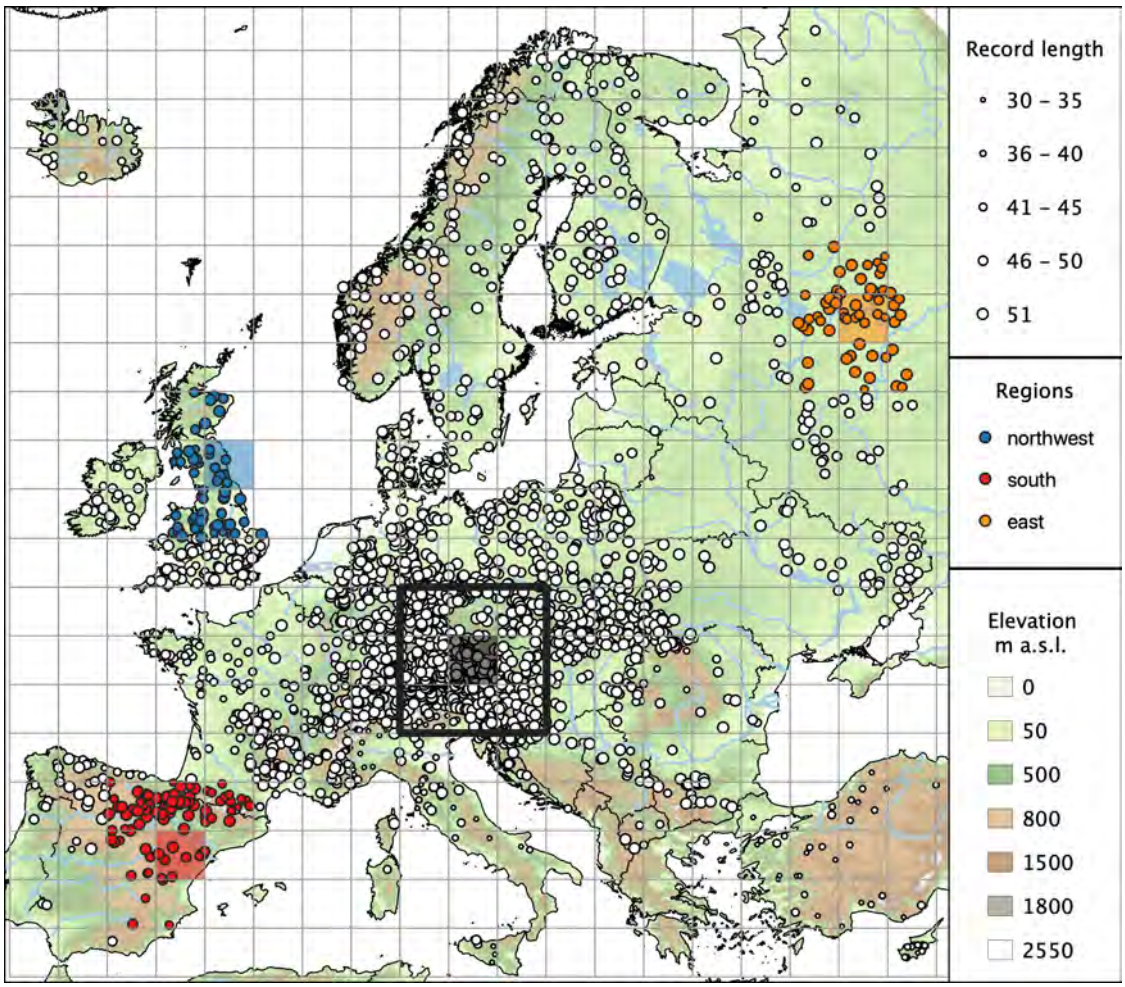

Fig. 4.1: Location of 2370 hydrometric stations in Europe and regions considered in this study. The size of the circles is proportional to the length of flood records. The grid size is 200 km. The black bordered region shows the size of the spatial moving windows analysed in Sect. 4.3.2. It consists of nine cells, corresponding to 600 km × 600 km, whose central cell is black shaded. Three regions analysed in Sect. 4.3.3, respectively located in northwestern, southern and eastern Europe, are shown with coloured circles and the shaded regions represent their central cells.

4.2.4 Drivers of flood change

Because stations with substantial artificial alterations are not included in the database, in this study we consider three potential climatic drivers of flood change: (i) extreme precipitation, (ii) antecedent soil moisture and (iii) snowmelt. For each driver we obtain catchment-averaged time series, as described in detail in the following paragraphs, which are used as covariates in the regional model of Sect. 4.2.1. Unlike Viglione et al. (2016), scale dependence is here accounted for by the data, as we use local (i.e. catchment-averaged) covariates, and not directly into the model.

Extreme precipitation

Daily series of catchment-averaged precipitation between 1960 and 2010 are calculated for each hydrometric station from the daily gridded E-OBS precipitation and the catchment boundaries.

For each station we identify a window around the average date of occurrence of floods $\bar{D}$, in which extreme precipitation is considered to be typically relevant for the generation of the annual peaks. The width of the window w is set between 90 and 360 days and it is taken proportional to $1 - R$, with R being the concentration of the date of occurrence around the average date, through the following equation:

$$w = 90 + (1 - R) \cdot 270 \; [days] \tag{4.10}$$

$\bar{D}$ and R are obtained with circular statistics (see Appendix C). The window of dates is centred around $\bar{D}$, in a way that two thirds of the window occur before the average date of occurrence of floods (as shown in Fig. 4.2 for an example series in one example year). For each year in the period of interest, we calculate the 7-day maximum precipitation within the identified window (which varies between catchments but is fixed between years).

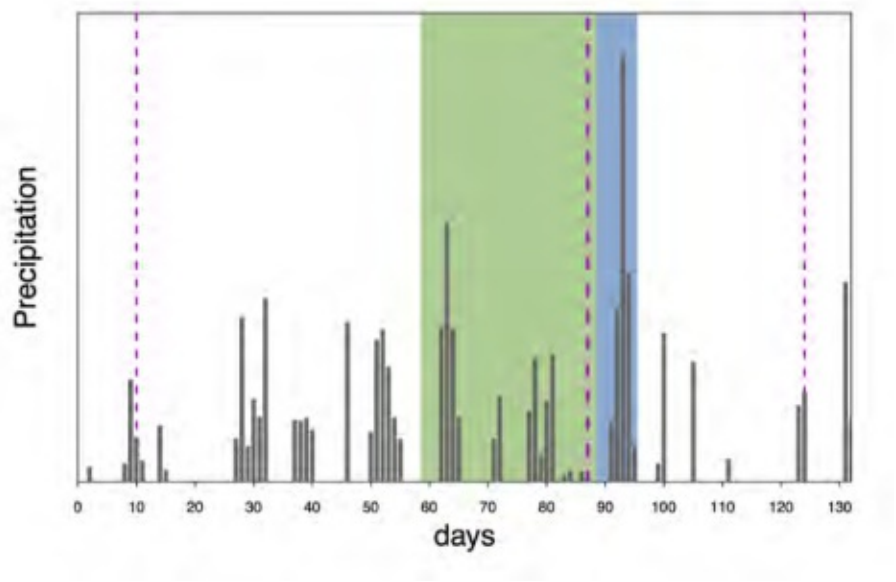

Fig. 4.2: Procedure used to obtain the time series of extreme precipitation and antecedent soil moisture index. The figure shows the daily series of catchment-averaged precipitation for one example station in one example year. The thick dashed magenta line represents the average date of occurrence of annual floods for the example station and the two thin dashed lines indicate the window of dates around the average date of occurrence, where extreme (7-day maximum) precipitation is selected (blue area). The respective preceding 30-day precipitation (green area) is representative of the antecedent soil moisture. The procedure is repeated for every year in the period of interest and every hydrometric station.

Antecedent soil moisture index

An index of antecedent soil moisture is obtained from daily catchment-averaged precipitation. For each year and each station, we calculate the 30-day precipitation preceding the 7-day window identified for extreme precipitation above. We use this index (for brevity, hereinafter referred to as 'antecedent soil moisture') based on precipitation instead of modelled soil moisture, as in Blöschl et al. (2019), in order to more strongly rely on observational data.

Snowmelt

Similar to precipitation, daily series of catchment-averaged temperature between 1960 and 2010 are obtained for each hydrometric station. We calculate daily series of catchment-averaged snowmelt according to a simple degree-day model (Parajka and Blöschl, 2008) as a function of mean daily air temperature T_A and precipitation P:

$$M = \begin{cases} 0 & for\ T_A < T_m \\ \min\left(\mathrm{DDF} \cdot (T_A - T_m); P_s\right) & for\ T_A \geq T_m \end{cases} \tag{4.11a}$$

$$P_S = \begin{cases} P & for\ T_A < T_s \\ P \cdot \frac{T_R - T_A}{T_R - T_S} & for\ T_S \leq T_A \leq T_R \\ 0 & for\ T_A > T_R \end{cases} \tag{4.11b}$$

Where M and P_s are the daily snowmelt depth and snow water equivalent storage, DDF is the degree day factor and T_m, T_s and T_R are the temperature thresholds that control the occurrence of melt, snow and rainfall, respectively. Here we assume $T_m = T_s = 0°$ C, $T_R = 2.5°$ C and DDF $= 2.5$ mm day^{-1} °C^{-1} (Parajka and Blöschl, 2008; He et al., 2014). For each station, the time series of 7-day maximum snowmelt is obtained from daily snowmelt, using the same procedure illustrated above for the case of extreme precipitation.

As in Bertola et al. (2019), this study aims at attributing flood changes to the long-term evolution of the covariates rather than their year-to-year variability. For this reason, we smooth the annual series of the drivers with the locally weighted polynomial regression LOESS (Cleveland, 1979) using the R function *loess*. The subset of data over which the local polynomial regression is performed is 10 years (i.e. 10 data-points of the series) and the degree of the local polynomials is set equal to 0, which is equivalent to a weighted 10-year moving average.

In this chapter, we select the potential drivers within the average season of occurrence of floods, as opposed to Chapter 3. This is necessary in order to take into account the large variability in flood types and seasonality across European regions, which is not observed within Upper Austria. Furthermore, in this chapter we separate the contribution of extreme precipitation (7-day maximum precipitation) and antecedent soil moisture (30-day precipitation antecedent the 7-day maximum window), while annual total precipitation is used in Chapter 3 as an indicator of both event precipitation and antecedent moisture conditions. This is because the climatic drivers are here used simultaneously in the non-stationary model (Sect. 4.2.1) as opposed to Chapter 3 where the potential atmospheric drivers were alternatively used (Sect. 3.3.4)."

4.2.5 A priori on model parameters

In the attribution analysis we use informative priors on the parameters controlling the relationship between flood and covariate changes (Bertola et al., 2019, see). This is done because we do not want to use the time patterns of the covariates X_i only to discriminate between drivers, which may lead to spurious correlations, but to hydrologically 'inform' the attribution analysis. Therefore, we set a priori constraints on the model parameters, based on qualitative reasoning and on prior literature. Given the covariates considered in this study, the elasticities of flood quantiles to the drivers (defined in Eq. 4.5) are expected to be positive (i.e. we expect the

changes in X_i and q_T to have the same sign). For T=2 and 100 years, this translates respectively into:

$$\alpha_{2_i} > 0 \tag{4.12a}$$

$$\alpha_{2_i} + \alpha_{g_i}\left(1 - \frac{1}{1 + x'_{100}}\right) > 0 \tag{4.12b}$$

Eq. 4.12a represents the lower limit for the elasticity parameters of q_2. The lower limit for α_{g_i} is obtained from Eq. 4.12b and depends on α_{2_i} and on the growth factor:

$$\alpha_{g_i} > -\frac{\alpha_{2_i}}{1 - \frac{q_2}{q_{100}}} \tag{4.13}$$

For simplicity, we assume $q_{100} = 2q_2$ as a reasonable approximation valid for Europe (Blöschl et al., 2013b; Alfieri et al., 2015), and we simplify Eq. 4.13 to:

$$\alpha_{g_i} > -2\alpha_{2_i} \tag{4.14}$$

The prior distributions of α_{2_i} and on α_{g_i} are modelled as normal distributions $\mathcal{N}(0, 2)$ with truncated lower tail, as summarised in Tab. 4.1. For the remaining parameters we set an improper uniform prior distribution.

Parameter	Meaning	Lower limit	Distribution type
α_{2_1}	Elasticity of q_2 to X_1	0	Truncated normal
α_{2_2}	Elasticity of q_2 to X_2	0	Truncated normal
α_{2_3}	Elasticity of q_2 to X_3	0	Truncated normal
α_{g_1}	Elasticity of x'_{100} to X_1	$-2\alpha_{2_1}$	Truncated normal
α_{g_2}	Elasticity of x'_{100} to X_2	$-2\alpha_{2_2}$	Truncated normal
α_{g_3}	Elasticity of x'_{100} to X_3	$-2\alpha_{2_3}$	Truncated normal

Tab. 4.1: A priori on model elasticity parameters

4.2.6 Regional analyses

Following the spatial moving window approach of Bertola et al. (2020), we identify several regions of size 600 km × 600 km across Europe, which overlap by 200 km in both directions. We fit the regional flood change model of Sect. 4.2.1 to pooled flood and covariate data of sites within each region. The resulting 200 km x 200 km grid cells are shown in Fig. 4.1 and each of the considered regions is composed of nine adjacent cells, (e.g. the black bordered region in Fig. 4.1). In each region, we estimate the elasticity of q_2 and q_{100} to the drivers X_i and the contribution of each driver to flood changes, obtained by multiplying the elasticity by the average driver trend in the region (Eq. 4.6). In regions where the average 7-day maximum snowmelt is less than 2 mm/day, only extreme precipitation and antecedent soil moisture are considered as potential drivers (i.e. Eq. 4.4a and 4.4b are modified by removing the contribution of X_3). The resulting elasticity and contribution are plotted in the central 200 km x 200 km cell of the region (e.g. the shaded cell in the black bordered region in Fig. 4.1). The rationale of the homogeneity assumption is that the spatial windows, given their size, have rather homogeneous climatic conditions (and hence flood generation processes and processes driving flood changes) relative to the overall variability within Europe. In a second step, the elasticities of flood quantiles to the drivers and their contributions

to flood change are further analysed as a function of the return period, for three regions located respectively in northwestern, southern and eastern Europe (see Fig. 4.1).

4.3 Results

4.3.1 Drivers of flood change

Time series of catchment-averaged (i) extreme precipitation, (ii) antecedent soil moisture and (iii) snowmelt are obtained for each hydrometric station for the period 1960-2010, as described in Sect. 4.2.4 Figure 4.3 shows maps of the mean value and the change of these drivers in the period of interest. Extreme precipitation (Fig. 4.3a) exhibits its largest mean values in central and western Europe, particularly in the Alpine region and on the western Atlantic coast. Positive changes of extreme precipitation are observed in the Alpine region, northwestern and central Europe, Scandinavia and Poland; negative changes are observed in southern countries and in few spots in central Europe (Fig. 4.3d). Similar spatial patterns appear for antecedent soil moisture (Fig. 4.3b and 4.3e), but the negative changes tend to be more widespread and with stronger (negative) magnitude. Mean snowmelt is largest in northeastern Europe and in the Alpine region (Fig. 4.3c). Its changes are mostly negative across all Europe, with the exception of the very North and few isolated spots (Fig. 4.3f).

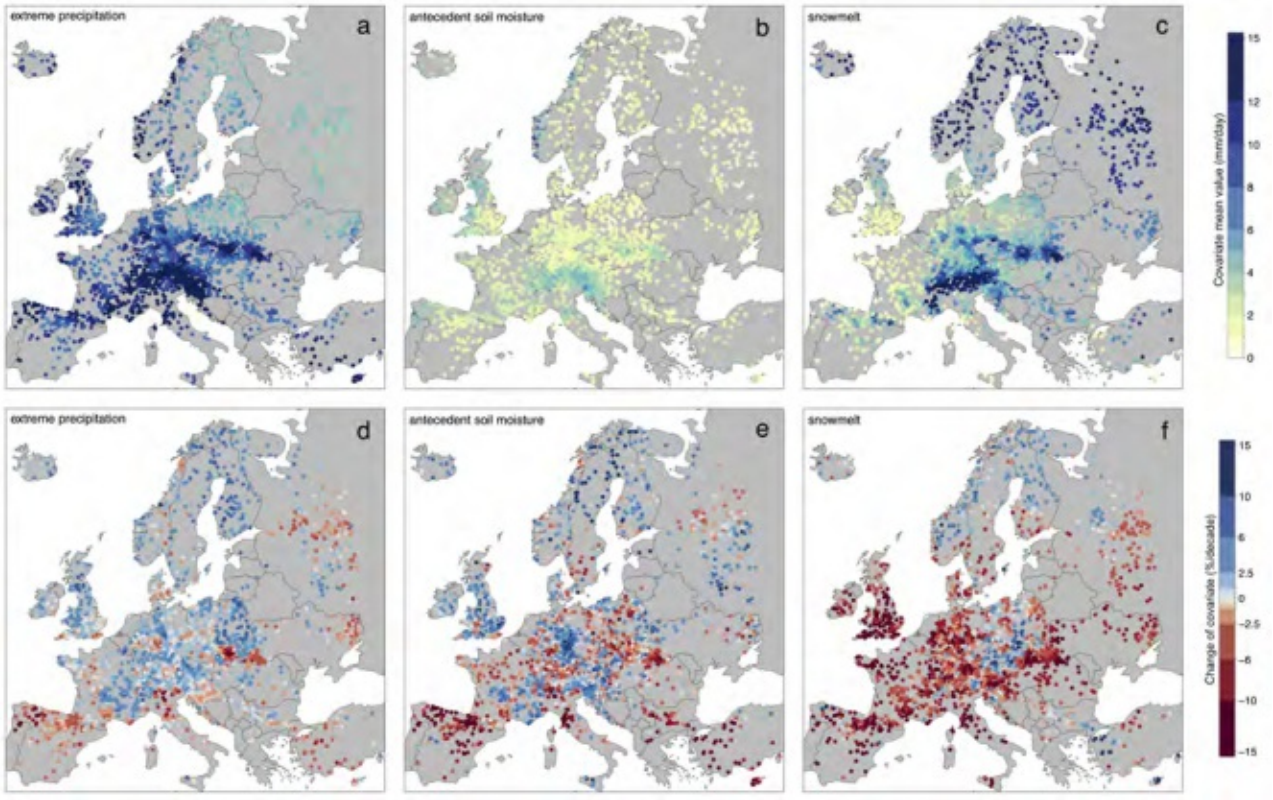

Fig. 4.3: Mean value and change of catchment-averaged extreme precipitation (a,d), antecedent soil moisture (b,e) and snowmelt (c,f) for each station over the period 1960-2010.

4.3.2 Contributions of the drivers to flood change across Europe

The obtained time series of catchment-averaged extreme precipitation, antecedent soil moisture and snowmelt are used as covariates in the regional driver-informed model. Figure 4.4 shows maps of the elasticity of the 2-year flood q_2 and the 100-year flood q_{100} to each of the three drivers, as defined in Eq. 4.5, resulting from fitting the regional model to the pooled flood and covariate data in moving windows across Europe. The value of the posterior median of the elasticities is shown together with the 90% credible bounds. The elasticity of q_2 to extreme precipitation (Fig. 4.4a) is large (0.6 to 1.5) in western, central and southern Europe and lower values (0 to 0.25) are observed in northeastern Europe. Similar values of elasticity to extreme precipitation are observed for the 100-year flood across Europe (Fig 4.4b), with small differences in northeastern Europe. This means that the elasticity of flood quantiles to extreme precipitation does not vary much with return period. In contrast, the elasticity of flood quantiles to soil moisture decreases with return period (Fig. 4.4b and 4.4e) and it is largest in southern Europe (0.25 to 0.6). Overall, the elasticities of q_2 and q_{100} to soil moisture are smaller than those to extreme precipitation. The elasticity of floods to snowmelt is largest in northeastern Europe (Fig. 4.4c and 4.4d), where values above 1 are observed (i.e. a change of 1% in snowmelt translates into a change in flood quantiles larger than 1%). In northeastern Europe the elasticities of q_2 and q_{100} to snowmelt are similar, while in central Europe and the Balkans they decrease with the return period.

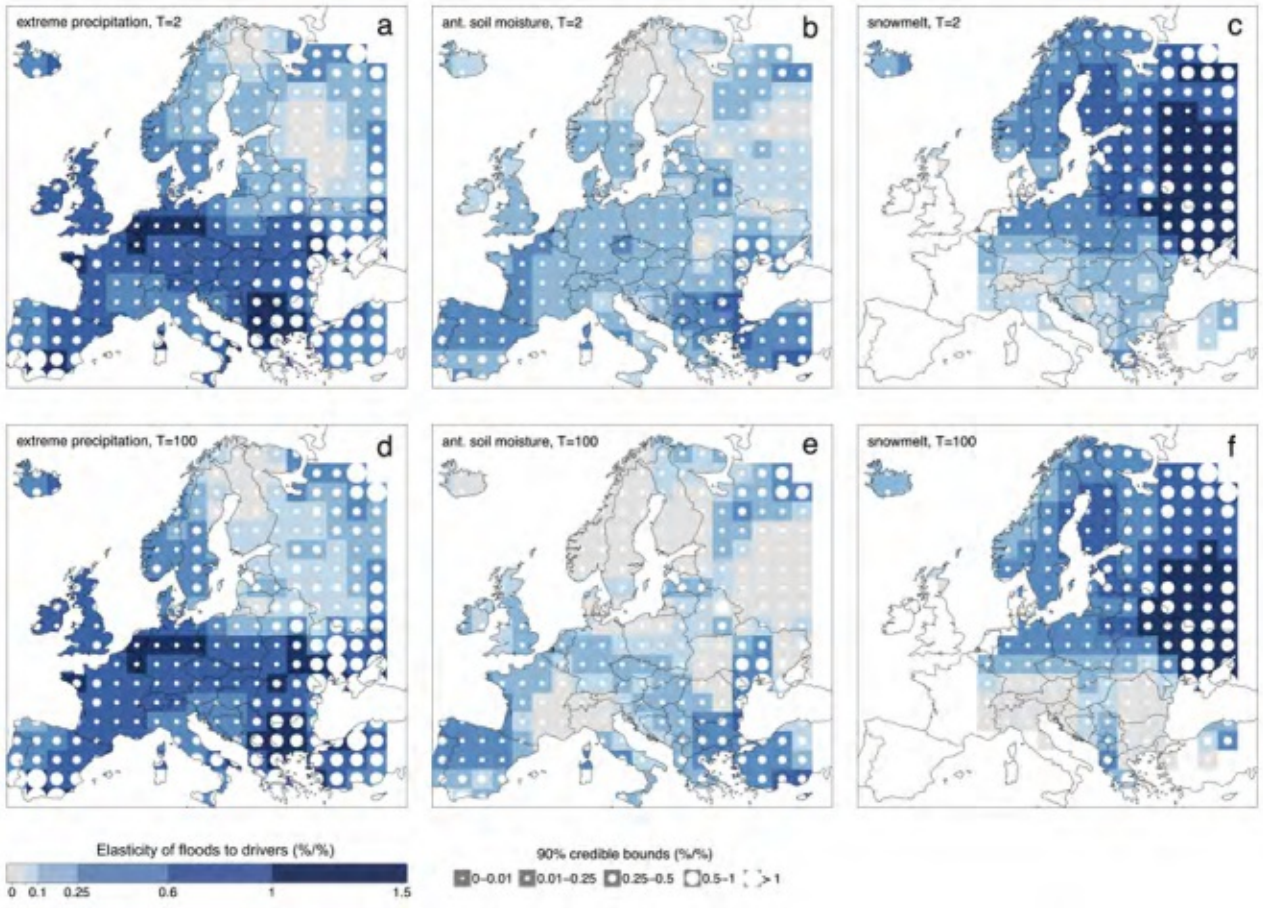

Fig. 4.4: Elasticity of the 2-year flood q_2 (upper panels) and the 100-year flood q_{100} (lower panels) to extreme precipitation (a, d), antecedent soil moisture (b, e) and snow melt (c, f). The median value of the posterior distribution of the elasticity is shown in each region with colours and the size of the white circles is proportional to the respective 90% credible bounds. The maps are shown for hypothetical catchment area of 1000 km^2

Figure 4.5 shows maps of the contributions of each of the three drivers to changes in q_2 and q_{100}, as defined in Eq. 4.6. They are obtained by multiplying the elasticities of flood quantiles to the drivers by the actual changes (in % per decade) in the drivers over the period 1960-2010 (Eq. 4.6) and represent the change in flood quantiles, in % per decade, caused by the change in a specific driver. Extreme precipitation (Fig. 4.5a and 4.5d) contributes positively to flood changes in northwestern and central Europe, and negatively in southern and eastern Europe. The absolute value of the contributions of extreme precipitation appears to slightly decrease when moving from q_2 to q_{100}. Antecedent soil moisture contributes mostly to negative flood changes in southern Europe (Fig. 4.5b and 4.5e) and the magnitude of this contribution decreases with the return period. The contributions of snowmelt to changes in q_2 and q_{100} are predominantly negative and marked in Eastern Europe, with small differences towards smaller contributions in absolute values with return period (Fig. 4.5c and 4.5f). In contrast, snowmelt contributes to positive flood changes in Scandinavia, and to a lesser extent for q_{100} than for q_2. Overall the uncertainties associated with the contribution of the drivers to changes in q_{100} do not seem to increase much compared to q_2.

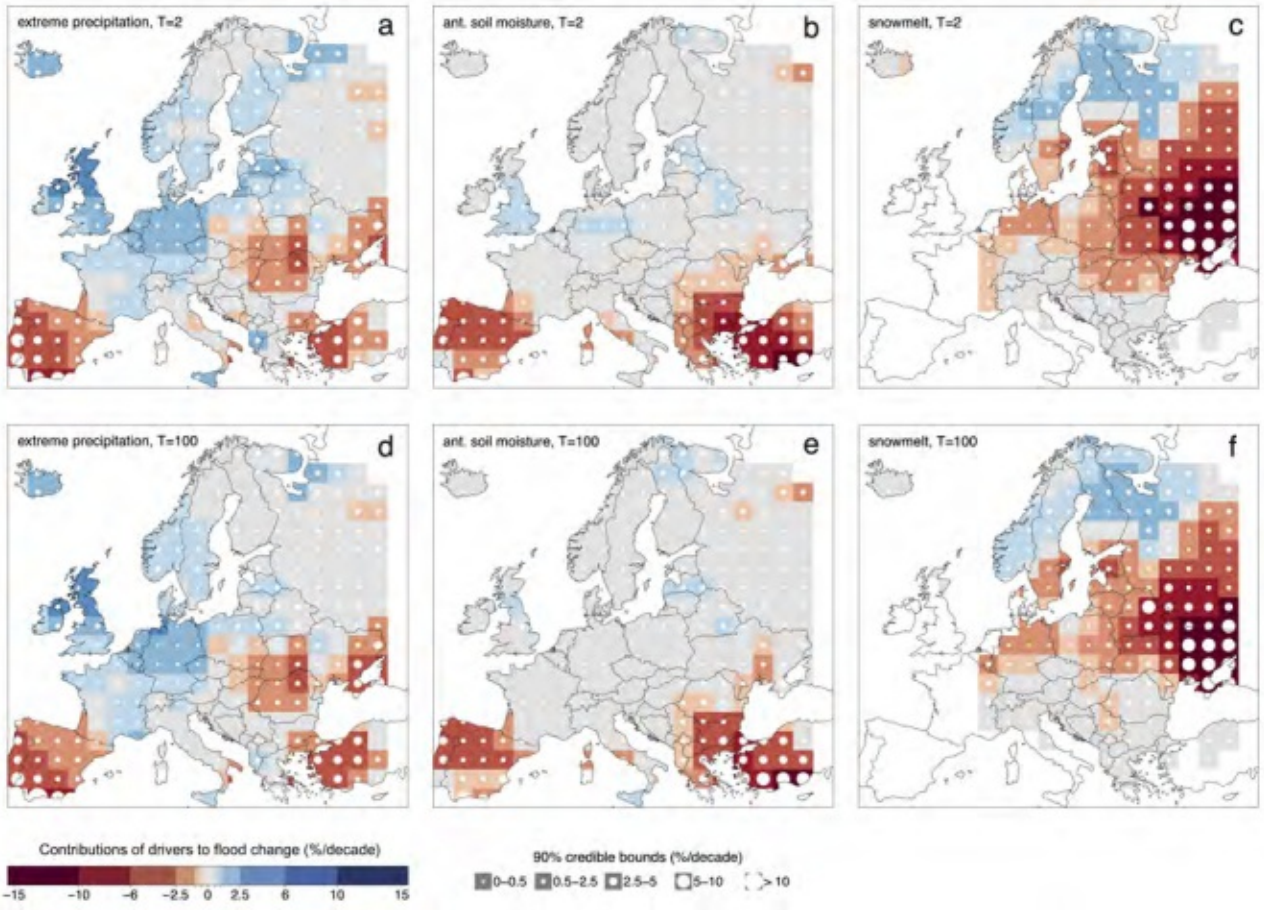

Fig. 4.5: Same as Fig. 4.4, but for contributions of extreme precipitation (a, d), antecedent soil moisture (b, e) and snow melt (c, f) to changes in q_2 and q_{100}.

In order to further investigate the differences in terms of (absolute) contributions of the drivers to changes in large (i.e. q_{100}) versus small floods (i.e. q_2), we compute for each driver the ratio between these two quantities (Fig. 4.6). In the case of extreme precipitation (Fig. 4.6a), the ratio between its contributions to changes in q_{100} and q_2 is between 0 and 1 in the Atlantic region, Spain, Italy, the Balkans, southern Germany, Austria and Finland, i.e., in these regions the contribution of extreme precipitation to changes in q_{100} is smaller, in absolute value, compared to changes in q_2. In southern France, eastern Europe and Turkey the opposite is observed (i.e. the ratio is larger than 1). Antecedent soil moisture and snowmelt generally contribute less to changes in q_{100} compared to q_2 (Fig. 4.6b and 4.6c). Large uncertainties in the ratio of elasticities are observed in northeastern Europe, in the case of extreme precipitation and antecedent soil moisture (Fig. 4.6a and 4.6b), and in southern Europe, in the case of snowmelt (Fig. 4.6c), and they result from values of the contribution of the drivers to q_2 that are close to zero in these regions (see Fig. 4.5).

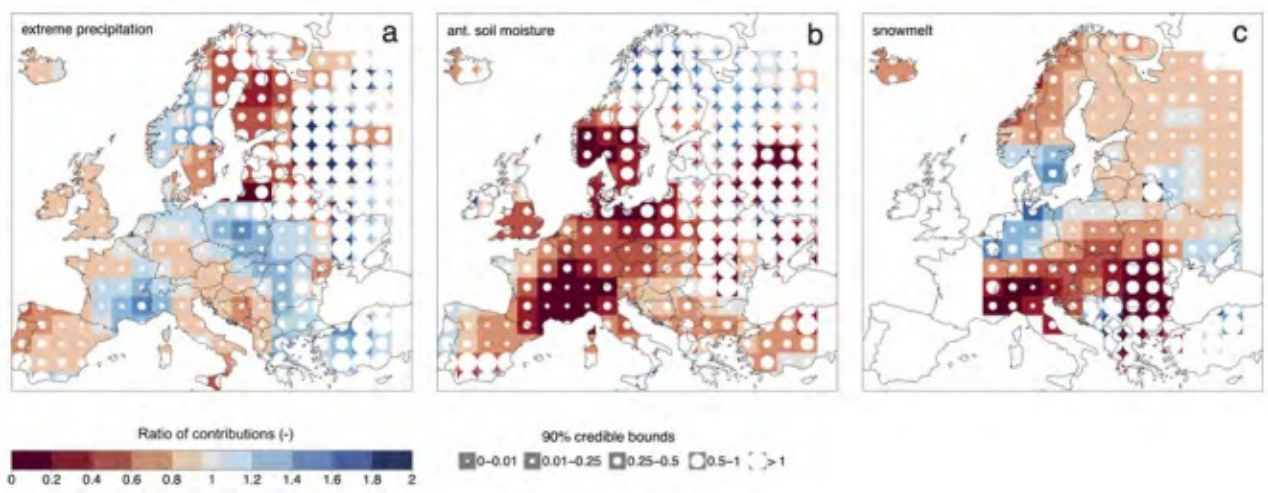

Fig. 4.6: Same as Fig. 4.4, but for the ratios of the contributions of extreme precipitation (a), antecedent soil moisture (b) and snow melt (c) to changes in q_{100} relative to q_2. Values below 1 (red colour) indicate that the contribution of the driver to q_{100} is smaller than the contribution to q_2; values above 1 (blue colour) indicate that the contribution of the driver to q_{100} is larger than the contribution to q_2.

Finally, for each region we obtain the relative contribution of the three drivers to changes in q_2 and q_{100} , as defined in Eq. 4.8 (Fig. 4.7). The relative contribution of extreme precipitation is the largest of all the drivers in most of western and central Europe for both q_2 and q_{100} (Fig. 4.7a and 4.7d). The relative contribution decreases somewhat with return period in northwestern Europe, while the opposite is the case in the South. In southern Europe antecedent soil moisture has the largest relative contribution to changes in q_2 (Fig. 4.7b) and its relative importance tends to decrease for more extreme floods (Fig. 4.7e). The relative contribution of snowmelt to flood changes clearly prevails in eastern Europe, with slightly decreasing strength for the higher return period.

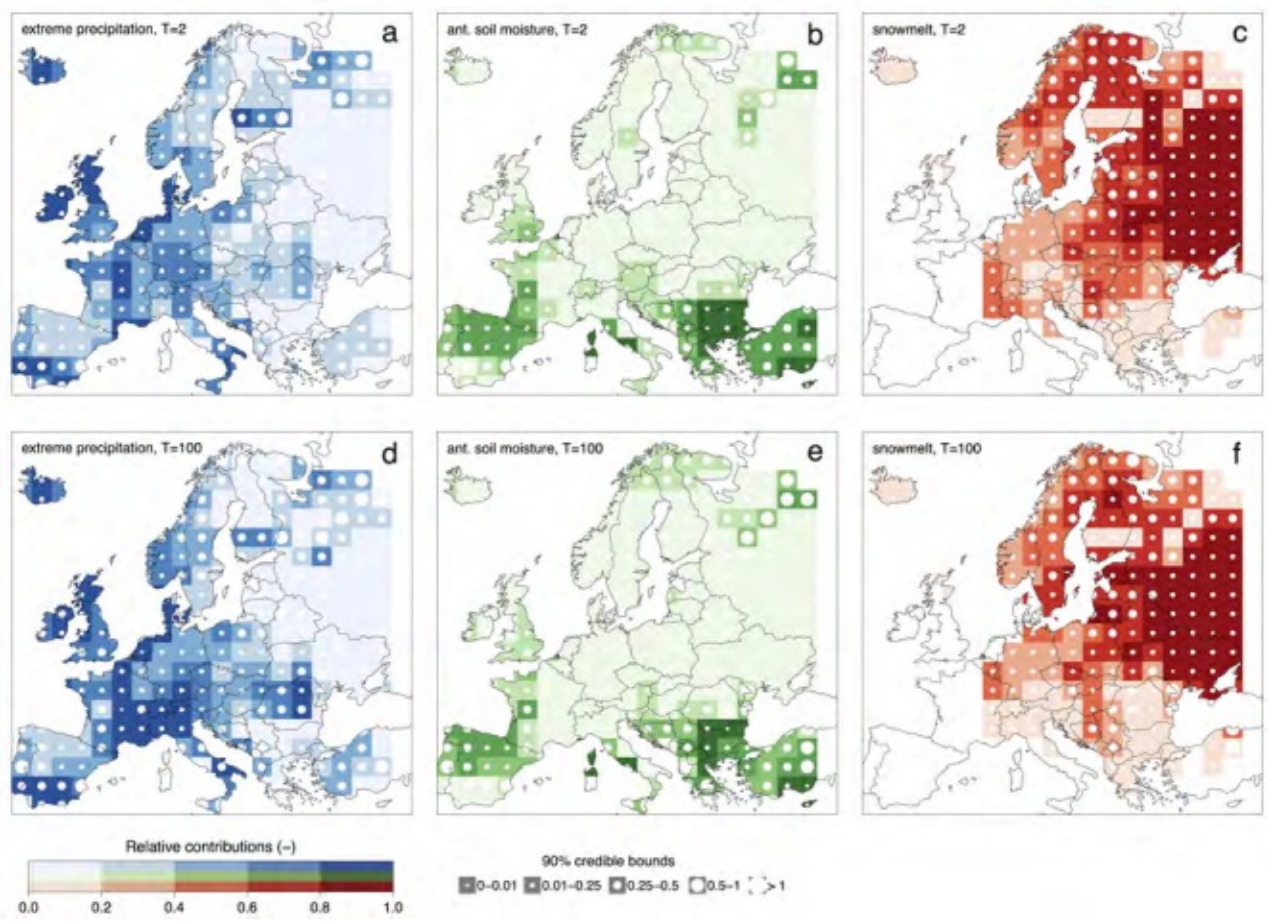

Fig. 4.7: Same as Fig. 4.4, but for relative contributions of extreme precipitation (a, d), antecedent soil moisture (b, e) and snow melt (c, f) to changes in q_2 and q_{100}.

4.3.3 Contributions to flood change of the drivers in northwestern, southern and eastern Europe

In this section we select three example regions among those analysed in Sect. 4.3.2, located respectively in northwestern, southern and eastern Europe (see Fig. 4.1). For these three regions we further show in Fig. 4.8 the elasticities of floods to the drivers (first row), the contributions (second row) and relative contributions (third row) of the drivers to flood change, as a function of the return period. In northwestern and southern Europe, snowmelt is excluded from the potential drivers as it does not represent a relevant process for most of the catchments in these regions (see Fig. 4.3c). In northwestern Europe extreme precipitation and antecedent soil moisture contribute positively to flood change, with extreme precipitation representing the most important driver. Its contribution to flood trends decreases with return period, while the contribution stays almost constant in the case of antecedent soil moisture (Fig. 4.8d and 4.8g). In southern Europe extreme precipitation and antecedent soil moisture represent both important drivers. The elasticity of floods to extreme precipitation is larger than that to antecedent soil moisture (Fig. 4.8b). However, antecedent soil moisture contributes (negatively) to a larger extent to flood changes for small return periods (i.e. T=2-10 years). Its contribution decreases in absolute values with increasing return period (Fig. 4.8e). For more extreme events (T>10 years) the relative contribution of extreme precipitation increases and becomes comparable to that of antecedent

soil moisture (Fig. 4.8h). In eastern Europe snowmelt is clearly the dominant driver at all return periods (Fig. 4.8c, 4.8f and 4.8i).

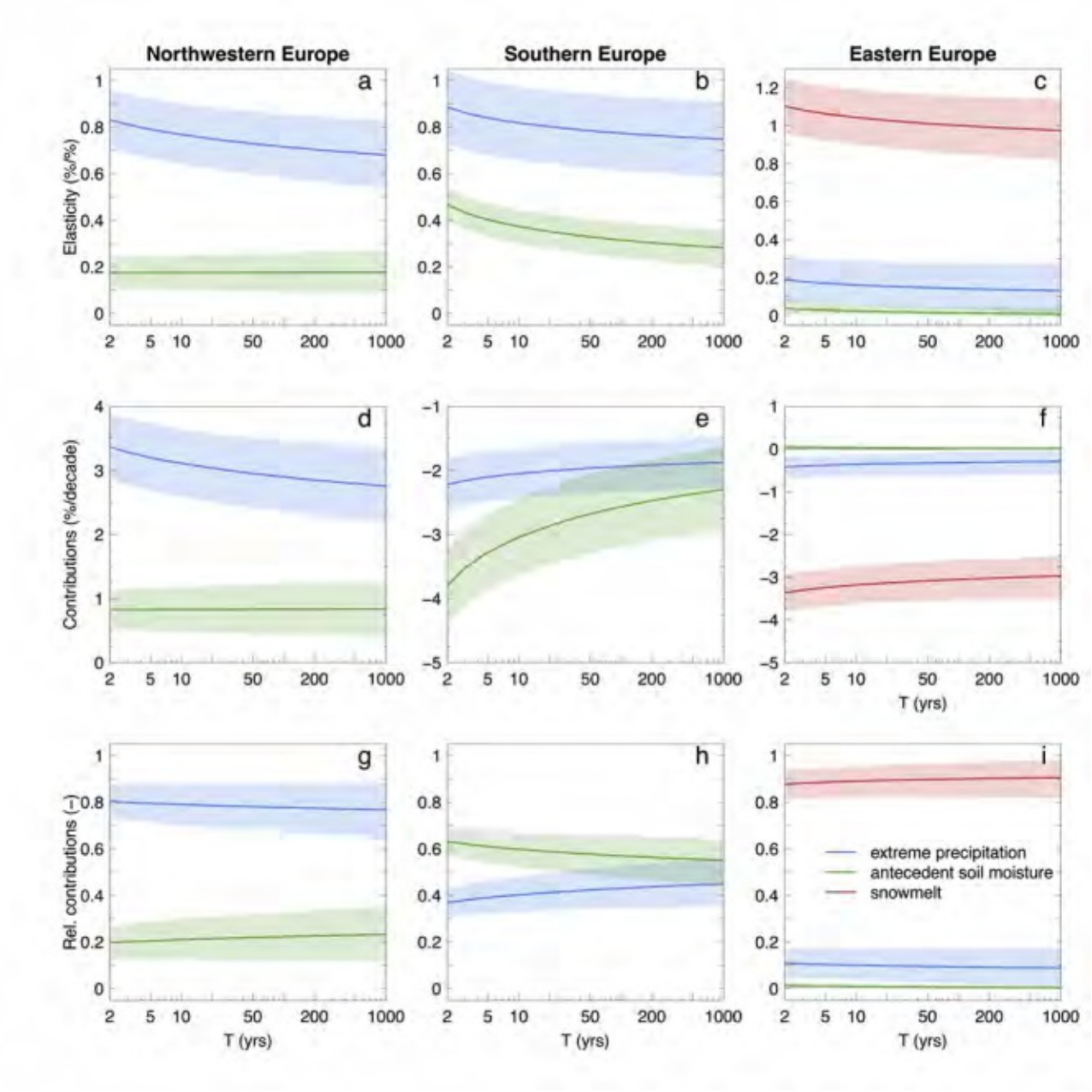

Fig. 4.8: Contributions of drivers to flood changes as a function of the return period in three regions (columns), respectively located in northwestern, southern and eastern Europe. Elasticity of floods to the drivers (a, b, c), contribution (d, e, f) and relative contribution (g, h, i) of the drivers to flood change are shown in the rows. The thick lines and the shaded areas represent respectively the median and the 90% credible intervals of their posterior distributions. The results are shown for hypothetical catchment area of 1000 km^2.

4.4 Discussion and conclusions

In this study, we attribute the changes in flood discharges that have occurred in Europe during the period 1960-2010 (Blöschl et al., 2019; Bertola et al., 2020) to potential drivers as a function of the return period, while previous detection and attribution studies have generally focused on the mean flood behaviour. In particular, we compare the relative contribution of extreme precipitation, antecedent soil moisture and snow melt to changes in the median and the 100-year flood. The attribution study is framed in terms of a non-stationary flood frequency analysis and the parameters of the distribution are estimated in a regional context with Bayesian inference.

Our results suggest that in northwestern and eastern Europe, changes in small and large floods are driven mainly by one single driver, which dominates at all return periods. In northwestern Europe, extreme precipitation contributes to changes in both q_2 and q_{100} for the most part and the contribution of antecedent soil moisture is of secondary importance. Similarly, in eastern Europe, snowmelt clearly drives flood changes at all return periods. In southern Europe both antecedent soil moisture and extreme precipitation significantly contribute to flood changes and their relative importance depends on the return period. Antecedent soil moisture contributes the most to changes in small floods (i.e. T=2-10 years), while the two drivers contribute with comparable magnitude to changes in more extreme events (T>10 years). Given the relative driver contributions and their credible bounds obtained in the analysis, the findings suggest that is indeed possible to identify the relative contributions to q_2 and q_{100} clearly.

The contribution of extreme precipitation is positive in northwestern Europe (about 3.3 to 2.8% per decade in Fig. 4.8) and decreases slightly with return period. In contrast, extreme precipitation in southern Europe contributes to 37 to 45% of the negative flood changes (corresponding to -2.2 to -1.8% per decade), depending on the return period. The contribution of antecedent soil moisture is negative in southern Europe and decreases in absolute value (from -3.8 to -2.3% per decade) with the return period. Finally, snowmelt strongly contributes to negative flood changes (about -3% per decade) in a similar way at all return periods. The sum of the contributions of the drivers of Fig. 5 is in overall agreement with the flood change patterns and trend magnitudes found by Blöschl et al. (2019) and Bertola et al. (2020), with the exception of Scandinavia, where the contributions of the drivers are all positive or close to zero, while mostly moderate negative flood trends were observed in previous studies (Blöschl et al., 2019; Bertola et al., 2020). This discrepancy points to other drivers not accounted for in the presented model, such as river regulation effects (Arheimer and Lindström, 2019), or non linear relationships between the drivers not captured by the model.

Prior information on the elasticities is used in order to 'inform' the attribution analysis, based on hydrological reasoning and the literature. Specifically, the prior distribution of the elasticities of q_2 and q_{100} to the drivers are assumed positive. This is because any changes in the considered covariates are expected to translate into flood changes with the same sign. In practice, the prior distribution of the elasticity of q_{100} is reflected in a lower bounded prior distribution on the elasticity of the growth factor x'_{100}, which depends on the ratio between q_{100} and q_2 (Sect. 4.2.5). For simplicity, we assume this ratio approximately equal to 2. This assumption is reasonably valid for humid catchments (see e.g., Blöschl et al., 2013b) and is in overall agreement with flood maps of the mean annual flood and q_{100} in Europe presented by Alfieri et al. (2015). However, in arid regions, larger values of this ratio (e.g. 4, see Blöschl et al., 2013b) would be more appropriate (corresponding to stricter priors on the elasticity of the growth factor) because the flood frequency curves tend to be steeper.

We fitted the change model of Sect. 4.2.1 to the pooled flood and covariate data of several regions across Europe, where elasticities of flood quantiles to their drivers are assumed homogeneous. This assumption is reasonable because of the spatial proximity of the catchments that is reflected

into similar climatic conditions, flood generation processes and processes driving flood changes. The attribution analysis is thereby performed at the regional scale, where average regional contributions of the decadal changes in the drivers to average regional trends in flood quantiles are estimated. Figure 4.8 shows the contributions of the drivers to flood changes as a function of the return period for three regions selected respectively in northwestern, southern and eastern Europe. Similar results would be obtained by fitting the model to larger regions over northwestern, southern and eastern Europe, that present comparatively homogeneous flood regime changes and processes driving flood changes (e.g. the three macro-regions in Blöschl et al. (2019) and Bertola et al. (2020)).

Overall the obtained uncertainties associated with the contribution of the drivers to changes in q_{100} do not seem to increase much compared to q_2, while a relevant increase would be reasonably expected. These results are valid under the assumption of the adopted model (i.e. Gumbel distribution) which may be too stringent. The model assumptions could be relaxed (e.g. adopting a Generalized Extreme Value distribution) in order to allow for larger model flexibility.

Spatial cross-correlation of floods at different sites is taken into account through an approach based on a magnitude adjustment to the likelihood. This results in larger uncertainties of the posterior distribution of the estimated parameters, compared to the case where floods are considered spatially independent.

As already noted, one of the main assumptions in our analysis is that the three drivers, i.e., extreme precipitation, soil moisture and snowmelt, are the only candidates for explaining river flood changes. The effects of other drivers not accounted for in this study, such as land cover change or river regulation, are probably not very large at the scale of Europe as we are focusing on catchments with minimum alteration. However, in contexts where anthropogenic alterations are important it will be useful to extend the analysis for such effects. This attribution analysis may be repeated with catchment (e.g. land-use or land-cover changes) and river drivers (e.g. construction of reservoirs in the catchment) in addition to atmospheric covariates, if detailed information about changes in land-use/land-cover and river structures were available for European catchments and flood data of affected stations were collected.

This study complements recent research on past changes in European floods by formally attributing the detected trends to potential drivers (i.e., extreme precipitation, antecedent soil moisture and snowmelt) as function of return period. The proposed method allows to identify the relative contribution of different drivers to changes in flood quantiles and to estimate the sign and magnitude of these contributions. The results show that in northwestern and eastern Europe changes in both the 2-year and the 100-year flood are driven by a single driver only (i.e. respectively extreme precipitation and snowmelt), while in southern Europe two drivers contribute to flood changes (i.e. soil moisture and extreme precipitation), with different relative contributions depending on the return period. Even though this study focuses on observed flood changes, the understanding of past processes is a fundamental step for the prediction of flood changes in future climate scenarios.

Chapter 5

Summary of the results and overall conclusions

This thesis complements recent research on flood regime changes in Europe (see e.g., Blöschl et al., 2017; Mangini et al., 2018; Blöschl et al., 2019; Kemter et al., 2020) in terms of both flood change detection and attribution to potential drivers. The results presented in this thesis contribute to a better understanding of the flood regime changes occurred in Europe during five decades (i.e. 1960-2010), by assessing regional flood trends as a function of the return period, as typically only changes in mean flood characteristics were investigated, and by estimating the relative contribution of three relevant climatic drivers to these trends. Two original approaches for the attribution of flood changes are proposed and applied at different scales.

In Chapter 2, regional trends of selected flood quantiles (i.e. the median and the 100-year flood), and the related uncertainties, are estimated and compared across Europe with a regional non-stationary flood frequency analysis, for different hypothetical catchment sizes between 1960 and 2010. Distinctive patterns of flood regime change are identified for large regions across Europe which depend on flood magnitudes and catchment areas. Results show that in northwestern Europe the trends in flood magnitude are generally positive. In small catchments (up to 100 km^2), the 100-year flood increases more than the median flood, while the opposite is observed in medium and large catchments. In southern Europe flood trends are generally negative. The 100-year flood decreases less than the median flood and, in the small catchments, the median flood decreases less compared to the large catchments. In eastern Europe the regional trends are negative and do not depend on the return period, but catchment area plays a substantial role: the larger the catchment, the more negative the trend.

In Chapter 3 a data-based attribution approach is proposed for selecting which driver best relates to variations in time of the flood frequency curve. This approach considers three groups of potential drivers (i.e. atmospheric, catchment and rivers system drivers) and consists in comparing and selecting alternative driver-informed models at the local (catchment) scale, based on an information criterion. The parameters of this attribution model are estimated by Bayesian inference. Prior information on one of these parameters (i.e. the elasticity of flood peaks to each driver) is taken from the existing literature to increase the robustness of the method to spurious correlations between flood and covariate time series. The application of this approach to a case study, consisting of 96 gauges in Upper Austria where flooding has become more intense during the last 50 years, made possible to identify changes in daily rainfall as the most probable cause of flood change, as well as to exclude the influence of human intervention on catchments and rivers.

In Chapter 4 we extend the approach of Chapter 3 to estimate the relative contributions of potential drivers to the flood changes detected in Chapter 2. The attribution model, based on regional non-stationary flood frequency analysis, is applied to European flood and covariate data and aims at attributing the observed trend in the median and the 100-year flood to specific drivers. Extreme precipitation, antecedent soil moisture and snowmelt are the potential drivers considered in this chapter. Catchment area is here implicitly taken into account by the use of local (i.e. catchment-averaged) covariates in the model. Results show that, in northwestern Europe, extreme precipitation mainly contributes to changes in both the median (q_2) and 100-year

flood (q_{100}), while the contributions of antecedent soil moisture are of secondary importance. In southern Europe, both antecedent soil moisture and extreme precipitation contribute to flood changes, and their relative importance depends on the return period. Antecedent soil moisture is the main contributor to changes in q_2, while the contribution of the two drivers to changes in larger floods (T>10 years) are comparable. In eastern Europe, snowmelt drives changes in both q_2 and q_{100}.

The results presented in this thesis are valid under the assumptions carefully described in each chapter and ways to overcome them are discussed. In particular, for simplicity and robustness, we assume flood peaks to follow the Gumbel distribution (Extreme Value distribution type I). Other distributions typically recommended by national guidelines, such as the generalized extreme distribution (GEV), could also be assumed. Salinas et al. (2014b) analysed the suitability of several two- and three-parameter distributions for flood frequency analysis in Europe. They showed that the Gumbel distribution well represents sample L-moment ratios in medium to large catchments, while the GEV distribution is the most suitable and versatile distribution for all catchment scales and climates, among those analysed. However, because the estimate of the GEV shape parameter is typically associated with high uncertainties (Coles and Tawn, 1996; Papalexiou and Koutsoyiannis, 2013) and in regional analyses it is often assumed constant for all sites within a region (see e.g. Renard et al., 2006a; Lima et al., 2016), we assume it equal to 0 (i.e. we assume a Gumbel distribution). The analyses presented in this thesis could be repeated relaxing this hypothesis and assuming more flexible distributions, such as the GEV distribution. Based on Salinas et al. (2014b) we expect this assumption to have effects mainly in arid and small catchments, which are typically associated with more skewed distributions.

In this thesis, log-linear and log-log non-stationary models are adopted to describe the potential relationships between floods and time (Chapter 2) or time-varying covariates (Chapter 3 and Chapter 4). The advantage of using log-linear and log-log models is that the elasticity of floods to the covariates (expressed as a percentage change) is directly represented by a parameter of the regression model. Other relationships with time or time-varying covariates could be investigated, such as linear (e.g. Renard et al., 2006b; Šraj et al., 2016; Steirou et al., 2019) or polynomial functions (e.g. Silva et al., 2017). The choice of the non-stationary model has clearly an effect on the results of the attribution analysis, which strongly depend on the model type and on the selected covariates. For instance, non-linear relationships between the drivers may be not captured by the assumed models or useful drivers (or combination of drivers) may have been left out.

The regional models of Chapter 2 and Chapter 4 are applied to several regions across Europe under the homogeneity assumption. This assumption is supported by evidence of flood similarity in terms of flood seasonality and trends in the mean annual flood (Blöschl et al., 2017; Blöschl et al., 2019), but this is not formally tested in this thesis, for which new methods should be developed ad hoc. In the attribution analyses (Chapter 3 and Chapter 4) we also make the assumption that flood changes can be fully explained by one driver, or by a combination of drivers, among those considered. In few sites or regions this resulted in difficulties to attribute observed flood trends to the pre-selected set of drivers and highlighted the need to further expand the analysis to other potential drivers.

Spatial cross-correlation of floods in regional analyses is taken into account through an approach based on a magnitude adjustment to the likelihood function in the Bayesian framework (Chapter 2 and Chapter 4). This approach consists in scaling the likelihood with a proper exponent and results in inflating the posterior variance of the estimated parameters, reflecting the overall effect of spatial dependence in the data (see Appendix B). Other approaches to obtain confidence intervals that account for spatial dependence may be adopted, such as bootstrap techniques (Efron, 1982; Efron and Tibshirani, 1986) with frequentist inference. These techniques allow to obtain

an approximation of the distribution of a statistic of interest from a large number of synthetic samples, generated by resampling the initial data with replacement. Moving block bootstrap (Künsch, 1989; Liu, Singh, et al., 1992) is adopted for bootstrapping time series, where the actual sequence of observations is relevant. It consists of resampling blocks of observations rather than single data points. This approach can be extended to spatial data by block bootstrapping in the same way in all data (spatial) dimensions. The advantage of this technique is that it preserves the cross correlation between timeseries without requiring its explicit estimation. The disadvantage is that it is computationally intensive, and it is sensitive to the size of the blocks (Wilks, 1997).

Unlike in Chapter 3, the effect of river structures on floods was not investigated in Chapter 4 because hydrometric stations strongly affected by dams were not included in the European flood database. In the next research phase, flood data from sites under anthropogenic effects will be collected and the effect of the construction of reservoirs on flood changes across Europe will be investigated.

This thesis contributes to the advancement of flood hydrology in two ways. First, it proposes two new data-based attribution approaches to formally identify drivers (Chapter 3) and estimate their contributions to flood changes as a function of return period (Chapter 4), at the local and regional scales. These approaches may be generalized and applied in other regions, where the explanation of past flood changes are of interest. Second, this thesis improves the understanding of past flood regime changes across Europe and it represents a continental-scale detection and attribution study. It shows differences between trends in big and small flood events and provides explanatory drivers. These results are useful for interpreting decadal changes in flood magnitudes at the regional scale. The understanding of past flood changes is important for better informed flood management strategies.

Acknowledgements

Financial support for this thesis was provided by the European Union's Horizon 2020 Research and Innovation Programme under the Marie Skłodowska-Curie grant agreement No 676027 "System-Risk", the FWF Vienna Doctoral Programme on Water Resource Systems (W1219-N28) and the Austian Science Funds (FWF) "SPATE" project I 3174.

We acknowledge the E-OBS dataset from the EU-FP6 project UERRA (`http://www.uerra.eu`) and the Copernicus Climate Change Service, and the data providers in the ECA&D project (`https://www.ecad.eu`). This product incorporates data from the GRanD database which is ®Global Water System Project (2011).

Bibliography

Akaike, H. (1973). "Information Theory and an Extension of the Maximum Likelihood Principle". In: *Selected Papers of Hirotugu Akaike*. New York, NY: Springer New York, pp. 199–213.

Alaoui, A., M. Rogger, S. Peth, and G. Blöschl (2018). "Does soil compaction increase floods? A review". In: *Journal of Hydrology* 557, pp. 631–642. ISSN: 00221694. DOI: 10.1016/j.jhydrol.2017.12.052.

Alfieri, L., P. Burek, L. Feyen, and G. Forzieri (2015). "Global warming increases the frequency of river floods in Europe". In: *Hydrology and Earth System Sciences* 19.5, pp. 2247–2260. ISSN: 16077938. DOI: 10.5194/hess-19-2247-2015.

Amponsah, W. et al. (2018). "Integrated high-resolution dataset of high-intensity European and Mediterranean flash floods". In: *Earth System Science Data* 10.4, pp. 1783–1794. ISSN: 1866-3516. DOI: 10.5194/essd-10-1783-2018.

Archfield, S. A., R. M. Hirsch, A. Viglione, and G. Blöschl (2016). "Fragmented patterns of flood change across the United States". In: *Geophysical Research Letters* 43.19, pp. 10,232–10,239. ISSN: 00948276. DOI: 10.1002/2016GL070590.

Arheimer, B. and G. Lindström (2019). "Detecting Changes in River Flow Caused by Wildfires, Storms, Urbanization, Regulation, and Climate Across Sweden". In: *Water Resources Research* 55.11, pp. 8990–9005. ISSN: 19447973. DOI: 10.1029/2019WR024759.

Ayalew, T. B., W. F. Krajewski, R. Mantilla, D. B. Wright, and S. J. Small (2017). "Effect of Spatially Distributed Small Dams on Flood Frequency: Insights from the Soap Creek Watershed". In: *Journal of Hydrologic Engineering* 22.7, p. 04017011. ISSN: 1084-0699. DOI: 10.1061/(ASCE)HE.1943-5584.0001513.

Ban, N., J. Schmidli, and C. Schär (2015). "Heavy precipitation in a changing climate: Does short-term summer precipitation increase faster?" In: *Geophysical Research Letters* 42.4, pp. 1165–1172. ISSN: 00948276. DOI: 10.1002/2014GL062588.

Barker, L., J. Hannaford, K. Muchan, S. Turner, and S. Parry (2016). "The winter 2015/2016 floods in the UK: a hydrological appraisal". In: *Weather* 71.12, pp. 324–333. DOI: 10.1002/wea.2822.

Berg, P., C. Moseley, and J. O. Haerter (2013). "Strong increase in convective precipitation in response to higher temperatures". In: *Nature Geoscience* 6.3, pp. 181–185.

Berghuijs, W. R., S. Harrigan, P. Molnar, L. J. Slater, and J. W. Kirchner (2019). "The Relative Importance of Different Flood-Generating Mechanisms Across Europe". In: *Water Resources Research*, pp. 1–12. ISSN: 19447973. DOI: 10.1029/2019WR024841.

Bertola, M., A. Viglione, and G. Blöschl (2019). "Informed attribution of flood changes to decadal variation of atmospheric, catchment and river drivers in Upper Austria". In: *Journal of Hydrology* 577.November 2018, p. 123919. ISSN: 00221694. DOI: 10.1016/j.jhydrol.2019.123919. URL: https://linkinghub.elsevier.com/retrieve/pii/S0022169419306390.

Bertola, M., A. Viglione, D. Lun, J. Hall, and G. Blöschl (2020). "Flood trends in Europe: are changes in small and big floods different?" In: *Hydrology and Earth System Sciences* 24.4, pp. 1805–1822. ISSN: 1607-7938. DOI: 10.5194/hess-24-1805-2020.

Besselaar, E. Van den, A. Klein Tank, and T. Buishand (2013). "Trends in European precipitation extremes over 1951–2010". In: *International Journal of Climatology* 33.12, pp. 2682–2689.

Beven, K. J. et al. (2008). *FD2120: Analysis of historical data sets to look for impacts of land use management change on flood generation*. Tech. rep. Defra/EA.

Blöschl, G., R. Merz, J. Parajka, J. L. Salinas, and A. Viglione (2012). "Floods in Austria". In: *IAHS Spec. Publ.* 10, pp. 169–177.

Blöschl, G., T. Nester, J. Komma, J. Parajka, and R. A. P. Perdigão (2013a). "The June 2013 flood in the Upper Danube Basin, and comparisons with the 2002, 1954 and 1899 floods". In: *Hydrology and Earth System Sciences* 17.12, pp. 5197–5212. ISSN: 1607-7938. DOI: 10.5194/hess-17-5197-2013.

Blöschl, G., M. Sivapalan, T. Wagener, A. Viglione, and H. Savenije (2013b). *Runoff Prediction in Ungauged Basins: Synthesis across Processes, Places and Scales*. Cambridge University Press, p. 484. ISBN: 9781107028180. DOI: 10.1017/CBO9781139235761.

Blöschl, G., A. Viglione, R. Merz, J. Parajka, J. L. Salinas, and W. Schöner (2011). "Auswirkungen des Klimawandels auf Hochwasser und Niederwasser". In: *Österreichische Wasser- und Abfallwirtschaft* 63.1, pp. 21–30. ISSN: 1613-7566. DOI: 10.1007/s00506-010-0269-z.

Blöschl, G., S. Ardoin-Bardin, M. Bonell, M. Dorninger, D. Goodrich, D. Gutknecht, D. Matamoros, B. Merz, P. Shand, and J. Szolgay (2007). "At what scales do climate variability and land cover change impact on flooding and low flows?" In: *Hydrological Processes* 21.9, pp. 1241–1247. ISSN: 08856087. DOI: 10.1002/hyp.6669.

Blöschl, G. et al. (2017). "Changing climate shifts timing of European floods". In: *Science* 357.6351, pp. 588–590. ISSN: 0036-8075. DOI: 10.1126/science.aan2506.

– (2019). "Changing climate both increases and decreases European river floods". In: *Nature*. DOI: 10.1038/s41586-019-1495-6.

Bouwer, L. M. (2011). "Have disaster losses increased due to anthropogenic climate change?" In: *Bulletin of the American Meteorological Society* 92.1, pp. 39–46.

Brady, A., J. Faraway, and I. Prosdocimi (2019). "Attribution of long-term changes in peak river flows in Great Britain". In: *Hydrological Sciences Journal* 00.00, pp. 1–12. ISSN: 0262-6667. DOI: 10.1080/02626667.2019.1628964.

Bronstert, A. et al. (2007). "Multi-scale modelling of land-use change and river training effects on floods in the Rhine basin". In: *River Research and Applications* 23.10, pp. 1102–1125. ISSN: 15351459. DOI: 10.1002/rra.

Burnham, K. and D. Anderson (2002). *Model Selection and Multimodel Inference: A Practical Information-Theoretic Approach (2nd ed)*. Vol. 172, p. 488. ISBN: 978-0-387-22456-5. DOI: 10.1016/j.ecolmodel.2003.11.004. arXiv: arXiv:1011.1669v3. URL: http://linkinghub.elsevier.com/retrieve/pii/S0304380003004526.

Carpenter, B., A. Gelman, M. Hoffman, D. Lee, B. Goodrich, M. Betancourt, M. Brubaker, J. Guo, P. Li, and A. Riddell (2017). "Stan: A Probabilistic Programming Language". In: *Journal of Statistical Software, Articles* 76.1, pp. 1–32. ISSN: 1548-7660. DOI: 10.18637/jss.v076.i01.

Castellarin, A., D. Burn, and A. Brath (2008). "Homogeneity testing: How homogeneous do heterogeneous cross-correlated regions seem?" In: *Journal of Hydrology* 360.1-4, pp. 67–76. ISSN: 00221694. DOI: 10.1016/j.jhydrol.2008.07.014.

Chamen, T., L. Alakukku, S. Pires, C. Sommer, G. Spoor, F. Tijink, and P. Weisskopf (2003). "Prevention strategies for field traffic-induced subsoil compaction : a review ; part 2, Equipment and field practices". In: *Soil & tillage research : an international journal on research and development in soil tillage and field traffic, and their relationship with land use, crop production and the environment* 73.1-2, pp. 161–174. ISSN: 0167-1987.

Cleveland, W. S. (1979). "Robust Locally Weighted Regression and Smoothing Scatterplots". In: *Journal of the American Statistical Association* 74.368, pp. 829–836. DOI: 10.1080/01621459.1979.10481038.

Coles, S. and J. Tawn (1996). "A Bayesian analysis of extreme rainfall data." English. In: *Journal of the Royal Statistical Society: Series C (Applied Statistics)* 45, pp. 463–478. ISSN: 0035-9254.

Cornes, R. C., G. van der Schrier, E. J. van den Besselaar, and P. D. Jones (2018). "An Ensemble Version of the E-OBS Temperature and Precipitation Data Sets". In: *Journal of Geophysical Research: Atmospheres* 123.17, pp. 9391–9409. ISSN: 21698996. DOI: 10.1029/2017JD028200.

Cunderlik, J. M. and D. H. Burn (2003). "Non-stationary pooled flood frequency analysis". In: *Journal of Hydrology* 276.1-4, pp. 210–223. ISSN: 00221694. DOI: 10.1016/S0022-1694(03)00062-3.

Dalrymple, T. (1960). "Flood frequency methods". In: *US geological survey, water supply paper A* 1543, pp. 11–51.

Delgado, J., B. Merz, and H. Apel (2012). "A climate-flood link for the lower Mekong River". In: *Hydrology and Earth System Sciences* 16.5, pp. 1533–1541.

Delgado, J. M., H. Apel, and B Merz (2009). "Flood trends and variability in the Mekong river." In: *Hydrology & Earth System Sciences Discussions* 6.5.

Dietrich, J. P., C. Schmitz, C. Müller, M. Fader, H. Lotze-Campen, and A. Popp (2012). "Measuring agricultural land-use intensity - A global analysis using a model-assisted approach". In: *Ecological Modelling* 232, pp. 109–118. ISSN: 03043800. DOI: 10.1016/j.ecolmodel.2012.03.002.

Douglas, E. M., R. M. Vogel, and C. N. Kroll (2000). "Trends in floods and low flows in the United States: Impact of spatial correlation". In: *Journal of Hydrology* 240.1-2, pp. 90–105. ISSN: 00221694. DOI: 10.1016/S0022-1694(00)00336-X.

Eagleson, P. S. (1972). "Dynamics of Flood Frequency". In: *Water Resources Research* 8.4, pp. 878–&. ISSN: 0043-1397.

Efron, B. (1982). *The jackknife, the bootstrap and other resampling plans*. SIAM.

Efron, B. and R. Tibshirani (1986). "Bootstrap methods for standard errors, confidence intervals, and other measures of statistical accuracy". In: *Statistical science*, pp. 54–75.

Estilow, T. W., A. H. Young, and D. A. Robinson (2015). "A long-term Northern Hemisphere snow cover extent data record for climate studies and monitoring". In: *Earth System Science Data* 7.1, pp. 137–142. ISSN: 1866-3516. DOI: 10.5194/essd-7-137-2015.

Falkenmark, M. and T. Chapman (1989). *Comparative hydrology: An ecological approach to land and water resources*. Paris: The Unesco Press, p. 479.

Fraser, C. E., N. Mcintyre, B. M. Jackson, and H. S. Wheater (2013). "Upscaling hydrological processes and land management change impacts using a metamodeling procedure". In: *Water Resources Research* 49.9, pp. 5817–5833. ISSN: 00431397. DOI: 10.1002/wrcr.20432.

Gelman, A., J. Hwang, and A. Vehtari (2014). "Understanding predictive information criteria for Bayesian models". In: *Statistics and Computing* 24.6, pp. 997–1016. ISSN: 0960-3174. DOI: 10.1007/s11222-013-9416-2. arXiv: 1307.5928.

Graf, W. L. (2006). "Downstream hydrologic and geomorphic effects of large dams on American rivers". In: *Geomorphology* 79.3-4, pp. 336–360. ISSN: 0169555X. DOI: 10.1016/j.geomorph.2006.06.022.

GRDC (2016). "The Global Runoff Data Centre". In: URL: http://www.bafg.de/GRDC/EN/Home/homepage_node.html.

Grillakis, M., A. Koutroulis, J. Komma, I. Tsanis, W. Wagner, and G. Blöschl (2016). "Initial soil moisture effects on flash flood generation – A comparison between basins of contrasting hydro-climatic conditions". In: *Journal of Hydrology* 541. Flash floods, hydro-geomorphic response and risk management, pp. 206 –217. ISSN: 0022-1694. DOI: https://doi.org/10.1016/j.jhydrol.2016.03.007.

Hall, J. et al. (2015). "A European Flood Database: facilitating comprehensive flood research beyond administrative boundaries". In: *Proceedings of the International Association of Hydrological Sciences* 370, pp. 89–95. ISSN: 2199-899X. DOI: 10.5194/piahs-370-89-2015.

Hall, J. and G. Blöschl (2018). "Spatial patterns and characteristics of flood seasonality in Europe". In: *Hydrology and Earth System Sciences* 22.7, pp. 3883–3901. ISSN: 1607-7938. DOI: 10.5194/hess-22-3883-2018.

Hall, J. et al. (2014). "Understanding flood regime changes in Europe: a state-of-the-art assessment". In: *Hydrology and Earth System Sciences* 18.7, pp. 2735–2772. ISSN: 1607-7938. DOI: 10.5194/hess-18-2735-2014.

Hanel, M., T. A. Buishand, and C. A. Ferro (2009). "A nonstationary index flood model for precipitation extremes in transient regional climate model simulations". In: *Journal of Geophysical Research Atmospheres* 114.15, pp. 1–16. ISSN: 01480227. DOI: 10.1029/2009JD011712.

Hannaford, J., G. Buys, K. Stahl, and L. M. Tallaksen (2013). "The influence of decadal-scale variability on trends in long European streamflow records". In: *Hydrology and Earth System Sciences* 17.7, pp. 2717–2733. ISSN: 10275606. DOI: 10.5194/hess-17-2717-2013.

Hannaford, J. and T. J. Marsh (2008). "High-flow and flood trends in a network of undisturbed catchments in the UK". In: *International Journal of Climatology* 28.10, pp. 1325–1338. ISSN: 08998418. DOI: 10.1002/joc.1643.

He, Z. H., J. Parajka, F. Q. Tian, and G. Blöschl (2014). "Estimating degree-day factors from MODIS for snowmelt runoff modeling". In: *Hydrology and Earth System Sciences* 18.12, pp. 4773–4789. ISSN: 1607-7938. DOI: 10.5194/hess-18-4773-2014.

Hiebl, J. and C. Frei (2018). "Daily precipitation grids for Austria since 1961—development and evaluation of a spatial dataset for hydroclimatic monitoring and modelling". In: *Theoretical and Applied Climatology* 132.1, pp. 327–345. ISSN: 1434-4483. DOI: 10.1007/s00704-017-2093-x.

Hirabayashi, Y., R. Mahendran, S. Koirala, L. Konoshima, D. Yamazaki, S. Watanabe, H. Kim, and S. Kanae (2013). "Global flood risk under climate change". In: *Nature Climate Change* 3.9, pp. 816–821.

Hodgkins, G. A., P. H. Whitfield, D. H. Burn, J. Hannaford, B. Renard, K. Stahl, A. K. Fleig, H. Madsen, L. Mediero, J. Korhonen, et al. (2017). "Climate-driven variability in the occurrence of major floods across North America and Europe". In: *Journal of Hydrology* 552, pp. 704–717.

Hosking, J. R. M. and J. R. Wallis (1993). "Some statistics useful in regional frequency analysis". In: *Water Resources Research* 29.2, pp. 271–281. ISSN: 00431397. DOI: 10.1029/92WR01980.

Hosking, J. and J. R. Wallis (1997). "Regional Frequency Analysis". In: *Regional Frequency Analysis, by JRM Hosking and James R. Wallis, pp. 240. ISBN 0521430453. Cambridge, UK: Cambridge University Press, April 1997.*, p. 240.

IPCC (2012). *IPCC, 2012: Managing the Risks of Extreme Events and Disasters to Advance Climate Change Adaptation. A Special Report of Working Groups I and II of the Intergovernmental Panel on Climate Change*. Cambridge, United Kingdom and New York, NY, USA: Cambridge University Press, p. 582. ISBN: 978-1-107-02506-6.

– (2013). *Climate Change 2013: The Physical Science Basis. Contribution of Working Group I to the Fifth Assessment Report of the Intergovernmental Panel on Climate Change*. Cambridge, United Kingdom and New York, NY, USA: Cambridge University Press, p. 1535. ISBN: ISBN 978-1-107-66182-0. DOI: 10.1017/CBO9781107415324. URL: www.climatechange2013.org.

Kemter, M., B. Merz, N. Marwan, S. Vorogushyn, and G. Blöschl (2020). "Joint Trends in Flood Magnitudes and Spatial Extents Across Europe". In: *Geophysical Research Letters* 47.7, pp. 1–8. ISSN: 19448007. DOI: 10.1029/2020GL087464.

Köppen, W. (1884). "Die Wärmezonen der Erde, nach der Dauer der heissen, gemässigten und kalten Zeit und nach der Wirkung der Wärme auf die organische Welt betrachtet". In: *Meteorologische Zeitschrift* 1.21, pp. 5–226.

Krumphuber, C. (Aug. 2016). *Crop farming in Upper Austria*. Tech. rep. www.ooe.lko.at. Landwirtschaftskammer Oberösterreich.

Kundzewicz, Z. W. et al. (2017). "Differences in flood hazard projections in Europe – their causes and consequences for decision making". In: *Hydrological Sciences Journal* 62.1, pp. 1–14. DOI: 10.1080/02626667.2016.1241398.

Künsch, H. R. (1989). "The jackknife and the bootstrap for general stationary observations". In: *Annals of Statistics* 17.3, pp. 1217–1241.

Lammersen, R., H. Engel, W van de Langemheen, and H. Buiteveld (2002). "Impact of river training and retention measures on flood peaks along the Rhine". In: *Journal of Hydrology* 267.1-2, pp. 115–124. ISSN: 00221694. DOI: 10.1016/S0022-1694(02)00144-0.

Lavers, D. A., R. P. Allan, E. F. Wood, G. Villarini, D. J. Brayshaw, and A. J. Wade (2011). "Winter floods in Britain are connected to atmospheric rivers". In: *Geophysical Research Letters* 38.23, n/a–n/a. ISSN: 00948276. DOI: 10.1029/2011GL049783.

Lavers, D. A. and G. Villarini (2013). "The nexus between atmospheric rivers and extreme precipitation across Europe". In: *Geophysical Research Letters* 40.12, pp. 3259–3264. ISSN: 00948276. DOI: 10.1002/grl.50636.

Leander, R., T. A. Buishand, B. J. van den Hurk, and M. J. de Wit (2008). "Estimated changes in flood quantiles of the river Meuse from resampling of regional climate model output". In: *Journal of Hydrology* 351.3-4, pp. 331–343. ISSN: 00221694. DOI: 10.1016/j.jhydrol.2007.12.020.

Leclerc, M. and T. B. Ouarda (2007). "Non-stationary regional flood frequency analysis at ungauged sites". In: *Journal of Hydrology* 343.3-4, pp. 254–265. ISSN: 00221694. DOI: 10.1016/j.jhydrol.2007.06.021.

Lehner, B. et al. (2011). "High-resolution mapping of the world's reservoirs and dams for sustainable river-flow management". In: *Frontiers in Ecology and the Environment* 9.9, pp. 494–502. ISSN: 1540-9295. DOI: 10.1890/100125.

Lima, C. H. and U. Lall (2010). "Spatial scaling in a changing climate: A hierarchical bayesian model for non-stationary multi-site annual maximum and monthly streamflow". In: *Journal of Hydrology* 383.3-4, pp. 307–318. ISSN: 00221694. DOI: 10.1016/j.jhydrol.2009.12.045.

Lima, C. H., U. Lall, T. Troy, and N. Devineni (2016). "A hierarchical Bayesian GEV model for improving local and regional flood quantile estimates". In: *Journal of Hydrology* 541, pp. 816–823. ISSN: 00221694. DOI: 10.1016/j.jhydrol.2016.07.042.

Liu, R. Y., K. Singh, et al. (1992). "Moving blocks jackknife and bootstrap capture weak dependence". In: *Exploring the limits of bootstrap* 225, p. 248.

López, J. and F. Francés (2013). "Non-stationary flood frequency analysis in continental Spanish rivers, using climate and reservoir indices as external covariates". In: *Hydrology and Earth System Sciences* 17.8, pp. 3189–3203. ISSN: 1607-7938. DOI: 10.5194/hess-17-3189-2013.

Machado, M. J., B. A. Botero, J. López, F. Francés, A. Díez-Herrero, and G. Benito (2015). "Flood frequency analysis of historical flood data under stationary and non-stationary modelling". In: *Hydrology and Earth System Sciences* 19.6, pp. 2561–2576. ISSN: 16077938. DOI: 10.5194/hess-19-2561-2015.

Madsen, H., D. Lawrence, M. Lang, M. Martinkova, and T. R. Kjeldsen (2014). "Review of trend analysis and climate change projections of extreme precipitation and floods in Europe". In: *Journal of Hydrology* 519.PD, pp. 3634–3650. ISSN: 00221694. DOI: 10.1016/j.jhydrol.2014.11.003.

Mangini, W., A. Viglione, J. Hall, Y. Hundecha, S. Ceola, A. Montanari, M. Rogger, J. L. Salinas, I. Borzì, and J. Parajka (2018). "Detection of trends in magnitude and frequency of flood peaks across Europe". In: *Hydrological Sciences Journal* 63.4, pp. 1–20. ISSN: 0262-6667. DOI: 10.1080/02626667.2018.1444766.

Martins, E. S. and J. R. Stedinger (2000). "Generalized maximum-likelihood generalized extreme-value quantile estimators for hydrologic data". In: *Water Resources Research* 36.3, pp. 737–744. ISSN: 00431397. DOI: 10.1029/1999WR900330.

Mediero, L. et al. (2015). "Identification of coherent flood regions across Europe by using the longest streamflow records". In: *Journal of Hydrology* 528, pp. 341–360. ISSN: 00221694. DOI: 10.1016/j.jhydrol.2015.06.016.

Mediero, L., D. Santillán, L. Garrote, and A. Granados (2014). "Detection and attribution of trends in magnitude, frequency and timing of floods in Spain". In: *Journal of Hydrology* 517, pp. 1072–1088. ISSN: 00221694. DOI: 10.1016/j.jhydrol.2014.06.040.

Merz, B., S. Vorogushyn, S. Uhlemann, J. Delgado, and Y. Hundecha (2012). "HESS Opinions "More efforts and scientific rigour are needed to attribute trends in flood time series"". In: *Hydrology and Earth System Sciences* 16.5, pp. 1379–1387. ISSN: 1607-7938. DOI: 10.5194/hess-16-1379-2012.

Merz, R. and G. Blöschl (2003). "A process typology of regional floods". In: *Water Resources Research* 39.12, pp. 1–20. ISSN: 00431397. DOI: 10.1029/2002WR001952. URL: http://doi.wiley.com/10.1029/2002WR001952.

Merz, R. and G. Blöschl (2008a). "Flood frequency hydrology: 1. Temporal, spatial, and causal expansion of information". In: *Water Resources Research* 44, W08432. DOI: 10.1029/2007WR006744.

– (2008b). "Flood frequency hydrology: 2. Combining data evidence". In: *Water Resources Research* 44, W08433. DOI: 10.1029/2007WR006745.

Miller, J. D., T. R. Kjeldsen, J. Hannaford, and D. G. Morris (2013). "A hydrological assessment of the November 2009 floods in Cumbria, UK". In: *Hydrology Research* 44.1, pp. 180–197. ISSN: 0029-1277. DOI: 10.2166/nh.2012.076.

Monfreda, C., N. Ramankutty, and J. A. Foley (2008). "Farming the planet: 2. Geographic distribution of crop areas, yields, physiological types, and net primary production in the year 2000". In: *Global Biogeochemical Cycles* 22.1, pp. 1–19. ISSN: 08866236. DOI: 10.1029/2007GB002947.

Montanari, A. and D. Koutsoyiannis (2014). "Modeling and mitigating natural hazards: Stationarity is immortal!" In: *Water Resources Research* 50.12, pp. 9748–9756. ISSN: 00431397. DOI: 10.1002/2014WR016092.

Mudelsee, M., M. Börngen, G. Tetzlaff, and U. Grünewald (2003). "No upward trends in the occurrence of extreme floods in central Europe". In: *Nature* 425.6954, pp. 166–169. ISSN: 0028-0836. DOI: 10.1038/nature01928.

Murawski, A., J. Zimmer, and B. Merz (2016). "High spatial and temporal organization of changes in precipitation over Germany for 1951–2006". In: *International Journal of Climatology* 36.6, pp. 2582–2597.

Niehoff, D., U. Fritsch, and A. Bronstert (2002). "Land-use impacts on storm-runoff generation: Scenarios of land-use change and simulation of hydrological response in a meso-scale catchment in SW-Germany". In: *Journal of Hydrology* 267.1-2, pp. 80–93. ISSN: 00221694. DOI: 10.1016/S0022-1694(02)00142-7.

O'Connell, P. E., J. Ewen, G. O'Donnell, and P. Quinn (2007). "Is there a link between agricultural land-use management and flooding?" In: *Hydrology and Earth System Sciences* 11.1, pp. 96–107. ISSN: 1607-7938. DOI: 10.5194/hess-11-96-2007.

Papalexiou, S. M. and D. Koutsoyiannis (2013). "Battle of extreme value distributions: A global survey on extreme daily rainfall". In: *Water Resources Research* 49.1, pp. 187–201. DOI: 10.1029/2012WR012557.

Parajka, J. and G. Blöschl (2008). "Spatio-temporal combination of MODIS images - Potential for snow cover mapping". In: *Water Resources Research* 44.3, pp. 1–13. ISSN: 00431397. DOI: 10.1029/2007WR006204.

Perdigão, R. A. and G. Blöschl (2014). "Spatiotemporal flood sensitivity to annual precipitation: Evidence for landscape-climate coevolution". In: *Water Resources Research* 50.7, pp. 5492–5509. ISSN: 19447973. DOI: 10.1002/2014WR015365.

Petrow, T. and B. Merz (2009). "Trends in flood magnitude, frequency and seasonality in Germany in the period 1951–2002". In: *Journal of Hydrology* 371.1-4, pp. 129–141. ISSN: 00221694. DOI: 10.1016/j.jhydrol.2009.03.024.

Pinter, N., R. R. Van der Ploeg, P. Schweigert, and G. Hoefer (2006). "Flood magnification on the River Rhine". In: *Hydrological Processes* 20.1, pp. 147–164. ISSN: 08856087. DOI: 10.1002/hyp.5908.

Ploeg, R. van der, G. Machulla, D. Hermsmeyer, J. Ilsemann, M. Gieska, and J. Bachmann (2002). "Changes in land use and the growing number of flash floods in Germany". In: *Agricultural Effects on Ground and Surface Waters: Research at the Edge of Science and Society* 273, pp. 317–321. ISSN: 01447815.

Prosdocimi, I., T. R. Kjeldsen, and J. D. Miller (2015). "Detection and attribution of urbanization effect on flood extremes using nonstationary flood-frequency models". In: *Water Resources Research* 51.6, pp. 4244–4262. ISSN: 00431397. DOI: 10.1002/2015WR017065.

Prosdocimi, I., T. R. Kjeldsen, and C. Svensson (2014). "Non-stationarity in annual and seasonal series of peak flow and precipitation in the UK". In: *Natural Hazards and Earth System Sciences* 14.5, pp. 1125–1144. ISSN: 16849981. DOI: 10.5194/nhess-14-1125-2014.

Prudhomme, C., D. Jakob, and C. Svensson (2003). "Uncertainty and climate change impact on the flood regime of small UK catchments". In: *Journal of Hydrology* 277.1-2, pp. 1–23. ISSN: 00221694. DOI: 10.1016/S0022-1694(03)00065-9.

Ramankutty, N., A. T. Evan, C. Monfreda, and J. A. Foley (2008). "Farming the planet: 1. Geographic distribution of global agricultural lands in the year 2000". In: *Global Biogeochemical Cycles* 22.1, pp. 1–19. ISSN: 08866236. DOI: 10.1029/2007GB002952.

Ray, D. K., N. Ramankutty, N. D. Mueller, P. C. West, and J. A. Foley (2012). "Recent patterns of crop yield growth and stagnation". In: *Nature Communications* 3, pp. 1293–1297. ISSN: 20411723. DOI: 10.1038/ncomms2296.

Renard, B., V. Garreta, and M. Lang (2006a). "An application of Bayesian analysis and Markov chain Monte Carlo methods to the estimation of a regional trend in annual maxima". In: *Water Resources Research* 42.12, pp. 1–17. ISSN: 00431397. DOI: 10.1029/2005WR004591.

Renard, B. and U. Lall (2014). "Regional frequency analysis conditioned on large-scale atmospheric or oceanic fields". In: *Water Resources Research* 50.12, pp. 9536–9554. ISSN: 00431397. DOI: 10.1002/2014WR016277. eprint: 2014WR016527 (10.1002).

Renard, B., M. Lang, and P. Bois (2006b). "Statistical analysis of extreme events in a non-stationary context via a Bayesian framework: case study with peak-over-threshold data". In: *Stochastic Environmental Research and Risk Assessment* 21.2, pp. 97–112. ISSN: 1436-3240. DOI: 10.1007/s00477-006-0047-4.

Renard, B. et al. (2008). "Regional methods for trend detection: Assessing field significance and regional consistency". In: *Water Resources Research* 44.8, pp. 1–17. ISSN: 00431397. DOI: 10.1029/2007WR006268.

Ribatet, M., D. Cooley, and A. C. Davison (2012). "Bayesian inference from composite likelihoods, with an application to spatial extremes". In: *Statistica Sinica*, pp. 813–845.

Rogger, M., H. Pirkl, A. Viglione, J. Komma, B. Kohl, R. Kirnbauer, R. Merz, and G. Blöschl (2012). "Step changes in the flood frequency curve: Process controls". In: *Water Resources Research* 48.5, pp. 1–15. ISSN: 00431397. DOI: 10.1029/2011WR011187. URL: http://doi.wiley.com/10.1029/2011WR011187.

Rogger, M et al. (2017). “Land use change impacts on floods at the catchment scale: Challenges and opportunities for future research”. In: *Water Resouces Research* 53.June 2013, pp. 5209–5219. DOI: 10.1002/2017WR020723.Received.

Rojas, R., L. Feyen, A. Bianchi, and A. Dosio (2012). “Assessment of future flood hazard in Europe using a large ensemble of bias-corrected regional climate simulations”. In: *Journal of Geophysical Research Atmospheres* 117.17. ISSN: 01480227. DOI: 10.1029/2012JD017461.

Roth, M., T. A. Buishand, G. Jongbloed, A. M. Klein Tank, and J. H. Van Zanten (2012). “A regional peaks-over-threshold model in a nonstationary climate”. In: *Water Resources Research* 48.11, pp. 1–12. ISSN: 00431397. DOI: 10.1029/2012WR012214.

Salazar, S., F. Frances, J. Komma, T. Blume, T. Francke, A. Bronstert, and G. Bloschl (2012). “A comparative analysis of the effectiveness of flood management measures based on the concept of "retaining water in the landscape" in different European hydro-climatic regions”. In: *Natural Hazards and Earth System Science* 12.11, pp. 3287–3306. ISSN: 15618633. DOI: 10.5194/nhess-12-3287-2012.

Salinas, J. L., A. Castellarin, S. Kohnová, and T. R. Kjeldsen (2014b). “Regional parent flood frequency distributions in Europe - Part 2: Climate and scale controls”. In: *Hydrology and Earth System Sciences* 18.11, pp. 4391–4401. ISSN: 16077938. DOI: 10.5194/hess-18-4391-2014.

Salinas, J. L., A. Castellarin, A. Viglione, S. Kohnová, and T. R. Kjeldsen (2014a). “Regional parent flood frequency distributions in Europe - Part 1: Is the GEV model suitable as a pan-European parent?” In: *Hydrology and Earth System Sciences* 18.11, pp. 4381–4389. ISSN: 16077938. DOI: 10.5194/hess-18-4381-2014.

Serinaldi, F. and C. G. Kilsby (2015). “Stationarity is undead: Uncertainty dominates the distribution of extremes”. In: *Advances in Water Resources* 77, pp. 17–36. ISSN: 03091708. DOI: 10.1016/j.advwatres.2014.12.013.

Sharkey, P. and H. C. Winter (2019). “A Bayesian spatial hierarchical model for extreme precipitation in Great Britain”. In: *Environmetrics* 30.1, e2529. DOI: 10.1002/env.2529.

Sharma, A., C. Wasko, and D. P. Lettenmaier (2018). “If Precipitation Extremes Are Increasing, Why Aren’t Floods?” In: *Water Resources Research* 54.11, pp. 8545–8551. ISSN: 19447973. DOI: 10.1029/2018WR023749.

Silva, A. T., M. M. Portela, M. Naghettini, and W. Fernandes (2017). “A Bayesian peaks-over-threshold analysis of floods in the Itajaí-açu River under stationarity and nonstationarity”. In: *Stochastic Environmental Research and Risk Assessment* 31.1, pp. 185–204. ISSN: 1436-3240. DOI: 10.1007/s00477-015-1184-4.

Sivapalan, M. and G. Blöschl (2015). “Time scale interactions and the coevolution of humans and water”. In: *Water Resources Research* 51.9, pp. 6988–7022. ISSN: 19447973. DOI: 10.1002/2015WR017896. arXiv: 2014WR016527 [10.1002].

Sivapalan, M., G. Blöschl, R. Merz, and D. Gutknecht (June 2005). “Linking flood frequency to long-term water balance: Incorporating effects of seasonality”. In: *Water Resources Research* 41.6, W06012. ISSN: 0043-1397. DOI: 10.1029/2004WR003439.

Skublics, D., G. Blöschl, and P. Rutschmann (2016). “Effect of river training on flood retention of the Bavarian Danube”. In: *Journal of Hydrology and Hydromechanics* 64.4, pp. 349–356. ISSN: 0042-790X. DOI: 10.1515/johh-2016-0035.

Smith, R. (1990). “Regional estimation from spatially dependent data”. In: *Preprint. http://www.stat. unc. edu/postscript/rs/regest. pdf*.

Šraj, M., A. Viglione, J. Parajka, and G. Blöschl (2016). “The influence of non-stationarity in extreme hydrological events on flood frequency estimation”. In: *Journal of Hydrology and Hydromechanics* 64.4, pp. 426–437. ISSN: 0042-790X. DOI: 10.1515/johh-2016-0032.

Stan Development Team (2018). *Stan Modeling Language Users Guide and Reference ManualVersion 2.18.0*. http://mc-stan.org.

Statistik Austria, S (2017). *Bundesanstalt Statistik Österreich: Crop production 1075 to 2017*. https://www.statistik.at/, Last accessed: 2018-01-17.

Stedinger, J. R. (1983). "Estimating a regional flood frequency distribution". In: *Water Resources Research* 19.2, pp. 503–510. ISSN: 00431397. DOI: 10.1029/WR019i002p00503.

Steirou, E., L. Gerlitz, H. Apel, X. Sun, and B. Merz (2019). "Climate influences on flood probabilities across Europe". In: *Hydrology and Earth System Sciences* 23.3, pp. 1305–1322. ISSN: 1607-7938. DOI: 10.5194/hess-23-1305-2019.

Sun, X., M. Thyer, B. Renard, and M. Lang (2014). "A general regional frequency analysis framework for quantifying local-scale climate effects: A case study of ENSO effects on Southeast Queensland rainfall". In: *Journal of Hydrology* 512, pp. 53–68. ISSN: 00221694. DOI: 10.1016/j.jhydrol.2014.02.025.

Szolgayova, E., J. Parajka, G. Blöschl, and C. Bucher (2014). "Long term variability of the Danube River flow and its relation to precipitation and air temperature". In: *Journal of Hydrology* 519.PA, pp. 871–880. ISSN: 00221694. DOI: 10.1016/j.jhydrol.2014.07.047.

Tasker, G. D. and J. R. Stedinger (1989). "An operational GLS model for hydrologic regression". In: *Journal of Hydrology* 111.1-4, pp. 361–375.

Thober, S., R. Kumar, N. Wanders, A. Marx, M. Pan, O. Rakovec, L. Samaniego, J. Sheffield, E. F. Wood, and M. Zink (2018). "Multi-model ensemble projections of European river floods and high flows at 1.5, 2, and 3 degrees global warming". In: *Environmental Research Letters* 13.1, p. 014003. ISSN: 1748-9326. DOI: 10.1088/1748-9326/aa9e35.

Tramblay, Y., L. Mimeau, L. Neppel, F. Vinet, and E. Sauquet (2019). "Detection and attribution of flood trends in Mediterranean basins". In: *Hydrology and Earth System Sciences* 23.11, pp. 4419–4431. DOI: 10.5194/hess-23-4419-2019. URL: https://hess.copernicus.org/articles/23/4419/2019/.

Tramblay, Y., L. Neppel, J. Carreau, and K. Najib (2013). "Analyse fréquentielle non-stationnaire des pluies extrêmes dans le Sud de la France". In: *Hydrological Sciences Journal* 58.2, pp. 280–294. ISSN: 02626667. DOI: 10.1080/02626667.2012.754988.

Ulbrich, U., T. Brücher, A. H. Fink, G. C. Leckebusch, A. Krüger, and J. G. Pinto (2003). "The central European floods of August 2002: Part 1 – Rainfall periods and flood development". In: *Weather* 58.10, pp. 371–377. ISSN: 00431656. DOI: 10.1256/wea.61.03A.

Van der Ploeg, R. and P. Schweigert (2001). "Elbe river flood peaks and postwar agricultural land use in East Germany". In: *Naturwissenschaften* 88.12, pp. 522–525. ISSN: 00281042. DOI: 10.1007/s00114-001-0271-1.

Van Der Ploeg, R. R., W. Ehlers, and F. Sieker (1999). "Floods and other possible adverse environmental effects of meadowland area decline in former West Germany". In: *Naturwissenschaften* 86.7, pp. 313–319. ISSN: 00281042. DOI: 10.1007/s001140050623.

Vehtari, A., A. Gelman, and J. Gabry (2017). "Practical Bayesian model evaluation using leave-one-out cross-validation and WAIC". In: *Statistics and Computing* 27.5, pp. 1413–1432. ISSN: 0960-3174. DOI: 10.1007/s11222-016-9696-4.

Vieux, B. E., J.-H. Park, and B. Kang (2009). "Distributed hydrologic prediction: Sensitivity to accuracy of initial soil moisture conditions and radar rainfall input". In: *Journal of Hydrologic Engineering* 14.7, pp. 671–689.

Viglione, A., F. Laio, and P. Claps (2007). "A comparison of homogeneity tests for regional frequency analysis". In: *Water Resources Research* 43.3, pp. 1–10. ISSN: 00431397. DOI: 10.1029/2006WR005095.

Viglione, A., J. Parajka, M. Rogger, J. L. Salinas, G. Laaha, M. Sivapalan, and G. Blöschl (2013a). "Comparative assessment of predictions in ungauged basins - Part 3: Runoff signatures in Austria". In: *Hydrology and Earth System Sciences* 17.6, pp. 2263–2279. ISSN: 10275606. DOI: 10.5194/hess-17-2263-2013.

Viglione, A., B. Merz, N. Viet Dung, J. Parajka, T. Nester, and G. Blöschl (2016). "Attribution of regional flood changes based on scaling fingerprints". In: *Water Resources Research* 52.7, pp. 5322–5340. ISSN: 00431397. DOI: 10.1002/2016WR019036.

Viglione, A., R. Merz, J. L. Salinas, and G. Blöschl (Feb. 2013b). "Flood frequency hydrology: 3. A Bayesian analysis". In: *Water Resources Research* 49.2, pp. 675–692. DOI: 10.1029/2011WR010782.

Villarini, G., J. A. Smith, F. Serinaldi, J. Bales, P. D. Bates, and W. F. Krajewski (2009). "Flood frequency analysis for nonstationary annual peak records in an urban drainage basin". In: *Advances in Water Resources* 32.8, pp. 1255–1266. ISSN: 03091708. DOI: 10.1016/j.advwatres.2009.05.003.

Villarini, G., J. A. Smith, F. Serinaldi, and A. A. Ntelekos (2011). "Analyses of seasonal and annual maximum daily discharge records for central Europe". In: *Journal of Hydrology* 399.3-4, pp. 299–312. ISSN: 00221694. DOI: 10.1016/j.jhydrol.2011.01.007.

Visser, H., A. C. Petersen, and W. Ligtvoet (2014). "On the relation between weather-related disaster impacts, vulnerability and climate change". In: *Climatic Change* 125.3-4, pp. 461–477.

Vogt, J., P. Soille, A De Jager, E Rimaviciute, W Mehl, S Foisneau, K Bodis, J Dusart, M. Paracchini, P Haastrup, et al. (2007). "A pan-European river and catchment database". In: *European Commission, EUR* 22920, p. 120.

Volpi, E., M. Di Lazzaro, M. Bertola, A. Viglione, and A. Fiori (2018). "Reservoir effects on flood peak discharge at the catchments scale". In: *Water Resources Research*.

Vorogushyn, S. and B. Merz (2013). "Flood trends along the Rhine: the role of river training". In: *Hydrology and Earth System Sciences* 17.10, pp. 3871–3884. ISSN: 1607-7938. DOI: 10.5194/hess-17-3871-2013.

Watanabe, S. (Dec. 2010). "Asymptotic Equivalence of Bayes Cross Validation and Widely Applicable Information Criterion in Singular Learning Theory". In: *J. Mach. Learn. Res.* 11, pp. 3571–3594. ISSN: 1532-4435.

Wilby, R. L., K. J. Beven, and N. S. Reynard (2008). "Climate change and fluvial flood risk in the UK: more of the same?" In: *Hydrological Processes* 22.14, pp. 2511–2523. ISSN: 08856087. DOI: 10.1002/hyp.6847.

Wilks, D. S. (1997). "Resampling hypothesis tests for autocorrelated fields". In: *Journal of Climate* 10.1, pp. 65–82.

Zanardo, S., L. Nicotina, A. G. J. Hilberts, and S. P. Jewson (2019). "Modulation of Economic Losses From European Floods by the North Atlantic Oscillation". In: *Geophysical Research Letters* 46.5, pp. 2563–2572. ISSN: 0094-8276. DOI: 10.1029/2019GL081956.

Zhu, Z., D. B. Wright, and G. Yu (2018). "The Impact of Rainfall Space-Time Structure in Flood Frequency Analysis". In: *Water Resources Research* 54.11, pp. 8983–8998.

Appendix A

Number of stations

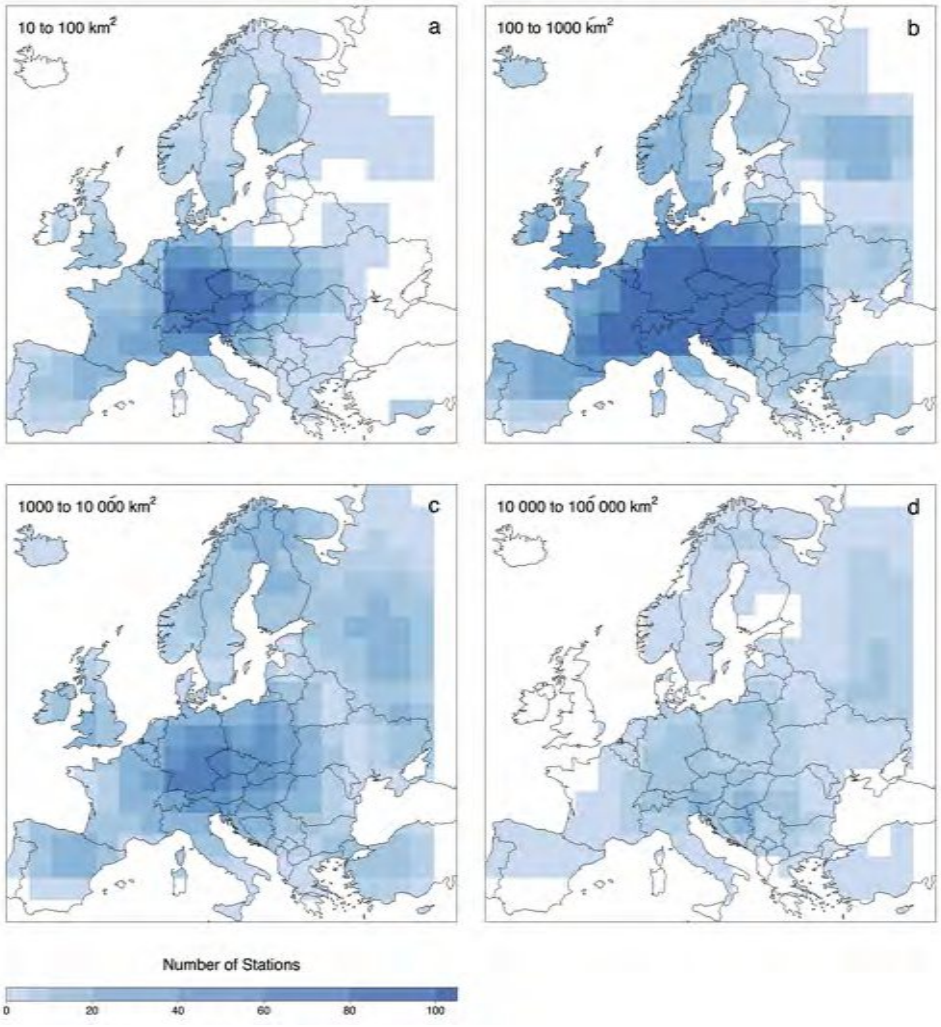

Fig. A.1: Number of stations in each 600x600 km region, stratified by catchment size: (a) 10 to 100 km^2, (b) 100 to 1000 km^2, (c) 1000 to 10 000 km^2 and (d) 10 000 to 100 000 km^2. The value representative for the region is plotted in the respective central 200x200 km cell.

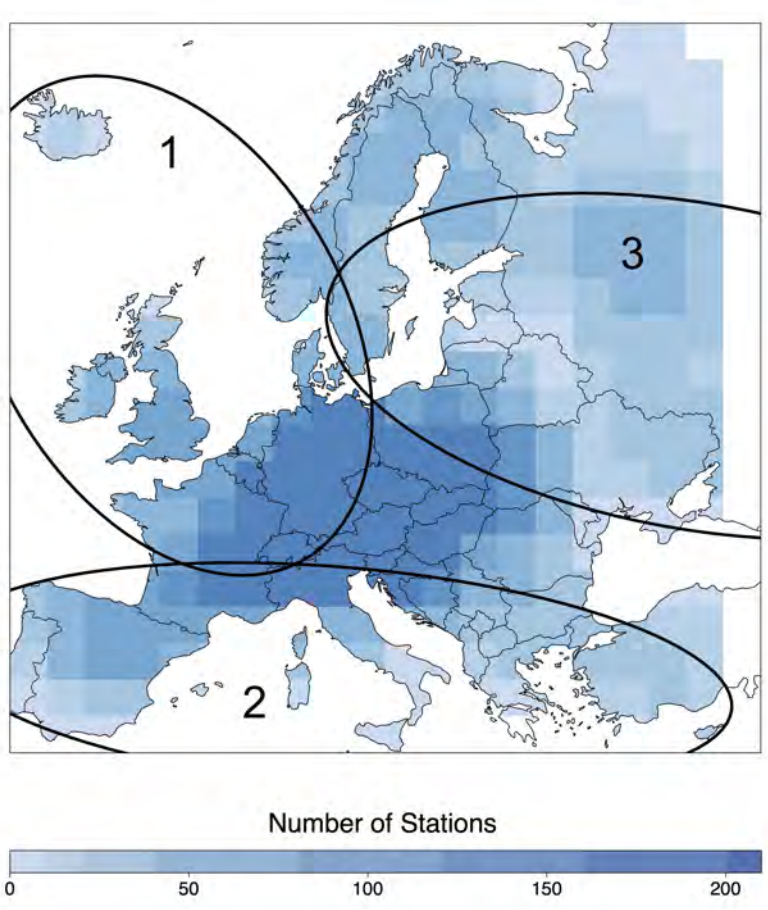

Fig. A.2: Total number of stations in each 600x600 km region. The value representative for the region is plotted in the respective central 200x200 km cell. The three macro-regions analysed in Chapter 2 are also represented: northewstern (1), southern (2) and eastern (3) Europe.

Appendix B

Adjustment to the likelihood

Regional frequency analyses typically assume spatial independence between time series and, when some degree of spatial dependence is apparent in the data, it may result in underestimating the variance of parameter estimates (Stedinger, 1983). Smith (1990) proposed a method for computing standard errors that accounts for spatial dependence using a modified covariance matrix. The asymptotic distribution of the maximum likelihood estimator $\hat{\theta}$ of the independence likelihood is:

$$\hat{\theta} \sim N\left(\theta^0, n^{-1}H^{-1}VH^{-1}\right) \tag{B.1}$$

where θ^0 is the value of the true value of θ and $H^{-1}VH^{-1}$ is the modified covariance matrix, where $H = -\mathbb{E}\nabla^2 l\left(\theta^0, \mathbf{y}\right)$ and $V = cov\nabla l\left(\theta^0, \mathbf{y}\right)$. If the assumption of spatial independence is correct, we have that $H = V$ which leads to the conventional approximation $cov\hat{\theta} \sim H^{-1}$. The matrix H is approximated by the observed information matrix $\nabla^2 l\left(\hat{\theta}, \mathbf{y}\right)$ and V is estimated by decomposing the likelihood into independent yearly contributions.

Based on the work of Smith (1990), Ribatet et al. (2012) proposed a method based on a magnitude adjustment to the likelihood function in the Bayesian framework, which accounts for the overall dependence in space and allows to obtain reliable credible intervals. The adjusted likelihood is defined as:

$$L^*\left(\theta, \mathbf{y}\right) = L\left(\theta, \mathbf{y}\right)^k \tag{B.2}$$

where $L\left(\theta, \mathbf{y}\right)$ is the likelihood under the assumption of spatial independence, θ is the vector of unknown parameters, and k is the magnitude adjustment factor to be estimated, such as $0 < k \leq 1$. Ribatet et al. (2012) proposed to set:

$$k = \frac{p}{\sum_{i=1}^{p} \lambda_i} \tag{B.3}$$

where p is the number of parameters in the independence likelihood and λ_i are the eigenvalues of the matrix $H^{-1}V$. This adjustment ensures that the expected value of the deviance function of the adjusted likelihood converges to that of the full (unavailable) likelihood. The magnitude adjustment to the likelihood results in inflating the asymptotic posterior variance of the parameters estimated, while parameter estimates are unchanged (Ribatet et al., 2012):

$$\hat{\theta} \sim N\left(\theta^0, np^{-1}tr(H^{-1}V)H^{-1}\right) \tag{B.4}$$

The magnitude adjustment factor k represents the overall reduction of hydrological information in the data caused by the presence of spatial correlation. For further details about the method and its application to hydrological data, see Smith (1990), Ribatet et al. (2012) and Sharkey and Winter (2019).

Appendix C

Seasonality of floods

As in Blöschl et al. (2017), the average date of occurrence of floods $\bar{D}$ and the concentration R of the date of occurrence around the average date are obtained with circular statistics, by conversion of the date of occurrence of a flood in the year i into an angular value D_i:

$$\bar{D} = \begin{cases} \tan^-1\left(\frac{\bar{y}}{\bar{x}}\right) \cdot \frac{\bar{m}}{2\pi} & \bar{x} > 0, \bar{y} \geq 0 \\ \tan^-1\left(\frac{\bar{y}}{\bar{x}} + \pi\right) \cdot \frac{\bar{m}}{2\pi} & \bar{x} \leq 0 \\ \tan^-1\left(\frac{\bar{y}}{\bar{x}} + 2\pi\right) \cdot \frac{\bar{m}}{2\pi} & \bar{x} > 0, \bar{y} \leq 0 \end{cases} \tag{C.1a}$$

$$R = \sqrt{\bar{x}^2 + \bar{y}^2} \tag{C.1b}$$

with:

$$\bar{x} = \frac{1}{n} \sum_{i=1}^{n} \cos\theta_i \tag{C.2a}$$

$$\bar{y} = \frac{1}{n} \sum_{i=1}^{n} \sin\theta_i \tag{C.2b}$$

$$\theta_i = D_i \cdot \frac{2\pi}{m_i} \tag{C.2c}$$

Where n is the number of peaks registered at that station, m_i is the number of days in the year i and $\bar{m}$ is the average number of days per year. When floods occur equally throughout the year $R = 0$, while $R = 1$ when floods always occur on the same date.

Appendix D

Drivers in northwestern, southern and eastern Europe

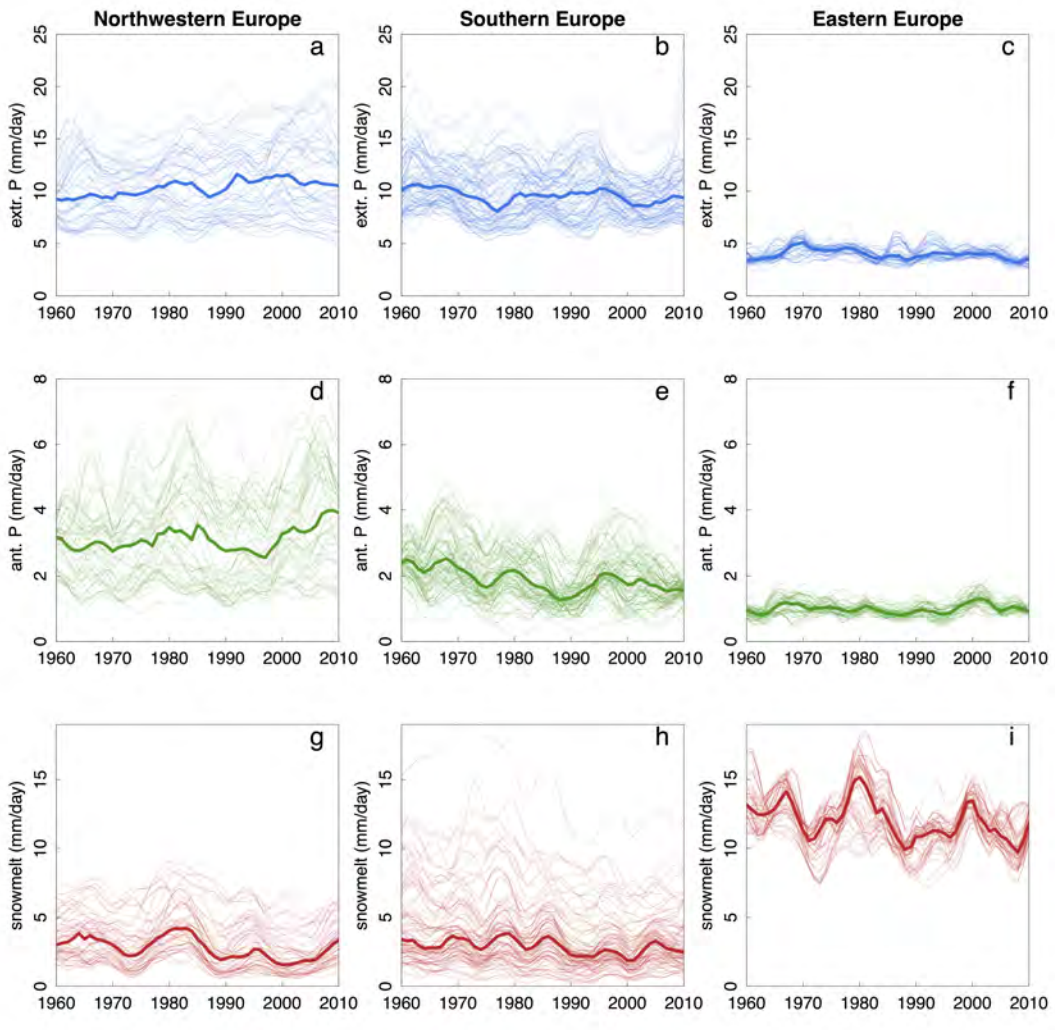

Fig. D.1: Smoothed time series (LOESS) of the drivers for each of the analysed regions in northwestern, southern and eastern Europe, as defined in Fig. 4.1. Thin lines represent catchment-averaged time series and thick lines represent the median value over the region.